



NUCLEAR WASTE MANAGEMENT ORGANIZATION SOCIÉTÉ DE GESTION DES DÉCHETS NUCLÉAIRES

# Phase 1 Geoscientific Desktop Preliminary Assessment, Processing and Interpretation of Geophysical Data

TOWNSHIP OF SCHREIBER, ONTARIO



**APM-REP-06144-0037**

**NOVEMBER 2013**

*This report has been prepared under contract to the NWMO. The report has been reviewed by the NWMO, but the views and conclusions are those of the authors and do not necessarily represent those of the NWMO.*

*All copyright and intellectual property rights belong to the NWMO.*

*For more information, please contact:*

**Nuclear Waste Management Organization**

22 St. Clair Avenue East, Sixth Floor

Toronto, Ontario M4T 2S3 Canada

Tel 416.934.9814

Toll Free 1.866.249.6966

Email [contactus@nwmo.ca](mailto:contactus@nwmo.ca)

[www.nwmo.ca](http://www.nwmo.ca)

**PHASE 1 GEOSCIENTIFIC DESKTOP  
PRELIMINARY ASSESSMENT**

**PROCESSING AND INTERPRETATION  
OF GEOPHYSICAL DATA**

**Township of Schreiber, Ontario**

Prepared for

AECOM

&

Nuclear Waste Management Organization

NWMO Report Number: APM-REP-06144-0037

By

Mira Geoscience Ltd.

Written by:



---

Thomas Campagne, M.Sc. Geophysics,  
Consultant  
Mira Geoscience Ltd.

Reviewed by:



---

Peter Kowalczyk, B.Sc., P.Geo.,  
Principal Consultant  
Mira Geoscience Ltd.



## **EXECUTIVE SUMMARY**

In December, 2011, the Township of Schreiber, Ontario, expressed interest in continuing to learn more about the Nuclear Waste Management Organization nine-step site selection process (NWMO, 2010), and requested that a preliminary assessment be conducted to assess potential suitability of the Schreiber area for safely hosting a deep geological repository (Step 3). This request followed the successful completion of an initial screening conducted during Step 2 of the site selection process.

The preliminary assessment is a multidisciplinary study integrating both technical and community well-being studies, including geoscientific suitability, engineering, transportation, environment and safety, as well as social, economic and cultural considerations. The findings of the overall preliminary assessment are reported in an integrated report (NWMO, 2013). The objective of the desktop geoscientific preliminary assessment was to determine whether the Township of Schreiber and its periphery, referred to as the “Schreiber area”, contains general areas that have the potential to meet NWMO’s geoscientific site evaluation factors.

This report presents the findings of a geophysical data interpretation assessment completed as part of the desktop geoscientific preliminary assessment of the Schreiber area (AECOM, 2013a). The purpose of this study was to perform a detailed interpretation of all available geophysical data (e.g., magnetic, electromagnetic, gravity and radiometric) for the Schreiber area, Ontario. The aim was to identify additional information that can be extracted from the data, in particular that relate to the coincidence of geophysical features with mapped lithology and structural features in the Schreiber area.

The geophysical data covering the Schreiber area are of variable data resolution. Low to medium resolution geophysical data, particularly the magnetic, gravity and radiometric data obtained from the Geological Survey of Canada (GSC), cover the entire Schreiber area. A magnetic/electromagnetic survey obtained from the Ontario Geological Survey (OGS) provided high resolution coverage over approximately 75% of the Schreiber area except for a north-south trending band along the western boundary.

The coincidence between the geophysical data and mapped lithology and structural features were interpreted using all the available geophysical data sets (e.g., magnetic, electromagnetic, gravity and radiometric). The pole reduced magnetic field (RTP) and its first vertical derivative (1VD of RTP) were the most reliable for the interpretation of geological contacts, and lithological heterogeneity. In addition, due to the limited overburden cover and the lack of large lakes on the land mass in the Schreiber area, the radiometric survey data was useful to highlight the lithological variations within and between the batholiths and greenstone units. Geophysical data analysis provided additional insight into compositional variations within mapped granitic intrusions of the Schreiber area. In general, the geophysical interpretations and the published geological maps were in good agreement.



## TABLE OF CONTENTS

<b>EXECUTIVE SUMMARY</b> .....	i
List of Figures (in order following text) .....	iv
List of Tables .....	iv
List of Abbreviations .....	v
<b>1. INTRODUCTION</b> .....	1
1.1 Study Objective .....	1
1.2 Schreiber Area .....	2
1.3 Qualifications of the Geophysical Interpretation Team .....	2
<b>2. SUMMARY OF PHYSICAL GEOGRAPHY AND GEOLOGY</b> .....	3
2.1 Physical Geography .....	3
2.2 Bedrock Geology .....	5
2.2.1 Granitoid Intrusive Rocks .....	5
2.2.2 Schreiber-Hemlo Greenstone Belt .....	6
2.2.3 Mafic Dykes .....	7
2.2.4 Faults .....	8
2.3 Structural Geology .....	8
2.4 Quaternary Geology .....	10
2.5 Land Use .....	12
<b>3. GEOPHYSICAL DATA SOURCES AND QUALITY</b> .....	12
3.1 Data Sources .....	13
3.1.1 Magnetic Data .....	15
3.1.2 Gravity Data .....	15
3.1.3 Radiometric Data .....	16
3.1.4 Electromagnetic Data .....	16
3.2 Data Limitations .....	17
<b>4. GEOPHYSICAL DATA PROCESSING</b> .....	18
4.1 Magnetic .....	18
4.2 Gravity .....	21
4.3 Radiometric .....	22
4.4 Electromagnetic .....	22
4.4.1 Very Low Frequency Electromagnetic .....	22

4.4.2	Frequency Domain Electromagnetic.....	22
5.	<b>GEOPHYSICAL INTERPRETATION</b> .....	24
5.1	Methodology .....	24
5.2	Results .....	25
5.2.1	Magnetic Data.....	25
5.2.2	Gravity Data.....	26
5.2.3	Radiometric Data .....	27
5.2.4	Electromagnetic .....	28
5.3	Geophysical Results for Batholiths in the Schreiber Area.....	30
5.3.1	Whitesand Lake Batholith.....	30
5.3.2	Crossman Lake Batholith.....	31
5.3.3	Terrace Bay Batholith .....	33
5.3.4	Mount Gwynne Pluton .....	34
6.	<b>SUMMARY OF RESULTS</b> .....	35
7.	<b>REFERENCES</b> .....	38

## List of Figures (in order following text)

- Figure 1: Township of Schreiber and surrounding area
- Figure 2: Regional Tectonic Setting of Schreiber and Surrounding Area
- Figure 3: Local Bedrock Geology of the Schreiber Area
- Figure 4: Terrain Features of the Schreiber Area
- Figure 5: Magnetic and Electromagnetic Survey Flight lines in the Schreiber Area
- Figure 6: Very Low Frequency Electromagnetic and Radiometric Flight Lines in the Schreiber Area
- Figure 7: Reduced to Pole Residual Magnetic Field in the Schreiber Area
- Figure 8: First Vertical Derivative of Reduced to Pole Residual Magnetic Field in the Schreiber Area
- Figure 9: Second Vertical Derivative of Reduced to Pole Residual Magnetic Field in the Schreiber Area
- Figure 10: Tilt Angle of Reduced to Pole Magnetic Field in the Schreiber Area
- Figure 11: Analytical Signal of Residual Magnetic Field in the Schreiber Area
- Figure 12: Bouguer Gravity Field with Station Locations in the Schreiber Area
- Figure 13: Radiometric Ternary Image in the Schreiber Area
- Figure 14: Very Low Frequency Electromagnetic (VLF EM) Data in the Schreiber Area
- Figure 15: Apparent Resistivity from Low Frequency (877 Hz) Electromagnetic Data in the Schreiber Area
- Figure 16: Geophysical Interpretation Showing Distribution of Bedrock units for the Schreiber area

## List of Tables

Table 1: Summary of the characteristics for the geophysical data sources in the Schreiber area .....	14
Table 2: CGRF-2005 magnetic field characteristics for retrieved surveys .....	19
Table 3: Radiometric responses for gamma-ray spectrometry parameters within the Schreiber area .....	28
Table 4: Apparent Resistivity statistics for 877 Hz .....	30

## List of Abbreviations

1VD	First Vertical Derivative
AFRI	Assessment File Research Imaging
AGIC	Advanced Geophysical Inversion Centre
AS	Analytic Signal
BA	Bouguer Anomaly
BP	Years Before Present
CDED	Canadian Digital Elevation Data
CGDB	Canadian Gravity Anomaly Database
CGRF	Canadian Geomagnetic Reference Field model
DAP	Geosoft server technology for distributing data
EM	Electromagnetic
eU	Equivalent Uranium
eTh	Equivalent ThoriumFA                      Free Air
FDEM	Frequency Domain Electromagnetic
FFT	Fast Fourier Transform
Ga	Billions of Years
GDAL	Geospatial data abstraction library
GRS80	Geodetic Reference ellipsoid 1980
GSC	Geological Survey of Canada
Hz	SI unit cycles per second
ICSD	Ice-Contact Stratified Drift
IAG	International Association of Geodesy
K	Potassium
Ka	Thousands of Years
L	Litre - SI unit of volume
m	Metre - SI unit of length
masl	metre above sea level
Ma	Millions of Years
Mira	Mira Geoscience Ltd.
MNDM	Ontario's Ministry of Northern Development and Mines
n/a	not applicable
nGy/h	nano Grays per hour (SI derived unit of absorbed dose)
NAD83	North American Datum 1983
NRCan	Natural Resources of Canada
nT	Nanotesla - Magnetic Field Strength
NWMO	Nuclear Waste Management Organisation
OGS	Ontario Geological Survey
ppm	parts per million concentration
RMI	Residual Magnetic Intensity
RMF	Reduced Magnetic Field
RTP	Reduced to pole (magnetic data)
SRK	SRK Consulting (Canada) Inc.
TC	Terrain Correction (Gravity)
TMI	Total Magnetic Intensity
TMF	Total Magnetic Field
UTM	Universal Transverse Mercator projection
VLF-EM	Very Low Frequency Electromagnetic
3D	3-dimensional

## 1. INTRODUCTION

In December, 2011, the Township of Schreiber, Ontario expressed interest in continuing to learn more about the Nuclear Waste Management Organization nine-step site selection process (NWMO 2010), and requested that a preliminary assessment be conducted to assess potential suitability of the Schreiber area for safely hosting a deep geological repository (Step 3). This request followed the successful completion of an initial screening conducted during Step 2 of the site selection process.

The preliminary assessment is a multidisciplinary study integrating both technical and community well-being studies, including geoscientific suitability, engineering, transportation, environment and safety, as well as social, economic and cultural considerations. The findings of the overall preliminary assessment are reported in an integrated report (NWMO, 2013). The objective of the desktop geoscientific preliminary assessment is to determine whether the Township of Schreiber and its periphery, referred to as the “Schreiber area”, contains general areas that have the potential to meet NWMO’s geoscientific site evaluation factors.

This report presents the findings of a geophysical data processing and interpretation study completed as part of the desktop geoscientific preliminary assessment of the Schreiber area (AECOM, 2013a).

### 1.1 Study Objective

This report documents the geophysical data processing and interpretation investigation completed by Mira Geoscience Ltd. for the Schreiber area as part of the Phase 1 Geoscientific Desktop Preliminary Assessment of Potential Suitability (AECOM, 2013a). Geophysical data are an important source of information for assessing the potential suitability of a region to host a deep geological repository, and can assist in the identification of general areas that have the potential to meet NWMO’s geoscientific site evaluation factors.

The purpose of this study is to review the available geophysical data for the Schreiber area, followed by a detailed interpretation of all available geophysical data sets (e.g., magnetic, electromagnetic, gravity and radiometric). This interpretation is to identify additional information that can be extracted from the data and evaluates the coincidence of geophysical features with mapped lithology and structural features in the Schreiber area.

The role of the geophysical interpretation is to extrapolate our current understanding of the mapped lithology and extent of overburden cover to assess how the distribution of rock units may change at depth. Boreholes, wells and other underground information may be available at individual points to supplement geological data acquired on surface. However, where these individual data points are limited (or non-existent), as is the case in the Schreiber area, the critical advantage of airborne geophysical data is that it provides a basis for interpreting the subsurface physical properties across the area. This is particularly important in areas where bedrock exposure is limited by surface water bodies and/or overburden cover (i.e., glacial sediments), which is the case in parts of the Schreiber area. A secondary role of geophysics is that it often elucidates certain characteristics of geological formations and structures that are not

easily discerned from surface mapping and analysis. Thirdly, it highlights tectonic and regional-scale features that may not be easily extracted from studies of a particular area on a more detailed scale.

## 1.2 Schreiber Area

The Township of Schreiber, located along the north shore of Lake Superior approximately 150 km east of Thunder Bay (~200 km by road), encompasses roughly 40 km<sup>2</sup> and is bounded to the east by the Township of Terrace Bay. The Township of Schreiber and its periphery, referred to as the “Schreiber area”, is approximately 1100 km<sup>2</sup> in size (Figure 1).

## 1.3 Qualifications of the Geophysical Interpretation Team

The team responsible for the geophysical review, processing and interpretation investigation component of the Phase 1 Geoscientific Desktop Preliminary Assessment for the Schreiber area consisted of qualified experts from Mira Geoscience Limited (Mira). The personnel assigned to this study were as follows:

**Thomas Campagne, M.Sc. Geophysics** – data processing, geophysical interpretation, report preparation, map preparation

Mr. Campagne is a consultant with the Advanced Geophysical Interpretation Centre (AGIC) at Mira Geoscience. Thomas has a Bachelor degree in Geosciences from the University of Strasbourg, France, and a Master/Engineering degree in Geophysics from the School of Engineering Geophysics within the Department of Earth Sciences of the University of Strasbourg, France. Thomas has worked as an undergrad geophysicist for Southern Geoscience Consultants in Perth, Australia, and as a project geophysicist for S.J.V. Consultants in Delta, Canada, prior to joining Mira Geoscience in May 2011. Thomas brings strong international experience, with specialization in geophysical modelling and inversions, focused on constrained inversions of potential field, electrical, and EM methods. He is part of a team of consultants whose experience ranges from modelling and interpretation of airborne gravity and magnetic data for large scale basin modelling studies, to integrated deposit targeting based on electrical, MT, and magnetic modelling, to environmental and geotechnical applications. Thomas is fluent in spoken and written French and English.

**Nigel Philips, M.Sc. Geophysics** – project management

Mr. Philips is a Senior Geophysicist and Manager of the Advanced Geophysical Interpretation Centre (AGIC) at Mira Geoscience in Vancouver, Canada. Nigel is focused on advancing the effectiveness of geophysics by specializing in the advanced processing and modelling of geophysical data to produce integrated solutions. He has over 15 years of experience in mineral exploration and has worked in many different exploration environments, his background ranges from field safety, acquisition, and logistics, to the development of data processing, modelling techniques, and software, to the communication of concepts and results through reports, publications, talks, and training. At AGIC, Nigel manages a group of highly skilled geophysicists providing specialized geophysical solutions to the mining industry.



**Peter Kowalczyk, P.Geo.** – report preparation

Mr. Kowalczyk is a Principal Consultant in Exploration Geophysics. Peter joined Mira Geoscience from Barrick Gold. Prior to Barrick purchasing Placer Dome, Peter was chief geophysicist for Placer Dome Inc. He joined Placer Dome in 1970 and has worked in porphyry copper, uranium, base metal and gold exploration. Peter coordinated Placer's geophysical research and was deeply involved in the introduction and implementation of digital processing, visualization and geophysical inversion methods in exploration at Placer. As chief geophysicist Peter worked with exploration, mine operations, academic research and government groups world-wide. Although an exploration generalist, he has particular experience in the processing and interpretation of electrical data. Peter graduated from UBC with a B.Sc. (geophysics) and is a registered geophysicist in British Columbia. He is currently associated with Ocean Floor Geophysics Inc. and Geoscience British Columbia.

## **2. SUMMARY OF PHYSICAL GEOGRAPHY AND GEOLOGY**

The Schreiber area is primarily located in the Archean Wawa Subprovince, Superior Province (Figure 2). The Wawa Subprovince comprises a volcano-sedimentary-plutonic terrane bounded to the east by the Kapuskasing structural zone (beyond the area of investigation) and to the north by the metasedimentary-dominated Quetico Subprovince. The western end of the Wawa Subprovince is bordered by the Proterozoic Trans-Hudson orogen. To the south, the Schreiber area is flanked by the Early Proterozoic Southern Province. A map sheet discontinuity is present in Figure 2 as an artificial break in the dyke traces indicated by the Marathon mafic dykes terminating through the Quetico Subprovince.

The Wawa Subprovince is composed of two semi-linear zones of greenstone belts, the northern of which includes the Shebandowan, Schreiber-Hemlo, Manitouwadge-Hornepayne, White River, Dayohessarah, and Kabinakagami greenstone belts (a portion of which is shown on Figure 2). The Schreiber area is situated in the western portion of the Schreiber-Hemlo greenstone belt (sometimes referred to as the Terrace Bay-Schreiber greenstone belt). This greenstone belt is divided into western and eastern portions by the Proterozoic Coldwell alkalic complex. The Schreiber-Hemlo greenstone belt consists of a number of narrow, arcuate segments of supracrustal rocks that are bounded and enclosed by granitoid bodies, including the Crossman and Whitesand Lake batholiths. The Schreiber-Hemlo greenstone belt is divided into three lithotectonic assemblages by Williams et al. (1991); the Schreiber, Hemlo-Black River, and Heron Bay assemblages. The Schreiber and Hemlo-Black River assemblages are separated by the Proterozoic Coldwell alkalic complex (north of the town of Marathon). The Hemlo-Black River and Heron Bay assemblages are located to the north and south of the Lake Superior Hemlo fault zone (LSHFZ; Figure 2), respectively.

### **2.1 Physical Geography**

Physical Geography of the Schreiber area is described in detail in AECOM (2013a,b). A summary of the main features is provided here for reference.

The elevation difference within the Schreiber area is significant with a maximum range of approximately 402 metres. The highest relief occurs just north of the Township of Schreiber,

where land elevation is approximately 585 metres above sea level (masl). The lowest point equals the elevation of Lake Superior, approximately 183 masl.

The Schreiber area is characterized by predominantly moderate to high relief over short distances, and rugged topography consisting of knobby bedrock hills and steep escarpments. The orientation of escarpments is parallel to the trend of major faults and lineaments which transect the area. Local areas of low relief (<20 m) occur between the Townships of Terrace Bay and Schreiber, and along the Aguasabon River system.

Across the Schreiber area, the elevation of hills and ridges is commonly between 400 and 500 metres. There is, however, a general southward decrease in the elevation of hill tops from the 400 to 500 metres range in the north to 300 to 400 metres range in the south. Lower elevations are encountered along the Aguasabon River in the east and in the vicinity of Whitesand and Lyne lakes in the southwest. A region of lower elevation, approximately 300 masl, characterizes the southeastern corner of the Schreiber area, around Hays Lake and the mouth of the Aguasabon River.

The Schreiber area is within the Little Pic tertiary watershed, which drains via the Great Lakes water system and the St. Lawrence River, and can be sub-divided into four watersheds at the quaternary scale. The Pays Plat River watershed is located in the northwestern part of the Schreiber area and enters into Lake Superior through the Pays Plat First Nation Reserve 51, 6 kilometres west of Rosspoint. The Whitesand River watershed is located immediately to the east and enters Lake Superior near Selim, approximately 8 kilometres west of Schreiber. The central portion of the Schreiber area is drained by the Big Duck Creek watershed, which drains into the Aguasabon River watershed at Hays Lake. The Aguasabon River watershed drains the eastern portion of the Schreiber area and enters Lake Superior near Terrace Bay.

The orientation of the drainage network within the Schreiber area is largely controlled by bedrock structural features and the irregular surface of the topography. Due to this control, the majority of waterways, including lakes, have a north, northwestward or northeastward orientation. While the overall drainage in the area is southward, the catchment areas of individual lakes within the watersheds results in short segments of northward flow.

The larger rivers draining the watersheds noted above are fed by numerous smaller creeks and rivers that effectively drain the vast majority of the Schreiber area. Creeks are lacking only in the region underlain by a notable thicknesses of glaciolacustrine and glaciofluvial deposits in the area surrounding Terrace Bay where drainage is through groundwater recharge. Typically, segments of the area's waterways are short, on the order of less than 2 kilometres, as they flow into and out of lakes occurring along the drainage paths.

Lakes within the Schreiber area are numerous and occur with an even distribution covering approximately 7.6% of the land surface (i.e., excluding Lake Superior). These lakes, many of which are elongate in shape, are generally small with only six lakes having a surface area of greater than 2 km<sup>2</sup>.

## 2.2 Bedrock Geology

The bedrock geology of the Schreiber area is shown in Figure 3. The main geological units in the Schreiber area include, several large granitoid intrusions (Terrace Bay, Crossman Lake and Whitesand Lake batholiths, and the Mount Gwynne pluton), the supracrustal rocks of the Schreiber assemblage of the Schreiber-Hemlo greenstone belt, and the several suites or swarms of mafic diabase dykes. Each of these sets of rock units is discussed in more detail below. In addition, the bedrock in the Schreiber area is overprinted by several orientations of brittle faults and the individual rock units have been subjected to varying amounts of metamorphism.

### 2.2.1 Granitoid Intrusive Rocks

Massive granite to granodiorite intrusions comprise a voluminous suite of rocks within and adjacent to the Schreiber-Hemlo greenstone belt (Figure 3). These are typically composite, ovoid intrusions that vary in size up to twenty-five kilometres in diameter. Their composite nature includes lithologies ranging from dominantly granite and granodiorite to quartz diorite, syenite and quartz monzonite (and their gneissic equivalents), as well as aplite and pegmatite dykes. These intrusions likely formed by partial melting of mafic to ultramafic sources (e.g., Polat, 1998).

Granitoid intrusions in the Hemlo assemblage of the Schreiber-Hemlo greenstone belt returned ages between ca. 2.688 and 2.678 billion years (Ga) (Corfu and Muir 1989). Due to the similar character and emplacement style of granitoid intrusions in the Schreiber area compared to the Hemlo area, and an absence of more precise age dating, the granitoid intrusions in the Schreiber area are also considered to be emplaced between ca. 2.690 and 2.680 Ga (Smyk and Schnieders, 1995; Corfu and Muir, 1989).

The granitoid intrusions in the Schreiber area include the Terrace Bay, Crossman Lake and Whitesand Lake batholiths, and the Mount Gwynne pluton (Figure 3). These intrusions cover approximately 495 km<sup>2</sup> within the Schreiber area. The emplacement of these batholiths overlapped with regional metamorphism dated at ca. 2.688 to 2.675 Ga (Muir, 2003) and resulted in the development of amphibolite grade contact aureoles within the surrounding greenschist grade greenstone belt rocks (Marmont, 1984).

The Terrace Bay batholith is located in the southeastern part of the Schreiber area (Figure 3) and trends northeast, at an angle to the generally east-trending greenstone belt rocks. The bulk of the Terrace Bay batholith is a massive, homogeneous, equigranular and medium-grained granodiorite with common variations in texture, grain size and colour, with minor masses of quartz monzodiorite and quartz-monzonite (Marmont, 1984; Carter, 1988). Apophyses and dykes derived from the Terrace Bay batholith intrude the greenstone belt rocks (discussed in Section 2.2.2) within the vicinity of the batholith contact. These minor phases include: 1) aplite and pegmatite dykes; 2) quartz-feldspar, feldspar and hornblende porphyries; 3) carbonate-rich lamprophyre dykes; and 4) narrow, magnetic diabase dykes. The Terrace Bay batholith covers 67 km<sup>2</sup> within the Schreiber area.

The Crossman Lake batholith occupies the majority of the northern part of the Schreiber area (Figure 3). The batholith is predominantly massive and consists of a mixture of medium-grained quartz-monzonite and monzodiorite, (alkali-feldspar) granite, tonalite and granodiorite. Minor dykes and irregular masses of microgranite, quartz (-feldspar) porphyry and aplite occur along

the margins of the batholith. The Crossman Lake batholith covers 300 km<sup>2</sup> within the Schreiber area.

The Whitesand Lake batholith occurs in the southwestern portion of the Schreiber area (Figure 3). This batholith is elongate in an east-west direction parallel to the structural trend within the surrounding greenstone belt rocks. The batholith consists of mostly massive (alkali-feldspar) granite with lesser porphyritic granite, monzodiorite, quartz monzonite and rare aplite. The Whitesand Lake batholith covers 123 km<sup>2</sup> within the Schreiber area.

The boundary between the Whitesand Lake and Crossman Lake batholiths is poorly defined. However, Carter (1988) places the boundary between the two batholiths along narrow band of east-trending supracrustal rocks along the western margin of the Schreiber area (Figure 3).

The Mount Gwynne pluton is located near the southern margin of the Schreiber area (Figure 3). It is located along the southern boundary of the supracrustal rocks of the Schreiber-Hemlo greenstone belt. The pluton comprises massive, medium-grained alkali-feldspar granite and biotite-hornblende granodiorite. The Mount Gwynne pluton covers 5 km<sup>2</sup> within the Schreiber area.

### **2.2.2 Schreiber-Hemlo Greenstone Belt**

Supracrustal rocks in the Schreiber area occur in the western part of the Schreiber-Hemlo greenstone belt and are considered to be part of the Schreiber assemblage (Williams et al., 1991; Figure 3). Carter (1988) identified three major types of supracrustal rocks in the Schreiber assemblage: 1) tholeiitic, mafic metavolcanic rocks comprising mainly massive to pillow basalt, tuff and related breccias; 2) calc-alkalic, mafic to felsic metavolcanic rocks dominated by pyroclastic units; and 3) clastic metasedimentary rocks of turbiditic origin interbedded with minor banded iron formation. These three supracrustal rock types are described in further detail below.

Tholeiitic, mafic metavolcanic rocks are massive or schistose and variably metamorphosed ranging from dominantly greenschist facies to amphibolite facies and locally pyroxene hornfels facies. Greenschist facies mafic volcanic rocks are either massive or foliated and are aphanitic to medium-grained, whereas amphibolite facies mafic volcanic rocks are medium-grained and well foliated (Carter, 1988). The greenschist facies tholeiitic rocks comprise aphanitic, fine-grained massive and pillowed flows, as well as porphyritic, amygdaloidal and variolitic flows. Interbedded with these flows are minor autoclastic flow breccias and mafic to intermediate tuff horizons. The amphibolite facies tholeiitic rocks include fine- to medium-grained foliated amphibolite and garnet amphibolite. The minimum age of mafic volcanism is constrained by crosscutting pluton apophyses in the eastern half of the Schreiber-Hemlo greenstone belt at ca. 2.697 Ga (Muir, 2003).

Calc-alkalic mafic to felsic metavolcanic rocks are mainly greenschist facies massive, aphanitic to fine-grained andesite to porphyritic dacite flows. Minor amygdaloidal felsic interbeds occur with the massive flows. In addition, fine-grained to aphanitic tuff units with rare lapilli tuff and tuff breccia are interlayered with the mafic to felsic flows. Muir (2003) indicated that felsic calc-alkalic volcanism occurred from ca. 2.698 to 2.692 Ga, and intermediate volcanism occurred around 2.689 Ga in the eastern half of the Schreiber-Hemlo greenstone belt. This is compatible

with U-Pb zircon age determinations for calc-alkaline volcanism that are generally within a narrow range between 2.698 and 2.688 Ga (Corfu and Muir, 1989).

Metasedimentary rocks are composed of greenschist facies wacke, silicified shale (including graphitic intervals), chert horizons and banded iron formation as well as minor amphibolite facies garnet- and sillimanite-bearing wacke. The wacke comprises foliated, fine- to medium-grained quartz-plagioclase-biotite rocks with minor epidote, apatite, muscovite and pyrite. Banded iron formations form thinly bedded units interlayered with the metavolcanic rocks comprising magnetite-chert or magnetite-only (oxide-facies) and pyrite-pyrrhotite-chert (sulphide-facies) horizons. Sedimentation of turbiditic wacke-mudstone in the Schreiber-Hemlo greenstone belt occurred after ca. 2.693 Ga for volcanoclastic deposits and possibly as late as ca. 2.685 Ga for wacke (Muir, 2003).

Rocks of the Quetico Subprovince consisting of metamorphosed turbiditic wacke with subordinate arenite-pegmatite migmatite and feldspar gneiss occupy the northern fringe of the Schreiber area (Carter, 1988). Deposition of these sedimentary rocks took place between 2.70 to 2.69 Ga, and amphibolite facies metamorphism occurred during the period 2.67 to 2.65 Ga (Williams et al., 1991).

Along the shore of Lake Superior in the Schreiber area, Mesoproterozoic sedimentary rocks of the ca. 2.200 Ga Animikie Group (Gunflint Formation, 24 in legend of Figure 3; Carter, 1988), the ca. 1.500 Ga Sibley and ca. 1.100 Ga Osler groups unconformably overlie Archean granitic and mafic metavolcanic rocks. These form discontinuous erosional remnants of an ancient fluvial-lacustrine system that comprises interbedded sandstone, conglomerate, ironstone, chert, shale, mudstone and limestone. These rocks are not metamorphosed and dip gently from 10 to 15 degrees to the southwest.

### 2.2.3 Mafic Dykes

Several suites of diabase dykes crosscut the Schreiber area (Figures 2 and 3), including:

- Northwest-trending Matachewan Suite dykes (ca. 2.473 Ga; Buchan and Ernst, 2004). This dyke swarm is one of the largest in the Canadian Shield. Individual dykes are generally up to 10 metres wide, and have vertical to subvertical dips. The Matachewan dykes comprise mainly quartz diabase dominated by plagioclase, augite and quartz (Osmani, 1991).
- North-trending Marathon Suite dykes (ca. 2.121 Ga; Buchan et al. (1996). These form a fan-shaped distribution pattern around the northern, eastern and western flanks of Lake Superior. The dykes vary in orientation from northwest to northeast, and occur as steep to subvertical sheets, typically a few metres to tens of metres thick, but occasionally up to 75 metres thick (Hamilton et al., 2002). The Marathon dykes comprise quartz tholeiite dominated by equigranular to subophitic clinopyroxene and plagioclase.); and
- East-west-trending, reversely polarized Keweenaw Suite dykes related to ca. 1.100 Ga mid-continental rifting that was centred on proto-Lake Superior (Thurston, 1991).

Potentially, a western extension of the ca. 2.167 Ga Biscotasing dyke swarm also occurs in the Schreiber area (Hamilton et al., 2002). These generally trend northeast; however, how these may be distinguished from northeast-trending Marathon dykes in the Schreiber area is undefined.

#### **2.2.4 Faults**

In the Schreiber area, several faults are indicated on public domain geological maps. These include the major (from west to east) Sox Creek, Ross Lake, and Cook Lake southeast-trending faults (Figure 3). Several northeast-trending faults are indicated on public domain maps including the Schreiber Point fault, the Worthington Bay fault (with the Syenite Lake fault along its extension), and the Ellis Lake fault. The timing and kinematics of these faults are not described in the literature.

Carter (1988) conducted a field mapping program and developed a geological map for the Schreiber area, primarily on the basis of 1:15,840 scale aerial photographs and north-south trending traverse mapping at roughly quarter mile intervals. As a result of this mapping program, Carter (1988) attempted an interpretation of the fault movement along some of the faults shown on public domain geological maps. No supporting structural information was included in Carter (1988), so it is assumed that the fault movement interpretation was derived from aerial photographs. Carter's (1988) interpretation is only included here for historical reference. Carter (1988) interpreted the Sox Lake fault and the Schreiber Point fault as dextral strike-slip faults; the Cook Lake fault and Syenite Lake fault as dip-slip faults; and the Worthington Bay fault as a sinistral strike-slip fault.

### **2.3 Structural Geology**

For the purpose of this report, a summary of structural geology for the Schreiber area was provided by AECOM and SRK Consulting and is outlined below.

Direct information on the geological and structural history of the Schreiber area is limited. The geological and structural history summarized below integrates the results from studies undertaken elsewhere throughout and proximal to the regional area shown in Figure 2, including structural investigations on the Hemlo gold deposit and surrounding region (i.e., the eastern portion of the Schreiber-Hemlo greenstone belt). It is understood that there are potential problems in applying a regional  $D_x$  numbering system into a local geological history. Nonetheless, the summary below represents an initial preliminary interpretation for the Schreiber area, which may be modified after site-specific information has been collected, if the community is selected by the NWMO and remains interested in continuing with the site selection process.

Regional studies revealed that the region has undergone complicated polyphase deformation but do not clarify the relationship between various structures and their significance for the regional tectonic evolution (Polat et al., 1998). Since the various structural studies were carried out on various scales and from different perspectives, disparate structural models and associated terminologies have developed for the Schreiber-Hemlo greenstone belt. In addition, because more than one generation of structures may develop in a single episode of progressive deformation, correlating the different structural studies is a challenge.

The most comprehensive structural study of the Schreiber-Hemlo greenstone belt was conducted by Muir (2003). Since no previous detailed structural studies have been undertaken in the Schreiber area, Muir's (2003) findings on the structural history are included in the summary below, and may be used as a "best-fit" for the structural history of the Schreiber area. The summary below integrates findings from Muir (2003) with information based on Carter (1988), Polat et al. (1998), Jackson (1998), Polat and Kerrich (1999) and Davis and Lin (2003).

Polat et al. (1998) interpreted that the Schreiber-Hemlo and surrounding greenstone belts represent collages of oceanic plateaus, oceanic arcs, and subduction-accretion complexes amalgamated through subsequent episodes of compressional and transpressional collision. On the basis of overprinting relationships between different structures, Polat et al. (1998) suggested that the Schreiber-Hemlo greenstone belt underwent at least two main episodes of deformation. These can both be correlated with observations from Muir (2003), who reported at least six generations of structural elements. Muir (2003) is therefore considered the better study to be used as a "best-fit" for the Schreiber area. Two of the six generations of structures account for most of the ductile strain, and although others can be distinguished on the basis of crosscutting relationships, they are likely the products of progressive strain events. The main characteristics of these deformation phases are described below.

The earliest deformation phase ( $D_1$ ) is associated with the development of  $S_1$  slaty cleavage and asymmetric boudins in metasedimentary rocks, and asymmetric boudins, mesoscopic closed to isoclinal (overturned)  $F_1$  folds and associated  $D_1$  thrust faults in the metavolcanic rocks. Muir (2003) included the development of  $S_1$  compositional layering as part of this deformation event. The orientation of  $F_1$  folds was modified during subsequent deformation; however, the regionally consistent asymmetry of the  $F_1$  overturned folds, combined with S-C fabrics along ductile  $D_1$  thrust faults, suggests a south-southeast tectonic vergence. Muir (2003) suggested that  $D_1$  likely occurred from ca. 2.719 to ca. 2.691 Ga.

$D_2$  deformation structures ( $D_1$  in Jackson, 1998) are ubiquitous in the Schreiber-Hemlo greenstone belt and include dominantly east-northeast trending overturned tight to isoclinal  $F_2$  folds,  $D_2$  thrust faults, and northeast- to east-trending  $D_2$  strike-slip faults (collectively forming  $D_2$  fold and thrust duplexes) that overprint or fold  $D_1$  structural elements. During  $D_2$  deformation, the dominantly steeply northward dipping  $S_2$  foliation was developed. The  $S_2$  foliation is characterized by a preferred alignment of phyllosilicate and mafic minerals and flattening and (or) elongation of clasts (Davis and Lin, 2003; Muir, 2003). Several kilometre-scale  $F_2$  folds, with dominant S-shaped asymmetry developed during  $D_2$  deformation (Muir, 2003). Whereas Polat et al. (1998) interpreted that  $D_2$  developed during dextral transpression, Lin (2001) interpreted  $D_2$  deformation as an episode of sinistral transpression based on local observations from the Hemlo shear zone. Muir (2003) suggested that  $D_2$  likely initiated at ca. 2.691 Ga and continued until ca. 2.683 Ga.

Lin (2001) further distinguished open to tight folds with a well-developed axial planar cleavage associated with north over south compression with a dextral strike-slip component. It is not clear whether these structures represent a separate deformation event. If  $D_2$  deformation represents a stage of dextral transpression, as interpreted by Polat et al. (1998), these structures can be interpreted to result from the prolongation of  $D_2$  deformation. However, if  $D_2$  represents a stage

of sinistral transpression, it follows that these structures must be related to a separate D<sub>3</sub> deformation phase.

Based on observations in the vicinity of the Hemlo gold deposit, Muir (2003) distinguished a variably developed S<sub>3</sub> mineral and (or) crenulation foliation associated with F<sub>3</sub> folds, which overprint D<sub>2</sub> structural elements. Muir (2003) noted that these features are particularly well-developed within schistose units. Local D<sub>3</sub> S-C shear fabrics and extensional shear bands record a dextral sense of shear, which conforms to their development during dextral transpression as interpreted by Lin (2001). Muir (2003) interpreted that a period of near peak metamorphic temperatures overlapped with the D<sub>2</sub>-D<sub>3</sub> transition from ca. 2.688 to ca. 2.675 Ga.

Again, founded on observations in the vicinity of the Hemlo gold deposit, Lin (2001) and Muir (2003) recognized D<sub>4</sub> structural elements, including F<sub>4</sub> kink folds and various sets of D<sub>4</sub> fractures and small-scale faults. Muir (2003) interpreted that the orientation of conjugate sets of D<sub>4</sub> contractional kink bands is consistent with their development during northwest- to west-northwest-directed shortening. Northwest-directed D<sub>3</sub>-D<sub>4</sub> shortening is estimated to have occurred from ca. 2.682 to ca. 2.679 Ga (Muir, 2003).

Based on this summary, it may be surmised that a protracted period of brittle-ductile deformation spanning D<sub>1</sub> to D<sub>4</sub> comprising elements of compression and sinistral and dextral transpression occurred between ca. 2.719 and ca. 2.679 Ga. It should be noted that this age range partly overlaps with the inferred ages for granitoid intrusions (ca. 2.690 to ca. 2.680 Ga) which suggests that these intrusions may have been affected by D<sub>2</sub>-D<sub>4</sub> deformation.

Lin (2001) highlighted the presence of post-D<sub>4</sub> brittle faults at various scales and with various orientations in the Schreiber-Hemlo greenstone belt. One set of post-D<sub>4</sub> brittle faults is parallel to the S<sub>2</sub> foliation, contains cataclasite, fault breccia and local pseudotachylite and commonly offsets Proterozoic diabase dykes. Another post-D<sub>4</sub> brittle fault set strikes southeast and displays a consistent dextral sense of shear. Other than that these faults post-date the intrusion of Proterozoic diabase dykes, no estimates for the timing of this post-D<sub>4</sub> brittle deformation are present in literature. Peterman and Day (1989) recorded reactivation of the Late Archean Quetico and Rainy Lake-Seine River faults at ca. 1.943 Ga in the Rainy Lake region of Minnesota and Ontario. It is possible that at least one stage of D<sub>4</sub> faulting occurred during this regional tectonic event, which coincides with the ca. 2.100 to 1.860 Ga Penokean Orogen.

## 2.4 Quaternary Geology

For the purpose of this report, a summary of Quaternary geology for the Schreiber area was provided by AECOM (2013b) as outlined below.

The Schreiber area is within the Abitibi Uplands physiographic region of Thurston (1991) who subdivided the extensive James Region physiographic region of Bostock (1970). The region is characterized by abundant bedrock outcrop with shallow drift cover and a rugged surface.

The Quaternary sediments, commonly referred to as drift, soil or overburden, are glacial and post-glacial materials which overlie the bedrock in the Schreiber area. The distribution, thickness and physical characteristics of these deposits have an important influence on several aspects of the current investigation. Areas of thicker drift can hinder the interpretation of



lineaments by masking their presence or muting the response obtained from geophysical surveys. Coarser-grained surficial sediments typically have a moderate to high transmissivity and can serve as local aquifers as well as being a potential source of mineral aggregates for use in building and road construction.

All glacial landforms and related materials within the Schreiber area are associated with the Wisconsinan glaciation which began approximately 115 Ka before present (BP) (Barnett, 1992). The Quaternary (i.e., surficial) geology of the Schreiber area has been mapped at a regional scale (>1:100,000) by several authors, including Zoltai (1965), Sado and Carswell (1987), and Barnett et al. (1991) and at a higher resolution by Gartner (1979a, 1979b) and Morris (2000, 2001). Quaternary deposits and landforms in the area are thought to have formed during the latter stages of ice cover (i.e., during the Late Wisconsinan, which began 30 Ka BP).

Morris (2000) reports bedrock erosional features (e.g., striae, roche moutonnée) and landforms that indicate a regional ice flow direction of 194° with a range of measured directions, due to local topographic conditions, of between 165° to 238°. For the majority of the Schreiber area drift thickness over bedrock is limited and the ground surface reflects the bedrock topography. Over the majority of the area bedrock outcrops are common and the terrain is classified, for surficial purposes, as a bedrock-drift complex; i.e., thin drift cover that only locally achieves thicknesses that mask or subdue the bedrock topography.

The remote sensing and terrain evaluation completed as part of the Phase 1 study provides the most detailed assessment of the type, distribution and thickness of surficial deposits in the Schreiber area (AECOM, 2013b; Figure 4). The most common glacial deposit in the Schreiber area is a thin, discontinuous till, generally less than two to three metres thick. Greater accumulations of till are found within bedrock depressions, large scale lineaments and on the down-ice (lee) side of bedrock highs. The till has a silty-sand matrix and contains abundant clasts in the pebble to cobble size range.

Two types of glaciofluvial deposits are present in the Schreiber area: ice-contact stratified drift deposits (ICSD) and outwash deposits. The ICSDs are associated with recessional moraines, dead-ice topography, eskers and valley fills (Morris, 2000). The largest ice-contact deposit forms the core of a 9 kilometre long feature situated between Terrace Bay and Schreiber, south of Hays Lake. The ICSDs consist primarily of stratified, well to poorly sorted, sand and gravel that locally can achieve thicknesses of several tens of metres.

Glaciofluvial outwash deposits occur as relatively level areas within some narrow, bedrock controlled valleys (Figures 3). While valley controlled outwash deposits are found within the Schreiber area, significant deposits are also located along the Aguasabon, Whitesand and Pays Plat rivers, and Big Creek (which drains Clean and Deep lakes) and its tributaries. The thicknesses of these deposits are likely to be variable, and may be locally substantial. Outwash deposits are generally well-sorted and comprised of stratified sand, gravel and, locally, boulders.

Following retreat of the glacial ice approximately 9.5 Ka BP, the Lake Superior basin was occupied by a series of glacial lakes. It is likely that only the later of these lakes, Glacial Lake Minong and younger, affected the Schreiber area (Farrand and Drexler 1985; Barnett 1992). Lake inundation was limited to the area along the Lake Superior shoreline, to an elevation of

~305 m, and for a short distance inland within bedrock controlled valleys. Elevations of the various glacial lakes were controlled by the position of the ice mass and isostatic recovery of the land surface following deglaciation.

Fine-grained glaciolacustrine silts and clay deposits associated with the glacial lake have been encountered at depth in boreholes in the Terrace Bay area and other embayments further west along the Lake Superior shoreline (Gartner, 1979a). Overlaying these deposits are coarse-grained glaciolacustrine sediments that were deposited in a deltaic environment where bedrock valleys served as drainage channels discharging to the glacial lake. The largest glaciolacustrine delta is located in the Terrace Bay area where a sediment thickness of 48.3 m has been recorded. Another notable but smaller deltaic feature is found at Selim, at the mouth of the Whitesand River (Figure 4).

Bogs and organic-rich alluvial deposits are present along water courses in the area and in rock floored basins. These deposits tend to have a limited thickness, as determined by regional studies, and areal extent.

In summary, the extent and thickness of surficial deposits in the Schreiber area is limited, and does not significantly influence the geophysics interpretation.

## **2.5 Land Use**

Land use in the Schreiber area is described in detail in AECOM (2013b). The vast majority of the Schreiber area is undeveloped Crown Land with residences almost exclusively within the build-up areas of Terrace Bay and Schreiber or in close proximity to the Highway 17, the Trans Canada Highway. Infrastructure to support the population, in the form of roads, power and rail lines, etc., is largely concentrated within 5 kilometres of the Lake Superior shore. Mineral exploration is active in the area and numerous active mining claims are held by prospectors and mining companies (Campbell et al., 2012; MNDM, 2012). The bulk of the claims are located over the two arms of the Schreiber-Hemlo greenstone belt and the immediate surrounding land. A number of aggregate operations are extracting sand and gravel in the area (MNR, 2012). The majority of the pits are located close to the Trans Canada Highway in the vicinity of Terrace Bay and Schreiber. A small number of pits are located near Selim.

In general, these features do not negatively impact the geophysics interpretation, with the exception of power lines in settlement areas which were taken into account for the Very Low Frequency Electromagnetic data interpretations.

## **3. GEOPHYSICAL DATA SOURCES AND QUALITY**

For the Schreiber area, geophysical data were obtained from available public-domain sources, particularly the Ontario Geological Survey (OGS) and the Geological Survey of Canada (GSC). To supplement these data, geophysical surveys performed in the Schreiber area by the mining industry were reviewed as assessment files, but no original digital data sources were obtained since it was determined that they would not contribute additionally to the geophysical interpretation over the Schreiber area.

The quality of the available data was assessed to determine which data sets are suitable for inclusion in this study. The geophysical surveys covering the Schreiber area show variability in data set resolution, which is a function of the flight line spacing, the sensor height and equipment sensitivity. In particular, where more than one data set overlaps, the available data were assembled using the highest quality coverage. Various geophysical data processing techniques were applied to enhance components of the data most applicable to the current study. The resolution of the higher quality data was maintained throughout the applied processing.

### **3.1 Data Sources**

Low-resolution geophysical data, particularly the magnetic, gravity, very low frequency electromagnetic (VLF-EM) and radiometric data obtained from the Geological Survey of Canada (GSC), cover most of the Schreiber area with the exception of some small areas covered by Lake Superior in the south of the Schreiber area. An Ontario Geological Survey (OGS) magnetic and frequency domain electromagnetic (FDEM) survey provides higher resolution coverage over approximately 75% of the Schreiber area, with the exception of a north-south trending band along the western boundary of the Schreiber area and an east-west trending band south of the Lake Superior shoreline along the southern boundary of the Schreiber area (Figure 5 and Figure 6). The OGS survey focuses primarily on the greenstone belts, but also encompasses plutonic rocks in the center, southern and western portions of the Schreiber area, particularly the Crossman Lake, Whitesand Lake, and Terrace Bay batholiths, and the Mount Gwynne pluton.

The OGS survey data were downloaded via the Ontario Geophysical (OGS, 2012) and OGS Earth applications, with this data being supplemented by a published DVD that contained flight line profile data. The GSC geophysical data utilized in this study were downloaded from the GSC's Geoscience Data Repository for Geophysical and Geochemical Data. The details of the geophysical data sets pertinent to the Schreiber area are summarized in Table 1.

**Table 1: Summary of the characteristics for the geophysical data sources in the Schreiber area**

Product	Source	Type	Line Spacing/ Sensor Height	Flight line Azimuth	Coverage	Date	Additional Comments
Coldwell, Hemlo, Schreiber (GSC2516)	GSC	Fixed Wing - Magnetic, VLF-EM, Radiometric data	1000m/120m	0°	Eastern third of Schreiber area without reaching south or north boundaries	1990	Quality control and initial processing applied by GSC.
Georgia Lake	GSC	Fixed Wing - Magnetic, VLF-EM, Radiometric data	1000m/120m	0°	One survey line covers the northwest corner of Schreiber area	1989	Quality control and initial processing applied by GSC.
North Shore Lake Superior (West)	GSC	Fixed Wing – Radiometric data	5000m/120m	0°	Almost the entire Schreiber area but stops at Lake Superior	1982	Quality control and initial processing applied by GSC.
Schreiber (GSC2514)	GSC	Fixed Wing - Magnetic, VLF-EM, Radiometric data	1000m/120m	0°	Entire Schreiber area but stops at Lake Superior. Denser survey lines in north central half of Schreiber area.	1990-1991	Covers entire Schreiber area but stops at Great Lake shoreline in the south. Denser survey lines in north central half of Schreiber area.
Superior, Lake	GSC	Fixed Wing – Magnetic data	1900m/300m	0°	Southern third of Schreiber area	1987	Flown at a higher elevation and with a low spatial resolution
Airborne Magnetic Compilation (Ontario #8)	GSC	Fixed Wing Magnetic data	805m/305m	0°	Entire Schreiber area	1962	Reduced and levelled to common datum magnetic data. August 2010 revision.
Ground Gravity (CGDB, SEP 2010)	GSC	Ground Gravity Measurements	5-15km	n/a	Thirteen stations sparsely located over entire Schreiber area.	1944-1962	Despite a good data quality at stations the sparse coverage of the Schreiber area makes the 2 km grid of low utility
Schreiber Area (GDS1104)	OGS	Heliborne - Magnetic, FDEM	200m/ MAG 30/45m FDEM–30m	0°	Central, north central, east central and northeast corner of Schreiber area	1999	Quality control applied by OGS. This recent high resolution survey flown at low altitude makes it the most reliable data set for the Schreiber study. Magnetics flown in vertical gradient configuration (upper and lower sensors)

Assessment files held in the AFRI database archived at the OGS were reviewed for the Schreiber area. There were ten airborne and thirteen ground geophysical surveys that focus on areas within the greenstone belts or on areas encompassing greenstone belts and plutonic rocks examined. Digital data from the assessment files were not available for public download from the AFRI database, and only poor quality scanned maps linked to the assessment reports were available. As airborne geophysical survey data were not available, despite repeated attempts to obtain them, and ground surveys focused on relatively small areas, AFRI assessment reports were not used in this geophysical interpretation.

### 3.1.1 Magnetic Data

Magnetic data were collected by various surveys (five fixed-wing and one helicopter based) using different equipment and survey parameters outlined in Table 1. Magnetic data assist in the understanding of geological and structural variations because different rock types differ in their content of magnetic minerals, such as magnetite and pyrrhotite, to which magnetometers are sensitive. Magnetic maps help to identify the distribution of magnetic and nonmagnetic geological bodies within the subsurface, and are particularly useful for delineating spatial geometry of bodies of rock, and the presence of faults and folds.

The quality of the retrieved magnetic data sets varies greatly. Surveys were flown over a period of thirty-eight years, over which time the quality and precision of the equipment as well as the quality of the processing improved consistently. The survey coverage was also taken into account when considering its ability to identify geological structures of interest relevant to this study. Data from the Lake Superior survey was acquired with flight line spacing of 1900 m and a high survey altitude (300 m) over the Schreiber area resulting in lower quality data. The Georgia Lake, Schreiber, and the Coldwell-Hemlo-Schreiber surveys are all flown at flight line spacing of 1000 m and at a constant altitude of 120 m and cover the entire Schreiber area. Although the line spacing is slightly wider, these surveys are considered to be of similar quality to the GSC airborne magnetic compilation (Ontario #8). The GSC airborne magnetic compilation was acquired at 805 m flight line spacing at a survey altitude of 305 m. In addition, data from this survey were digitized from paper maps in locations where flight lines intersect with contour intervals, resulting in poorer resolution of subtle magnetic variations. The GSC airborne magnetic compilation from August 2010, based on the Ontario #8 survey, provides leveled magnetic data to the GSC magnetic datum, and surrounds the high resolution Schreiber Area survey done by the OGS which is also available as magnetic data leveled to the GSC magnetic datum. The OGS survey (GDS1104) is flown at tighter flight line spacing (200 m) and lower altitude (lower magnetic sensor at 30 m above ground surface) over roughly 75% of the Schreiber area.

The GSC airborne magnetic compilation (Ontario #8) and the OGS Schreiber Area survey (GDS1104) provide the best available data quality and complete coverage over the Schreiber area. Data from these surveys were predominantly used for our interpretation. Lower quality data sets were investigated; however, they were not actively utilized as part of our geophysical interpretation.

### 3.1.2 Gravity Data

Gravity data indicate the local changes in the strength of Earth's gravitational field. Measurements were made between 1944 and 1962 acquired using gravimeters at stations scattered over the Schreiber area. The measurements were recorded in milli-Gals (mGal) and can be used to infer density variations in the subsurface rocks.

Measurements from thirteen gravity station locations in the Schreiber area (Table 1) were acquired from the Canadian Gravity Anomaly Data Base (NRCAN, 2012b; CGDB, September 2010) and downloaded from the NRCAN DAP server and are sparsely distributed with roughly 5 – 15 km between measurements.

The raw gravity measurements were downloaded as well as the Free Air (FA) and Bouguer anomaly (BA) corrected data. The FA correction is applied to correct for the elevation at which a measurement is made and adjusts measurements of gravity to what would have been measured at sea level. The complete Bouguer correction is applied to the FA corrected data as a correction for the height at which the measurements were made and the attraction of surrounding topographic features. (more details in section 4.2).

Despite the fact that data are of good quality, the coarseness of the gravity data can only be used to provide regional information of large scale geologic features due to the sparse gravity data stations in the Schreiber area.

### **3.1.3 Radiometric Data**

A radiometric or Gamma-Ray Spectrometry survey infers the concentration of natural radioactive elements at surface: uranium (U), thorium (Th) and potassium (K). Despite the fact that radiometric surveys have no significant depth of penetration (30 to 100 cm depth; Campbell et al., 2002), resulting maps or grids provide mineralogical and geochemical information about bedrock, surficial geology and alteration associated with mineral deposits, often indicating geological features not revealed by other techniques. Interpretation of radiometric data has to be done carefully as the presence of overburden can affect the interpretation of geological contacts.

Available radiometric data sets for the Schreiber area (Table 1) were acquired from the NRCAN DAP server (NRCAN, 2012c). All retrieved radiometric data sets are considered to be of high reliability as the system used is the well calibrated and highly sensitive GSC “Skyvan” airborne system. Even though the data are of high quality, the user should be aware that the elevated flight height (120 m above ground surface) combined with a wide line spacing (1000 m) limit the level of interpretation to regional structures, and that the almost insignificant depth of penetration hinders the identification of structures of interest if they are covered by any overburden. Signal to noise of any particular part of an image is difficult to assess without a detailed investigation of count rates and an assessment of background count rates. The most recent data set (Schreiber GSC2514, 1991) provides superior quality and coverage, and was utilized for the interpretation in this report. Lower quality data sets were investigated, however, they were not utilized as part of our geophysical interpretation.

### **3.1.4 Electromagnetic Data**

#### ***3.1.4.1 Very Low Frequency Electromagnetic***

Available very low frequency electromagnetic (VLF-EM) data sets for the Schreiber area (Table 1 and Figure 6) were acquired from the NRCAN DAP server. The VLF-EM signal is sensitive to conductors in the ground that channel the induced secondary currents in the survey area. These conductors are typically faults, or conductive geological units such as graphitic horizons. The VLF-EM signal is also perturbed by the topography.

The VLF-EM data were acquired in the Georgia Lake, Schreiber, and the Coldwell-Hemlo-Schreiber surveys flown at flight line spacing of 1000 m and at a constant altitude of 120 m. The Schreiber survey (GSC2514) provides complete VLF-EM coverage over the Schreiber area, with the Georgia Lake and Coldwell-Hemlo-Schreiber surveys providing coverage of the surrounding region. Retrieved VLF-EM data sets covering the Schreiber area are considered to be moderate

resolution as only basic survey parameters (such as lines orientation and partial sensor specifications) are provided with the data, and VLF-EM frequencies used for the measurements are unspecified. Moreover the elevated flight height combined with a wide line spacing limit the level of interpretation to regional structures.

#### **3.1.4.2 Frequency Domain Electromagnetic**

Only one Frequency domain electromagnetic (FDEM) data set was available for the Schreiber area (Table 1); this was acquired as part of the OGS Schreiber area survey (GDS1104). The EM system used for the OGS Schreiber Area survey measured the in-phase and quadrature components of five transmitter/receiver coil pairs in a system towed below a helicopter on a 30 m long cable with a nominal terrain clearance of the sensor of 30 m. Most of the parameters, such as survey design and sensor specifications, are well described and the survey has the finest spatial resolution, and the lowest flight height of all the airborne geophysical surveys considered in this study.

The coplanar coil geometry measures the vertical component of the EM field from a transmitter coil with a vertically oriented dipole moment and is sensitive to lateral variations in the bulk earth conductivity. Conversely the coaxial coil geometry measures the horizontal component of the EM field from a transmitter coil with a horizontally oriented dipole moment and is useful when current is induced in subvertical structures.

Data from the coplanar geometry were used by the OGS to produce three apparent resistivity grids. Each grid was calculated using a different frequency (877 Hz, 4891 Hz or 33840 Hz). As lower EM frequencies penetrate deeper into the Earth, each calculated frequency corresponds to different crustal depths. A detailed report provided by the OGS contains accurate information on survey design, equipment sensitivity and survey parameters (GDS1104).

### **3.2 Data Limitations**

The wide range of survey designs and methods used in the Schreiber area means that the available geophysical data are highly variable from one source to another. Resolution varies between high altitude surveys with large line spacing to low altitude surveys with tight line spacing. Equipment sensors have evolved through time from analog to digital and sampling frequencies have increased. Modern processing methods range from basic rejection of poor measurements to advanced filtering and processing and transformations of the data.

The magnetic data yield consistent responses that elucidate the mapped geology and this is useful in areas of limited bedrock exposure. Compositional differences and zonation are seen within the plutonic rocks and can be differentiated by the geophysical data depending on their characteristics. Similarly, the main structural regimes are clearly delineated by the magnetic, VLF-EM and FDEM data, but at different levels of detail depending upon the spatial resolution of the survey. All four data types considered, magnetic, gravity, radiometric and electromagnetic, contribute to the geophysical interpretation. Limitations in applying these data types to the Schreiber area are governed mainly by the following factors:

- Coverage and quality of data – types of data available, density of coverage, vintage, and specifications of the instrumentation;

- Overburden – areal extent, thickness and physical properties; and
- Bedrock lithologies – physical properties and homogeneity (e.g., batholith contacts can be easily mapped but batholiths themselves are sometimes quite homogeneous, making geophysical characterization of internal structure difficult).

The user of the geophysical information must bear in mind that each method relies on characterizing a certain physical property of the rocks. The degree to which these properties can be used to translate the geophysical responses to geological information depends mainly on the amount of contrast and variability in that property within a geological unit and between adjacent geological units. The usability of each data set also depends on its quality and resolution.

## 4. GEOPHYSICAL DATA PROCESSING

All geophysical data sets available for the Schreiber area were assessed, processed and imaged using the following software packages:

- GOCAD Mining Suite (GOCAD Mining Suite, 2012) for data compiling and filtering;
- WinDisp from Scientific Computing and Applications for data filtering and format conversion (WinDisp, 2012);
- The GDAL library (GDAL, 2012) for data format and coordinate reference system conversions.

### 4.1 Magnetic

The magnetic survey data acquired from the GSC and OGS consists of total magnetic field (TMF) and reduced magnetic field (RMF) grids. The RMF was determined by the GSC and the OGS by removing the Earth's ambient magnetic field recorded at the time of the survey from the data. The retrieved grids of the magnetic datasets have also been leveled using an upward continuation transformation to convert the data to a common elevation datum of 305 m used by the Geological Survey of Canada (GSC). While the upward continuation transformation acted in part as a low pass filter to the magnetic data, it was deemed to be the best approach to leveling these particular datasets and did not adversely affect the geophysical interpretation. The essential theoretical aspects of the leveling methodology are fully discussed in Gupta et al. (1989), and Reford *et al.* (1990).

The resulting survey data were integrated to form a single GSC-levelled RMF grid defined by 40 m grid cells and covering the entire Schreiber area. Gridding of the data was generated through a minimum curvature interpolation based on points extracted from the 200 m grid cell size compiled grid and from the 40 m grid cell size Schreiber Area grid.

Additional magnetic data processing was performed on GSC-levelled gridded data using filters to perform Reduction to Pole (Figure 7), first vertical derivative of RTP (Figure 8), second vertical derivative of RTP (Figure 9), tilt angle of RTP (Figure 10) and analytic signal of TMF (Figure 11).



**Table 2: CGRF-2005 magnetic field characteristics for retrieved surveys**

Source	Name	X	Y	Date	Declination (°)	Inclination (°)	Field Strength (nT)
NRCan	Coldwell, Hemlo, Schreiber	539654.79	5405364	23/07/1990	-5.348	76.052	59,291
NRCan	Georgia Lake	441720.9	5449997	24/07/1989	-3.882	76.395	59,564
NRCan	Ontario #08	589213.15	5288089	15/07/1962	-3.092	76.937	60,131
NRCan	Schreiber	486114.06	5431920	27/02/1991	-4.661	76.199	59,351
NRCan	Lake Superior	394282.07	5246121	24/08/1987	-2.196	75.156	59,224
OGS	Schreiber Area	505860.77	5418566	28/11/1999	-5.440	75.562	58,438

### Reduction to Pole (RTP)

Reduction to pole recalculates total magnetic intensity data as if the inducing magnetic field had a 90° inclination, such as it does at the Earth's magnetic poles. This transforms asymmetric magnetic anomalies to symmetric anomalies centred over their causative bodies which can simplify the interpretation of the data. The CGRF magnetic field characteristics at the time of each survey, shown in Table 2, were used to identify the geomagnetic inclination and declination used to perform the RTP.

The RTP filter, computed from the residual magnetic field after it is transformed to the Fourier domain, is defined as follows (Baranov, 1957):

$$L(\theta) = \frac{[\sin(I) - i \cdot \cos(I) \cdot \cos(D - \theta)]^2}{[\sin^2(I_a) + \cos^2(I_a) \cdot \cos^2(D - \theta)] \cdot [\sin^2(I) + \cos^2(I) \cdot \cos^2(D - \theta)]} \quad eq. 4.1$$

If: ( $|I_a| < |I|$ ),  $I_a = I$

Where:

- $L(\theta)$  = pole-reduced magnetic field for wavenumber  $\theta$
- $I$  = geomagnetic inclination
- $I_a$  = inclination for amplitude correction (never less than  $I$ ).
- $D$  = geomagnetic declination
- $i$  = imaginary number in the Fourier domain

### First Vertical Derivative of the Pole Reduced Field

First vertical derivative (IVD) of RTP data computes the vertical rate of change in the magnetic field and tends to sharpen the edges of anomalies and enhance shallow features (Telford *et al.*, 1990). The 1VD in the spatial domain is shown as

$$1VD = \frac{dRTP}{dZ} \quad eq. 4.2$$

where  $Z$  is the vertical offset. The computation was done using a 5x5 spatial filter in the software package WinDisp from Scientific Computing and Applications. The weights were computed by transforming the 1VD operator defined in the Fourier domain into the spatial domain.

#### Second Vertical Derivative of the Pole Reduced Field

Second vertical derivative (2VD) of RTP data is a measure of curvature and large curvatures are associated with shallow anomalies (Telford *et al.*, 1990). The 2VD enhances near-surface effects at the expense of deeper anomalies and is shown in equation 4.3.

$$2VD = \frac{d^2RTP}{dZ^2} \quad eq. 4.3$$

where  $Z$  is the vertical offset. The computation was done using a 5x5 spatial filter in the software package WinDisp from Scientific Computing and Applications. The weights were computed by transforming the 2VD operator defined in the Fourier domain into the spatial domain.

#### Tilt Angle of the Pole Reduced Field

The tilt angle (Miller and Singh, 1994) calculates the arctangent of the angle between the vertical gradient and the horizontal gradient of the magnetic field to normalize data and to help discriminate between signal and noise. The tilt angle in the spatial domain is shown in equation 4.4.

$$TILT = \tan^{-1} \frac{\frac{dRTP}{dZ}}{\sqrt{\left(\frac{dRTP}{dX}\right)^2 + \left(\frac{dRTP}{dY}\right)^2}} \quad eq. 4.4$$

where  $X$  and  $Y$  are the horizontal offsets in the east and north directions. The first vertical derivative, as well as horizontal derivatives in  $X$  and  $Y$  directions are computed in the spatial domain. The computation was applied to the reduced to pole magnetic field data using a 5x5 spatial filter in the software package WinDisp from Scientific Computing and Applications. The weights were computed by transforming the TILT operator defined in the Fourier domain into the spatial domain.

#### Analytic Signal Amplitude

Analytic Signal (AS) of TMF is calculated by taking the square root of the sum of the squares of the derivatives in the horizontal ( $X$  and  $Y$ ), and vertical ( $Z$ ) directions of the magnetic field at a given location. The resulting shape of the analytic signal is independent of the orientation of the magnetization of the source for 2D bodies and is centered on the causative body (Nabighian, 1972). This has the effect of transforming the shape of the magnetic anomaly from any magnetic inclination to one positive, body-centered anomaly. The analytic signal in the spatial domain is shown in equation 4.5.

$$AS = \sqrt{\left(\frac{dRMF}{dX}\right)^2 + \left(\frac{dRMF}{dY}\right)^2 + \left(\frac{dRMF}{dZ}\right)^2} \quad eq. 4.5$$

where RMF is the reduced magnetic field from the magnetic survey data. The computation was done using a 5x5 spatial filter in the software package WinDisp from Scientific Computing and Applications. The weights were computed by transforming the AS operator defined in the Fourier domain into the spatial domain.

A low-pass (Butterworth) filter was applied to the 1VD, 2VD, and Tilt angle of the RTP magnetic field, and the analytic signal of the RMF grids. This filtering was performed in the Fourier domain using GOCAD and is based on a Gaussian curve defined by a cut-off frequency twelve times the grid cell size and a roll-off frequency six times the grid cell size. Users of the above filtering products for interpretation often assume the absence of remnant magnetization and self-demagnetization. Their effects are commonly ignored or assumed to be insignificant.

## 4.2 Gravity

The retrieved gravity data are from the Canadian Gravity Anomaly Database (CGDB) consists of point data collected at gravity stations plus 2 km by 2 km gridded data of observed, free air (FA) and Bouguer data (Figure 12). All CGDB gravity are leveled to the control stations of the Canadian Gravity Standardization Network (CGSN) which is itself based on the International Gravity Standardization Network of 1971 (IGSN71). Both networks are using the ellipsoid GRS80 as reference. FA and Bouguer anomalies for a station on land were calculated from the observed gravity by GSC.

The FA anomaly incorporates a correction to the observed gravity to account for the difference in elevation between the observed station and the reference ellipsoid. The FA anomaly is detailed in equation 4.6 (NRCAN, 2005).

$$FA = g_0 - g_t + \frac{dg}{dz}h \quad 4.6$$

Where  $g_0$  is the observed gravity,  $g_t$  is the theoretical gravity at the surface of the reference ellipsoid (GRS80),  $h$  is station elevation above mean sea level in metres, and  $dg/dz$  equals 0.3086 mGal  $m^{-1}$  which reflects the average vertical gravity gradient per metre of elevation above sea level).

The Bouguer anomaly includes a further correction for the mass between the station and the reference ellipsoid (GRS80). The Bouguer anomaly (BA) is detailed in equation 4.7 (NRCAN, 2005).

$$\begin{aligned} BA &= g_0 - g_t + \left(\frac{dg}{dz} - 2\pi G\rho_c\right)h + TC \quad 4.7 \\ &= FA - 2\pi G\rho_ch + TC \end{aligned}$$

Where the constant of gravitation  $G$  equals  $6.672 \times 10^{-6} \text{m}^3 \text{kg}^{-1} \text{s}^{-2}$  (IAG, 1975),  $\rho_c$  is the average density of crustal rock ( $2670 \text{kg m}^{-3}$ ),  $TC$  is the terrain correction in mGal, and  $dg/dz$  equals  $0.3086 \text{mGal m}^{-1}$  which reflects the average vertical gravity gradient per metre of elevation above sea level (NRCan, 2005).

### 4.3 Radiometric

The following radiometric grids (radioelement concentrations and ratios) were acquired from the Schreiber Survey (GSC2514) at 200 m grid cell size. No additional processing beyond typical survey quality control was applied to the retrieved radiometric data set.

The data consisted of measurements of three radioelement concentrations and a dose rate:

- Potassium, K (%)
- Equivalent uranium, eU (ppm)
- Equivalent thorium, eTh (ppm)
- Total Air Absorbed Dose Rate (nGy/h)

Three additional grids were calculated from these measurements by the GSC based on the ratios of radioelement concentrations:

- Equivalent Uranium/equivalent Thorium ratio (eU/eTh)
- Equivalent Uranium/Potassium ratio (eU/K)
- Equivalent Thorium/Potassium ratio (eTh/K)

An additional ternary image of the concentrations in K, eU and eTh was generated (Figure 13). The determination of the radioelement concentrations, dose rate and ratios followed the methods and standards published by the International Atomic Energy Agency (IAEA, 2003), many of which were developed at the GSC. The dose rate is a calibrated version of the measured “total count” that considers the energy of different parts of the radiation spectrum, and reflects the total radioactivity from natural and man-made sources.

### 4.4 Electromagnetic

#### 4.4.1 Very Low Frequency Electromagnetic

The GSC performed quality assurance on the VLF-EM data from the Coldwell-Hemlo-Schreiber, Georgia Lake and Schreiber surveys. No additional processing was applied to the retrieved VLF-EM total field and quadrature data. The data are shown in Figure 14 as profile lines along the flight path.

#### 4.4.2 Frequency Domain Electromagnetic

The OGS oversaw quality control and processing of the Frequency Domain Electromagnetic (FDEM) data. Their work is detailed in the GDS1104 report (OGS, 2003) and is summarized below.

Profile data were levelled and assigned co-ordinates based on the flight path data. Raw in-phase and quadrature data were de-spiked using a spike rejection filter. Further spikes were removed manually after examination of profile data and then a 7-point Hanning filter was applied. Noise less than one second in wavelength on the low coplanar data was removed using an FFT filter. Linear interpolation of corrections between high level background checks were applied to the data, and the data were examined in profile form to look for levelling discrepancies. Minor level adjustments were applied where warranted after examination of all frequencies.

The inphase and quadrature data were individually gridded and inspected for levelling errors. Several small errors were noticed which were not related to altitude. A decorrugation filter was applied to the inphase and quadrature data separately to create preliminary correction grids. The corrections were limited to data where the response was in the range of  $\pm 4$  ppm and a low pass filter was applied to the corrections. The low pass filter was carefully designed to have minimal effect in reducing the amplitudes of conductive areas in either the inphase or quadrature channels. The correction channels were applied to the data to create the final inphase and quadrature channels used to calculate the resistivity. The data were rigorously analyzed after each stage to ensure no anomalies were being introduced or deleted and the final correction was a smoothly varying function.

The coplanar resistivities were calculated in Ohm-metres from the inphase and quadrature data in parts per million using the Fugro pseudo-layer model (i.e., finite thickness resistive layer over a homogeneous half-space). These channels were gridded with a 40 m cell size, and Akima spline interpolation was applied. The grids were then smoothed with a 3 by 3 convolution filter for presentation.

The resulting 40 m grids from the coplanar geometry were used to produce three apparent resistivity grids. Each grid was calculated using a different frequency (877 Hz, 4891 Hz or 33840 Hz) and therefore investigates a different depth, as lower EM frequencies penetrate deeper into the Earth. The apparent resistivity for 877 Hz is shown on Figure 15.

EM anomalies were manually picked with conductor types and dips assigned by the interpreter based upon the mid-frequency profiles. Cultural anomalies were verified by power line response, topographic correlation and examination of the flight path video. Identified EM anomalies were located, given a unique ID number and classified as one of four anomaly types as detailed in the GDS1104 report:

- Bedrock is assigned to an anomaly whose response matches that of a bedrock conductor, but is not thin and/or near vertical. This anomaly type might include other shapes of conductors: roughly pod-shaped, thick dykes, short strike length bodies, or conductors sub-parallel to the flight path;
- Dyke is assigned to an anomaly whose shape matches that of a steeply dipping thin dyke-like conductor. The thickness appears to be less than about 3 m. These are commonly conductors in steeply dipping geology, but may also be conductive shear zones;
- Flat lying conductors, generally surficial, are geologic anomalies that might represent conductive overburden, swamps or clay layers. They would not appear to be conductive at depth;

- Line current is an anomaly with a shape typical of an elongated line of channeled electrical current - typically cultural (human sources) such as power lines, train tracks, fences, etc.

## 5. GEOPHYSICAL INTERPRETATION

### 5.1 Methodology

The coincidence of geophysical features with mapped lithology and structural features were identified and interpreted for the Schreiber area using all available geophysical data sets. In particular, the pole reduced magnetic field (Figure 7) and its first vertical derivative (Figure 8), as well as radiometric data sets (Figure 13) were the most accurate data for mapping variations in geological contacts, identifying heterogeneity, and delineation and classification of structural lineaments (faults, dykes). The methodology and results from the structural lineament interpretation are presented in the lineament report for the Schreiber area (SRK, 2013). Corroborating observations from the other data sets sensitive to some specific characteristics of the geology were considered and used if they were of value. The following enhanced grids of the total magnetic field data provided the most valuable information and were used to assist in the interpretation:

- Pole reduced magnetic field – distribution of magnetic units (Figure 7);
- Pole-reduced first and second vertical derivative –boundaries, texture, foliation (Figure 8 and 9);
- Tilt angle (Figure 10) – subtle magnetic responses. In particular, tilt angle maps allow the identification of contacts in the presence of a varying magnetic background;
- Analytic signal (Figure 11) – anomaly character, texture, boundaries.

Gravity data (Figure 12) were considered to be of insufficient resolution to be used for detailed interpretation of geological units and boundaries, based on the sparse number of measurements in the Schreiber area. However, some general characterizations of the regional scale units were possible (see section 5.2.2 for details).

From a mapping perspective in the Schreiber area, the geophysical interpretations were initially conducted using the magnetic data sets (Figures 7 to 11). The frequency domain electromagnetic (FDEM) (Figure 15), radiometric (Figure 13) and very low frequency electromagnetic (VLF-EM) (Figure 14) data were used to provide supporting evidence for interpreting variations in bedrock lithologies. In most cases, the magnetic data proved to be greatly superior in the Schreiber area.

The magnetic anomaly characteristics and geophysical contacts were compared to the current mapped bedrock geology in order to identify similarities and/or changes in the lithological contact locations. The coincidence of the lithological units with the geophysical data was mainly recognized in the magnetic images from their anomaly amplitude, texture, width, and orientation characteristics. Similarly, variations in the radiometric element concentrations from radiometric

surveys show good agreement with the mapped bedrock units. In some cases, differences in the boundaries determined from the magnetic data and the mapped boundaries may reflect a subsurface response which may not match the mapped surface contacts (e.g., dipping unit) and/or a contact extended through locations with limited outcrop exposure (e.g., under overburden and drainage cover). This might indicate that geology is incorrectly mapped, or that geology is actually more complicated than represented on the geological map. Similarities and differences noted between geophysical interpretations and mapped bedrock geology are discussed in the following sections (see Figure 16).

The geophysical data were evaluated against the following published geological maps:

- Ontario Geological Survey, 2011, 1:250 000 Scale Bedrock Geology of Ontario, Miscellaneous Release Data 126-Revision 1 (OGS, 2011), Figure 3;
- OGS Map 2665 Precambrian Geology Compilation Series - Schreiber Sheet (Santaguida, 2002);
- OGS Map 2667 Precambrian Geology Compilation Series - Longlac Sheet (Johns *et al.*, 2003).

## 5.2 Results

The following section presents a regional-scale description and interpretation of each geophysical data set in the Schreiber area, which includes detailed interpretations of geophysical responses associated with the four major granitoid intrusions (Crossman Lake batholith, Whitesand Lake batholiths, Terrace Bay batholith and the Mount Gwynne pluton) identified within the Schreiber area (Figure 3). The interpretation also discusses how well the geophysical data relate to the Bedrock Geology of Ontario map (OGS, 2011, MRD126-REV).

### 5.2.1 Magnetic Data

The magnetic field data for the Schreiber area are displayed as images of the reduced to pole (RTP) residual magnetic field (Figure 7), its first and second vertical derivatives (Figure 8 and Figure 9), tilt angle (Figure 10) and analytic signal (Figure 11). Where the Schreiber area is overlain by the high-resolution magnetic data (GDS1104), the residual magnetic field shows an exceedingly variable signature reflecting changes in both bedrock geology and structure. This variation in magnetic signal typically reflects the relative intensity of the magnetic field by highlighting areas that are strongly or weakly magnetized. The reduced magnetic field within the Schreiber area has a range of 8791 nT, from a minimum of -2298 nT to a maximum of 6493 nT.

The observed magnetic signal over most of the granitic intrusions in the Schreiber area (i.e., Crossman Lake and Terrace Bay batholiths) show a generally subdued and low magnetic response, with the exception of the Whitesand Lake batholith. The Whitesand Lake batholith, as well as much of the adjacent greenstone belt in the area to the northeast of the Township of Schreiber displays a strongly positive anomaly. This anomaly extends to the mid-point of the eastern boundary of the Schreiber area, where an especially strong response correlates with the felsic to intermediate metavolcanic rocks. First and second vertical derivatives over this anomaly exhibit variability in the magnetic texture and amplitudes indicating a high degree of lithological

heterogeneity within the greenstone belt (see Figure 8 and Figure 9). This area also encompasses a small granitic intrusion surrounding Ellis Lake, bordered by the Syenite Lake Fault to the north-west and by the Schreiber-Hemlo greenstone belt to the south-west.

A weak magnetic anomaly is displayed overlying the granitic intrusion throughout the central portion of the Schreiber area, corresponding predominantly to the Crossman Lake batholith. As observed in Figure 7, the first vertical derivative of the reduced magnetic field emphasizes the individual geological features reflected in the bedrock, where the observed patterns are interpreted to reflect variations in the detail of structural fabric within an area.

High analytic signal responses observed in the Schreiber area tend to highlight contacts with magnetic source rocks, corresponding to the Schreiber-Hemlo greenstone belt as well as some of the major faults within the project area (Figure 11). The interpretation of geologic bedrock units and structures made using the analytic signal and the first vertical derivative is also supported by a review of the tilt angle (Figure 10). In general, the interpretation of the magnetic data and the enhanced grids correspond well with the distribution of mapped bedrock geology and structures from the OGS (MRD126-REV1). This is to be expected as the distributions of bedrock units shown on the bedrock geology maps in the Schreiber area is the result of previous interpretation of the magnetic data by the OGS, as shown in the Precambrian Geology Compilation map series (M2665). Cross-cutting anomalies show up both as normally magnetized as well as reversely magnetized in the Schreiber-Terrace Bay area and are better imaged with reduced to pole data (Figure 7).

### **5.2.2 Gravity Data**

The widespread shape, and lack of detail shown in the gravity anomaly distribution, reflects the sparse arrangement of gravity stations used to generate the grid in the Schreiber area. Thus, confidence in the ability to interpret the gravity data to assess spatial variations in geology is low. Despite the low spatial resolution of the gravity data some observations can be made and are detailed below.

The Bouguer gravity anomaly and the gravity station locations in the Schreiber area are presented in Figure 12. Results show a positive gravity response over the Township of Schreiber that extends in a northeast direction from Lake Superior. The positive gravity response underlying Lake Superior is presumed to be associated with a thick sequence of metavolcanic rocks of the Osler Group associated with the 1.1 Ga Mid-Continent Rift. Variations in gravity measurements for the Schreiber area tend to be related to the relative densities of geologic units within the subsurface. Similar observations are shown at a regional scale in the Superior Province where granitic intrusive units typically show lower gravity response, corresponding to lower rock densities (i.e. Szewczyk and West 1976). In comparison, mafic rocks typical of greenstone belts generally show positive gravity responses and thus higher densities. Different phases of a same intrusion may also have different densities. It is noted that gravity responses in themselves may not uniquely define geology, and could be derived from multiple geological configurations. Resulting from the sparse distribution of gravity stations, the broad shape of the anomaly in the Schreiber area does not appear to reflect the mapped bedrock geology. However, the positive anomaly broadly encompasses the greenstone belt units surrounding the Township of Schreiber, as well as the southern end of the Whitesand Lake batholith, the Mount Gwynne



pluton, and a part of the granitic intrusion bordering the southern margin of the Crossman Lake batholith.

A slight negative gravity response is present to the east of the Township of Schreiber that corresponds broadly to the outline of the Terrace Bay batholith. To the north and northwest of the Township of Schreiber a large negative gravity response underlies the Crossman Lake and Whitesand Lake batholiths, as well as the northern arm of the Schreiber-Hemlo greenstone belt. Although, the shape of these negative anomalies is only based on a few gravity station measurements, individual gravity values suggest the batholiths may either have lower densities or may extend to some depth.

### 5.2.3 Radiometric Data

Radiometric data in the Schreiber area were of sufficient resolution to be used, as a complementary data set to magnetic data, for interpretation of geological contacts and boundaries. Considering that outside of the areas covered by lakes, bedrock is exposed or near surface over the majority of the Schreiber area, due to the limited thickness of Quaternary cover, it is considered that the radiometric signal broadly portrays bedrock geological features.

Variations in the radiometric parameters (potassium, uranium and thorium) for the Schreiber area reflect changes in bedrock lithology. Airborne radiometric data for the Schreiber area are provided in Figure 13 as a composite RGB ternary diagram representing the three radiometric parameters (Red – Thorium, Green – Uranium, and Blue – Potassium). Their extremes and mean value per radiometric parameter are shown in Table 3. Note that radiometric assays are statistical and at low values have a large standard error; at low concentrations a radio-assay may be negative due to the statistical error introduced by correction factors. The radiometric responses identified on the ternary image for the Schreiber area appear to be predominantly related to the mapped distribution of bedrock geology. Variations in the radiometric responses within a single mapped intrusive batholith may be related to different intrusive phases or a differentiated lithology within the single domain.

The granitic intrusions show elevated responses in potassium (K), thorium (eTh) and uranium (eU) concentrations, with radioelement responses generally above 0.75% K, 2.0 ppm eTh, and 0.5 ppm eU. The greenstone belts show much lower radiometric response, which corresponds to a general depletion of radioactive elements, with radioelement responses generally below 0.75 % K, 2.0 ppm eTh, and 0.5 ppm eU. The exception is a region over the northern portion of the Crossman Lake batholith, adjacent to the mafic metavolcanic rocks of the greenstone belt and mostly located east of the Schreiber Point fault. This region is characterized by a radiometric anomaly which exhibits similar concentrations of equivalent uranium and equivalent thorium to the greenstone belt. It is highlighted by the equivalent thorium and equivalent uranium mean values, respectively around 2.3 ppm, and 0.47 ppm eU, but differs on the potassium concentration which matches the average observed over the granitic intrusions, with average values around 0.84 %. This anomaly may represent a different phase of the Crossman Lake batholith.

**Table 3: Radiometric responses for gamma-ray spectrometry parameters within the Schreiber area**

Radioelement	Minimum*	Maximum	Mean
Potassium (%)	-0.03	2.83	1.09
Uranium (ppm)	-0.92	3.13	0.74
Thorium (ppm)	-0.31	10.75	3.44
Natural air absorbed dose rate (nGy/h)	-2.59	75.01	24.42

\*Negative values are not unusual due to the statistical nature of gamma-ray spectrometer data and grid interpolation effects

The Whitesand Lake batholith and the southern portion of the Crossman Lake batholith show elevated responses in all three radioelements, with mean values being 1.47 % K, 5.14 ppm eTh, and 1.18 ppm eU. The elevated radiometric response extends north and west from the Whitesand Lake batholith and displays a sharp gradation into the Crossman Lake batholith, which may represent a subtle change in lithologies between the two batholiths. Based on mapping by the OGS, no boundary has been defined to differentiate between the Whitesand Lake and the Crossman Lake batholiths. The elevated radiometric response shown along the southern margin of the Crossman Lake batholith tends to be limited to the granitic intrusion that is bordered by the Syenite Lake Fault to the north-west and by the Schreiber-Hemlo greenstone belt to the south-west. This response shows similar concentrations in all three radiometric elements as the Whitesand Lake batholith, with mean values being 1.26 % K, 4.07 ppm eTh, and 0.88 ppm eU, and may represent a change in bedrock lithology interpreted as a separate intrusive phase in contrast to the adjacent Crossman Lake batholith.

Most of the Terrace Bay batholith within the Schreiber area is covered by Quaternary sediments with exception of an area southwest of Hays Lake (Figure 4). Despite the presence of cover the radiometric response shown on the ternary diagram (Figure 13) is quite consistent with mean values being 1.02 % K, 2.47 ppm eTh, and 0.55 ppm eU. Peaks in radiometric concentrations above 1.3 % K, 3.5 ppm eTh and 1.0 ppm eU are observed in absence of cover which corresponds to the general trend within the Schreiber area.

## 5.2.4 Electromagnetic

### 5.2.4.1 Very Low Frequency Electromagnetic Data

Results of the VLF-EM total field and quadrature data from the Schreiber survey are presented in Figure 14. The total field, which shows a maximum over conductive linear features, indicates multiple linear structures interpreted from one survey line to another with the general trends being southeast, east-southeast, and west-southwest (Figure 14). The measured quadrature gives corroborating evidence for the interpretation and anomalous trends are coincident with several faults and geological contacts between the batholiths and the greenstone belts mapped on the OGS Bedrock Geology of Ontario map (MRD126-REV) as well as on OGS Precambrian geology maps 2665 and 2667. Several interpreted geological contacts are identified and presented in Figure 14. The locations of these interpreted features either correspond to contacts between the batholiths and greenstone units, or reflect internal heterogeneities within individual bedrock units. In particular, a major geological contact is interpreted in the northern portion of the Schreiber area between the mafic metavolcanic rocks of the greenstone belt and metasedimentary rocks of the Quetico Subprovince. As expected, the same major geological

contact appears to be well defined in the frequency domain electromagnetic data, as well as the radiometric and processed components of the RTP magnetic field data.

In addition, two power lines located in the southern half of the Schreiber area, with a general east-west trend, greatly affect the VLF-EM signal. The overwhelming response of such highly conductive anthropogenic features masks the EM response from the underlying geological bedrock.

#### ***5.2.4.2 Frequency Domain Electromagnetic Data***

The FDEM data responses for the Schreiber area correspond to a mixture of sources, including cultural (e.g., roads, power lines, railways) surficial (lake sediments, wetlands, aquifers) and bedrock (e.g., sulphide mineralization, resistive horizons). Both, cultural and surficial sources highly affect the data by minimizing the depth of penetration of the electromagnetic signal. The three frequencies of the survey investigate different depths, however, these depths of investigation are not consistent for a given frequency, but depend on the resistivity of the medium through which the EM signal has to travel. Interpretation of the EM data focused primarily on delineating bedrock sources.

Only the lowest frequency data are presented in Figure 15 and detailed in Table 4 as it is the frequency with the highest depth of penetration. Linear low resistivity anomalies identified through the Schreiber area generally are coincident with several mapped bedrock faults and geological contacts. Review of the apparent resistivity maps shows that majority of the greenstone units and associated mafic metavolcanic rocks possess relatively high apparent resistivity values. Localized zones of low resistivity anomalies are identified in the northern portion of the greenstone belt, south of the contact with the Quetico metasedimentary units, and to the east of the Syenite Lake Fault. Both of these anomalies appear as closely spaced, subparallel conductors that are trending in the east-west direction, parallel to the dominant structural fabric, and are interpreted to reflect the internal heterogeneities associated with the metavolcanic rocks. In addition, the locations of these anomalies agree with the results from the OGS electromagnetic anomaly database, where a number of conductive features are interpreted to be dyke structures, or faults infilled by dykes.

The granitic batholiths in the Schreiber area are highly resistive for the most part, which is typical of granitic rocks. Apparent resistivity gridded images are relatively undifferentiated in the Schreiber area with some localized low resistivity patterns throughout the batholith regions which may reflect lake-bottom sediments. On the other hand, portions of the Terrace Bay batholith exhibit somewhat reduced resistivities in comparison to the Crossman Lake and Whitesand Lake batholiths, which is likely to result from the occurrence of thick morainal, glaciofluvial and glaciolacustrine deposits over a large portion of the batholith near Terrace Bay (Figure 4), as well as a number of localized surface water bodies, which typically possess low resistivities. In general, the apparent resistivity data have proven useful for mapping linear structures, minor bedrock conductive horizons in the greenstone units, and for identifying the presence of conductive overburden. It does not exhibit a clear apparent resistivity contrast between the greenstone belts and the granitic batholith units. To a large extent, most of the linear structures identified in the electromagnetic data are coincident with structures that have been highlighted by other geophysical methods.

**Table 4: Apparent Resistivity statistics for 877 Hz**

<b>Resistivity Values</b>	<b>Minimum</b>	<b>Maximum</b>	<b>Mean</b>
Low	0.50	1150	995
Medium	1.22	8001	5851
High	3.24	46407	12997

As discussed in section 4.5, several FDEM anomalies are located and classified into four categories: Bedrock, Dyke, Flat Lying Conductor, and Line Current and are presented in Figure 15. Bedrock anomalies located on the western edge of the survey are presented, but should not be considered for this interpretation as they are likely to represent artifacts from the survey edge as they follow the survey outline. Most of the dyke-like conductors are clustered within the greenstone belt and over metasedimentary rocks of the Quetico Subprovince in the north. These anomalies are interpreted based on an anomaly shape which is consistent with a steeply dipping thin dyke. However, the interpretation of these anomalies is also consistent with either steeply dipping geology or conductive shear zones. Most of the flat-lying conductors are located in the south over the Schreiber greenstone belt and the Terrace Bay batholith. Few bedrock conductors were identified over the eastern portion of the Crossman Lake batholiths. Instead, most of the line current anomalies occur east of Terrace Bay and north of Selim. Since EM anomalies are generally concentrated over the greenstone belt, little useful information can be extracted to improve the understanding of the granitic intrusive rocks.

### **5.3 Geophysical Results for Batholiths in the Schreiber Area**

The following section provides more detailed geophysical interpretations of the Whitesand, Crossman Lake and Terrace Bay batholiths and the Mount Gwynne pluton in the Schreiber area. The interpretations include a description of the geophysical characteristics of each unit, as well as a refinement of geologic contacts, where possible, and the identification of internal heterogeneities within the unit, if present. The geophysical interpretation benefited from all of the datasets in the Schreiber area, albeit geological contacts and internal heterogeneities were largely mapped using the magnetic data to extrapolate to depth. In areas where geologic features are obscured in the magnetic data, the radiometric data were used for mapping. These interpreted features are presented alongside the current bedrock geology mapping on Figure 16, noting that the interpretations are preliminary and require future geologic validation.

#### **5.3.1 Whitesand Lake Batholith**

With the exception of the greenstone belt units, the dominant magnetic signature of moderate to high magnetic signal shown in the reduced to pole magnetic data in the Schreiber area corresponds to the Whitesand Lake batholith, extending along the north shore of Lake Superior west of the Township of Schreiber. The reduced to pole magnetic field data show a range of values from -286 nT to 798 nT, with an average of 78 nT. The reduced to pole magnetic field and the processed magnetic data presented in Figure 7 and Figure 8 indicate that the overall outline of the Whitesand Lake batholith is consistent with mapping performed by the OGS (Figure 16). The eastern contact with the greenstone belt consists of an abrupt transition, expressed as a relatively flat response associated with greenstone units transitioning westward into an elevated response with a change of approximately 600 nT along the edge of the

Whitesand Lake batholith. The northeastern boundary of the Whitesand Lake batholith, adjacent to the greenstone belt, displays a magnetic feature which is coincident with the location of the Cook Lake Fault and follows a major magnetic low interpreted to reflect depletion of magnetite along the fault. Much of the batholith displays a similarly high magnetic response; even though the reduced magnetic field, as well as the vertical derivatives, shows that the Whitesand Lake batholith is characterized by several obvious magnetic perturbations indicative of heterogeneity within the intrusion. The internal heterogeneity corresponds to linear magnetic lows that have been interpreted within the Schreiber area lineament report as bedrock structural features (SRK, 2013), and a number of them are coincident with faults mapped by the OGS, in particular the Sox Creek Fault. Additionally, some of the noisy magnetic response of the area underlain by the Whitesand Lake batholith may reflect the presence of remnant mafic metavolcanic rocks identified in bedrock maps intermixed with the internal batholith (Figure 16; unit A). Further north, the RTP and processed magnetic data display a general decrease in the magnetic intensity, which may indicate a subtle change in bedrock lithology. Although a discrete contact has never been mapped between the Whitesand Lake and the Crossman Lake batholiths, this transition zone may correspond to the change between the two batholiths. Similar lithological changes are observed in the radiometric data as discussed below.

Radiometric highs in potassium, thorium and uranium contents are associated with the southern margin of the Whitesand Lake batholith along Lake Superior in the Schreiber area. The ratio of equivalent uranium to potassium is consistent with the remainder of the Schreiber area. Locations to the north and west of the Whitesand Lake batholith display a gradation in the radiometric response into the Crossman Lake batholith. This change in the radiometric response may represent a subtle change in lithologies between the two batholiths, and may correspond to the geological contact between the two intrusions. Based on mapping by the OGS, no boundary has been defined to differentiate between the Whitesand Lake and the Crossman Lake batholiths. However, Carter (1988) places the boundary between the two batholiths along the narrow band of east-trending supracrustal rocks along the western margin of the Schreiber area (Figure 3 and Figure 16; SRK, 2013). In addition, the signature of the Whitesand Lake batholith on the radiometric ternary image is similar to the one observed in the granite unit located on the southern contact of the Crossman Lake batholith with the greenstone units, adjacent to the Syenite Lake Fault (Figure 16; unit B).

Apparent resistivity of the Whitesand Lake batholith shows significant variability with a range of 66 to 1150 Ohm-m for the low frequency response. The higher end of the apparent resistivity range is consistent with resistivity values for granitic bedrock elsewhere in the Schreiber area. Several linear features observed in the electromagnetic data are characterized by a decrease in apparent resistivity of roughly 500 Ohm-m and are observed to largely correspond to the locations of faults mapped by the OGS. The locations of these features are similarly reflected in the magnetic data, suggesting a relative depletion in magnetic minerals and an increased presence of conductive minerals. A number of small localized apparent resistivity anomalies are coincident with the location of surficial water bodies, and localized overburden deposits.

### **5.3.2 Crossman Lake Batholith**

The Crossman Lake batholith has been mapped by the OGS as relatively uniform granodiorite to granite at the regional scale (OGS, 2011). The magnetic response observed over the batholith is

characterized generally by a low magnetic intensity, consisting mainly of negative values ranging from -462 nT to 4301 nT. The western half of the batholith exhibits a slightly higher magnetic response which gradually decreases in an eastern direction. Peak anomaly values of above +400 nT are observed over the batholith which may correspond to localized increases in the presence of magnetic minerals (e.g. remnant volcanic units - Figure 16; unit C), though few well-defined linear magnetic highs crossing the batholith attain peak values interpreted as dykes in the lineament study (SRK, 2013). Field examination of outcrops supports the current bedrock mapping for the two eastern-most areas on Figure 16 labelled as unit C (Figure 3; Carter, 1981a, b). It is, however, a possibility that remnant volcanic units may be present in the subsurface.

Processed magnetic images reveal the magnetic texture of the Crossman Lake batholith to be relatively flat, although it expresses several distinct linear structural trends coincident with the local faults and dykes mapped by the OGS. In addition, the overall outline of the Crossman Lake batholith is consistent with the bedrock geology map compiled by the OGS (Figure 3). Contacts between the greenstone units and the Crossman Lake batholith generally are evident as an abrupt transitional boundary in the magnetic and processed magnetic field data, though locally the contact is reflected as a subtle gradational change, particularly along the northern boundary of the Crossman Lake batholith adjacent to the mafic and ultramafic units. This transitional magnetic response may suggest that the mapped mafic and ultramafic units have a similar magnetic susceptibility as the granitic batholith. As noted above, no boundary has been defined to differentiate between the Whitesand Lake and the Crossman Lake batholiths based on field mapping by the OGS. Although a discrete contact has never been mapped, a transition zone is interpreted that may correspond to the change between the two batholiths. Similarly, lithologic changes are observed in the radiometric data as discussed below. The magnetic field and processed magnetic data within the Crossman Lake batholith in the northwest corner of the Schreiber area are marked by a quiescent pattern (Figure 16; unit D) interpreted to reflect increased lithological homogeneity within the batholith.

A slightly higher magnetic response is evident in the granitic unit that extends to the south of the Crossman Lake batholith, bordered by the Syenite Lake fault to the north-west and by the Schreiber-Hemlo greenstone belt to the south-west (Figure 16, unit B). This unit possesses an anomalously high magnetic response in comparison to the Crossman Lake batholith itself, where the magnetic signature, as well as a radiometric response (discussed below), is more consistent with that of the Whitesand Lake batholith. These responses may be interpreted to reflect a different granitic phase flanking the Crossman Lake batholith to the south. At this point there is a lack of additional mineralogical and lithological evidence to support this inference. The geologic contacts interpreted from the magnetic data in this area show some deviation from the bedrock geology map (Figure 16). Recognition of the contact between the granite unit (Figure 16; unit B) and the adjacent greenstone unit to the west was restricted due to an apparent low magnetic contrast between the two units; however, variations in the radiometric response between the two rock units enabled the placement of an interpreted boundary (Figure 16; unit E). As field mapping of outcrops supports the geologic boundaries illustrated on the bedrock geology map (Figure 3; Carter 1981b), the geophysical signature may reflect subsurface conditions.

Radiometric data show a moderate response in thorium, uranium and potassium concentrations throughout the Crossman Lake batholith in comparison to a more elevated response over the

Whitesand Lake batholith. To the west of the Crossman Lake batholith a gradational change of radioelement concentrations towards the Whitesand Lake batholith can be observed, which may represent a subtle change in lithology between the two batholiths. Based on mapping by the OGS, no boundary has been defined between the Whitesand Lake and the Crossman Lake batholiths. The signature of the Whitesand Lake batholith on the radiometric ternary image is similar to that observed in the granite unit separated from the southern margin of the Crossman Lake batholith by the Syenite Lake Fault (Figure 16; unit B).

Apparent resistivity of the Crossman Lake batholith is relatively uniform with average values of 1060 Ohm-m, which is consistent with resistivity values for granitic bedrock elsewhere in the Schreiber area. Several linear features observed in the electromagnetic data are characterized by a decrease in apparent resistivity of roughly 500 Ohm-m and largely correspond to the locations of faults mapped by the OGS. The locations of these features are similarly reflected in the magnetic data, suggesting a relative depletion in magnetic minerals and an increased presence of conductive minerals. A number of smaller apparent resistivity perturbations are coincident with the location of surficial water bodies, and localized overburden deposits.

### **5.3.3 Terrace Bay Batholith**

The Terrace Bay batholith is mapped as a homogeneous, granodiorite with minor masses of quartz-monzodiorite and quartz-monzonite (Marmont, 1984; Carter, 1988; Figure 16). The magnetic response observed over the batholith is characterized generally by moderate magnetic intensity, with values ranging from -1591 nT to 1565 nT. Locally, few peak anomaly values are observed throughout the batholith which may correspond to localized increases in the presence of magnetic minerals. Processed magnetic images reveal the magnetic texture of the Terrace Bay batholith to be relatively flat. The magnetic response is generally lower in magnitude and smoother than that of the Whitesand Lake batholith, and appears to have a similar response to the Crossman Lake batholith, with the exception of the southwestern edge located adjacent to the Worthington Bay Fault. The southwestern edge of the batholith exhibits a higher magnetic response, with peak values of +1500 nT, which rapidly decreases in a northeast direction (-50 nT) along a sharp magnetic boundary (Figure 16; unit F). The high magnetic response near the southwestern contact may be associated with the occurrence of aplite and pegmatite along the batholith margin associated with molybdenite and chalcopyrite mineralization identified through field mapping by Carter (1988). In addition, mineralogical analysis of hand samples identified in the OGS PetROCH database suggests that the southwestern margin of the Terrace Bay batholith is elevated in the amounts of both ferrous and ferric iron. The northern contact between the Terrace Bay batholith locally appears as an abrupt transition into the adjacent greenstone units, expressed as an increased magnetic response and magnetic intensity passing from the batholith units in the greenstones. The transition shown in the magnetic data sets forms a well-defined east-northeast trend that is generally coincident with the mapped bedrock geology. Although there is general agreement throughout the batholith, locally the magnetic response may suggest minor deviations in the location of the geological contact as indicated by regional-scale compilation mapping (OGS, 2011). In the area between Hayes Lake and the eastern boundary of the Schreiber area the northern boundary of the Terrace Bay batholith may be 1 km further north (Figure 16). The position of the batholith's northern boundary as interpreted from the magnetic data is in agreement with the boundary shown by Carter (1981b, c) as determined by field mapping.

Much of the Terrace Bay batholith is transected by several uniformly spaced, E-W trending linear magnetic perturbations, which extend through the entire batholith into adjacent greenstone units to the west and northwest, and extend well outside of the Schreiber area to the east. Although the magnetic response corresponds to a decrease of -200 nT compared to the background units, these linear features have been interpreted as Keweenawan Suite dykes cross-cutting the Terrace Bay batholith (SRK, 2013). This interpretation is based on the consistency in orientation and spacing of these linear features with mapped Keweenawan dykes in the region, in particular they are suggested to represent the northward continuation of a set of E-W trending dykes located in the southwest corner of the Terrace Bay batholith (Figure 8). In addition, Keweenawan-aged intrusive rocks commonly exhibit a reversely magnetized character (Pesonen and Halls, 1982). Mapping performed by the OGS has not identified the presence of diabase dykes within this area; therefore this interpretation will require future geologic validation.

Radiometric data show a moderate response in all radioelement concentrations throughout the Terrace Bay batholith (Figure 13), and a discrete contact between the batholith and the greenstone units to the north. In general, the radiometric response agrees well with the mapped bedrock geology for the batholith. Where present, overburden material shows a similar radioelement response to the batholith, which suggests that the material may be locally derived from the underlying bedrock. In this case it may serve as a proxy when interpreting the radiometric data. Few local anomalous zones to the north and northwest of the Community of Terrace Bay are observed as being depleted in all radioelement concentrations, which are coincident with the locations of Hays Lake and the Aguasabon River.

Apparent resistivity of the Terrace Bay batholith shows significant variability with a range of 0.5 to 1150 Ohm-m for the low frequency response. Much of this variability is reflected as apparent resistivity low coincident with the location of surficial water bodies, and localized overburden deposits. The apparent resistivity lows are consistently observed in all frequencies of the electromagnetic data. A small number of anomalous linear features trending in an east-west direction are observed in the electromagnetic data and are determined to be associated with interference from utility lines crossing the Schreiber area. The diabase dykes interpreted in the magnetic data are not evident in the apparent resistivity data, suggesting that sulphide mineralization or other electrically conductive minerals along the magnetic low linear features may be limited or absent.

#### **5.3.4 Mount Gwynne Pluton**

The Mount Gwynne pluton has been mapped by the OGS as a small, fault bounded intrusion located on the Schreiber Peninsula, south of the Township of Schreiber (Carter 1988; OGS 2011; Figure 16).

The residual magnetic response observed over the pluton is characterized generally as a high amplitude positive anomaly observed in the pole reduced magnetic field data with values ranging from -114 nT to 1490 nT (Figure 7). This response over the Mount Gwynne pluton, and over the southwest corner of the granitic intrusion surrounding Terrace Bay, could be due to the presence of a high magnetite content in the granodiorite to granite rocks, or magnetized mafic to felsic and



intermediate metavolcanic rocks mapped in the area. The vertical derivative data sets show the presence of linear magnetic lows extending from the Terrace Bay batholith into the Mount Gwynne pluton, and beyond the edge of the survey data. These features are interpreted as the western extent of the same dyke systems observed in the Terrace Bay batholith.

The northern half of the Mount Gwynne pluton corresponds to a slight increase in radiometric concentrations of thorium, uranium and potassium, located approximately 1 km southwest of the Township of Schreiber, and is consistent with other intrusive batholiths in the Schreiber area. However, the pluton is only identified by a single flight line from the airborne survey that crosses the pluton resulting in the inability to readily identify the geological contacts using the radiometric data.

Typical apparent resistivity values calculated from the low frequency electromagnetic data for the pluton show a relatively uniform distribution, which is difficult to differentiate from the adjacent metavolcanic units of the greenstone belt. The apparent resistivity values range from 850 Ohm-m to 1150 Ohm-m.

## **6. SUMMARY OF RESULTS**

The purpose of this study was to identify and obtain the available geophysical data for the Schreiber area of the western Wawa Subprovince, Ontario, followed by a detailed interpretation of all available geophysical data (e.g., magnetic, electromagnetic, gravity and radiometric). The aim was to identify additional information that could be extracted from the data, in particular with regard to the coincidence of geophysical features with mapped lithology and structural features in the Schreiber area.

The geophysical data covering the Schreiber area are of variable data resolution. Low to medium resolution geophysical data, particularly the magnetic, gravity and radiometric data obtained from the Geological Survey of Canada (GSC) cover the entire Schreiber area. An additional magnetic/electromagnetic survey obtained from the Ontario Geological Survey (OGS) provided higher resolution coverage over approximately 75% of the Schreiber area except for a north-south band along the western boundary of the Schreiber area. These surveys mainly covered greenstone belts, but also encompassed intrusive rocks in the central, west, south-west and south-east regions of the Schreiber area, namely the Crossman Lake, Whitesand Lake and Terrace Bay batholiths, and Mount Gwynne pluton.

The coincidence between the geophysical data and mapped lithology and structural features has been interpreted using all available geophysical data sets (e.g., magnetic, electromagnetic, gravity and radiometric). In particular, the pole reduced magnetic field (RTP) and its first vertical derivative (1VD of RTP) were the most reliable for identifying variations in geological contacts, and lithological heterogeneity. In addition, due to the limited overburden cover and the small size of water body features in the Schreiber area the radiometric survey data were useful to discriminate the lithological variations of the batholith and greenstone units, as well as differences within the batholiths. Geophysical data analysis provides additional insight into

compositional variations within mapped granitic intrusions of the Schreiber area. In general, the geophysical interpretations and the published geological maps are in reasonable agreement.

The magnetic response in the Schreiber area is observed as a generally subdued response over most of the granitic intrusions (e.g., Crossman Lake, and Terrace Bay batholiths) with the exception of the Whitesand Lake batholith. The Whitesand Lake batholith, as well as much of the greenstone belt in the area to the northeast of the Township of Schreiber, displays a strongly positive anomaly. This anomaly extends to the mid-point of the eastern boundary of the Schreiber area, where an especially strong response correlates with the felsic to intermediate metavolcanic rocks. With the exception of the greenstone belt units, the dominant magnetic signature corresponds to the Whitesand Lake batholith, reflecting an increased abundance of magnetic minerals. The eastern and northeastern boundary of the Whitesand Lake batholith, adjacent to the greenstone belt, displays an abrupt magnetic transition which is coincident with mapped contact in the bedrock geology, and with several mapped faults which follow major magnetic lows. Further north, the magnetic data show a general decrease in the magnetic intensity, which may indicate a subtle change in bedrock lithology approaching the Crossman Lake batholith. Although a discrete contact has never been mapped between the Whitesand Lake and the Crossman Lake batholiths, this transition zone may correspond to the change between the two batholiths. Similar lithological changes are observed in the radiometric data as discussed below. Much of the batholith displays an elevated magnetic response; even though the reduced magnetic field and the vertical magnetic derivative maps show several obvious magnetic perturbations indicative of heterogeneity within the intrusion. Additionally, some of the noisy magnetic response of the area underlain by the Whitesand Lake batholith may reflect the presence of remanent mafic metavolcanic rocks identified in bedrock maps intermixed with the internal batholith.

The magnetic response observed over the Crossman Lake batholith is characterized generally by a negative anomaly. The western half of the batholith exhibits a slightly higher magnetic response, which gradually decreases in an eastern direction. Peak anomaly values observed over the batholith may correspond to localized increases in the presence of magnetic minerals (e.g. remnant volcanic units), though a few well-defined linear magnetic highs are attributed to the presence of mapped diabase dykes (SRK, 2013). Processed magnetic images reveal the magnetic texture of the Crossman Lake batholith to be relatively flat, with several distinct linear structural trends superimposed that are coincident with the local faults and dykes mapped by the OGS. Contacts between the greenstone units and the Crossman Lake batholith generally are evident as an abrupt transitional boundary in the magnetic and processed magnetic field data, though locally the contact is reflected as a subtle gradational change, particularly along the northern boundary of the Crossman Lake batholith adjacent to the mafic and ultramafic units. This transitional magnetic response suggests that the mapped mafic and ultramafic units have a similar magnetic susceptibility as the granitic batholith. In addition, the overall outline of the Crossman Lake batholith is consistent with the bedrock geology map compiled by the OGS.

The Terrace Bay batholith is well delineated by several of the available geophysical data sets. It exhibits a generally subdued and fairly uniform magnetic response with the exception of a western region where a higher magnetic response is noted that could be due to an increased presence of magnetic minerals. A series of reversely magnetized diabase dykes oriented nearly

east-west is observed across the entire batholith and is identified in the magnetic data sets. However, these dykes are not evident in the apparent resistivity data, suggesting the limited presence or total absence of sulphide mineralization or other electrically conductive minerals along the magnetic low linear features. Radiometric data show a relatively moderate response in all radioelement concentrations.

The Mount Gwynne pluton possesses a distinct high magnetic signature that has similar characteristics to the Whitesand Lake batholith, which could be due to the presence of underlying and outcropping felsic metavolcanic rocks. The magnetic vertical derivative data sets show the presence of linear magnetic lows extending from the Terrace Bay batholith into the Mount Gwynne pluton, and beyond the edge of the survey data. These features are interpreted as the western extent of the same dyke systems observed in the Terrace Bay batholith. Apparent resistivity values calculated from the low frequency electromagnetic data for the pluton show a relatively uniform distribution, which is difficult to differentiate from the adjacent metavolcanic units of the greenstone belt.

The lack of detail shown by the gravity data reflects the sparse arrangement of gravity stations used to generate the grid in the Schreiber area. Thus, confidence in the ability to use the gravity data to interpret spatial variations in geology is low. However, some regional scale characterizations of the geological units are possible. Results show a positive gravity response is present through the Township of Schreiber that extends in a northeast direction from Lake Superior. Although the shape of the anomaly in the Schreiber area does not appear to reflect the mapped bedrock geology, the positive anomaly broadly encompasses the greenstone belt units surrounding the Township of Schreiber, as well as the southern end of the Whitesand Lake batholith, the Mount Gwynne pluton, and a part of the granitic intrusion bordering the southern margin of the Crossman Lake batholith.

A slight negative gravity response is present to the east of the Township of Schreiber that corresponds broadly to the outline of the Terrace Bay batholith. To the north and northwest of the Township of Schreiber a large and relatively negative gravity response underlies the Crossman Lake and Whitesand Lake batholiths, as well as the northern arm of the Schreiber-Hemlo greenstone belt. Although, the shape of these negative anomalies corresponds to only a few gravity station measurements, individual gravity values suggest the batholiths may either comprise a lower rock density or may extend to some depth.

## 7. REFERENCES

AECOM Canada Ltd., 2013a. Phase 1 Geoscientific Desktop Preliminary Assessment, Terrain and Remote Sensing Study, Township of Schreiber, Ontario. Prepared for Nuclear Waste Management Organization (NWMO). NWMO Report Number: APM-REP-06144-0036.

AECOM Canada Ltd., 2013b. Phase 1 Geoscientific Desktop Preliminary Assessment, Terrain and Remote Sensing Study, Township of Schreiber, Ontario. Prepared for Nuclear Waste Management Organization (NWMO). NWMO Report Number: APM-REP-06144-0036.

Baranov, V., 1957. A new method for interpretation of aeromagnetic maps: pseudo-gravimetric anomalies. *Geophysics*, vol. 22 (2), pp. 359–383.

Barnett, P.J., Henry, A.P. and Babuin, D. 1991. Quaternary geology of Ontario, west-central sheet; Ontario Geological Survey, Map 2554, scale 1:1,000,000.

Barnett, P.J. 1992. Quaternary Geology of Ontario. *In* Geology of Ontario, Ontario Geological Survey, Special Volume 4, Part 2, pp.1010–1088.

Bostock, H.S. 1970. Physiographic subdivisions of Canada. *In*: Geology and Economic Minerals of Canada, Geological Survey of Canada, Economic Geology Report no. 1, pp.11-30.

Buchan K.L., Halls, H.C. and Mortensen, J.K. 1996. Paleomagnetism, U-Pb geochronology, and geochemistry of Marathon dykes, Superior Province, and comparison with the Fort Frances swarm. *Canadian Journal of Earth Sciences*, vol. 33, pp. 1583-1595.

Buchan, K.L. and Ernst, R.E. 2004. Diabase dyke swarms and related units in Canada and adjacent regions. Geological Survey of Canada, Map 2022A, scale 1:5,000,000.

Campbell, J.E., Shives, R.B.K. and Klassen, R.A. 2002. Integrated Field Investigations of airborne Radiometric Spectral Domains, NEA–IAEA Test Area, Eastern Athabasca basin: A Preliminary Report. Summary of Investigations 2002, Volume 2, Saskatchewan Geological Survey, Sask. Industry Resources, Misc. Rep. 2002-4.2, CD-ROM, Paper D-13, 22p.

Campbell, D.A., Scott, J.F., Cooke, A., Brunelle, M.R., Lockwood, H.C. and Wilson, A.C. 2012. Report of Activities 2011, Resident Geologist Program, Thunder Bay South Regional Resident Geologist Report: Thunder Bay South District; Ontario Geological Survey, Open File Report 6273, 59p.

Canadian Geomagnetic Reference Field model (CGRF), [http://geomag.nrcan.gc.ca/mag\\_fld/cgrf-eng.php](http://geomag.nrcan.gc.ca/mag_fld/cgrf-eng.php)

Carter, M. W. 1981a. Precambrian Geology of the Schreiber Area, East Part, Thunder Bay District; Ontario Geological Survey Preliminary Map P. 2391, Geological Series, at a scale of 1:15,840 or 1 inch to 1/4 mile. Geology 1979.

Carter, M. W. 1981b. Precambrian Geology of the Terrace Bay Area, West Sheet, Thunder Bay District; Ontario Geological Survey Preliminary Map P. 2417, Geological Series, at a scale of 1:15,840 or 1 inch to 1/4 mile. Geology 1980.

Carter, M. W. 1981c. Precambrian Geology of the Terrace Bay Area, East Sheet, Thunder Bay District; Ontario Geological Survey Preliminary Map P. 2418, Geological Series, at a scale of 1:15,840 or 1 inch to 1/4 mile. Geology 1979.

Carter, M.W. 1988. Geology of Schreiber-Terrace Bay area, District of Thunder Bay. Ontario Geological Survey, Open File Report 5692, 287p.

Corfu, F. and Muir, T.L. 1989. The Hemlo-Heron Bay greenstone belt and Hemlo Au-Mo deposit, Superior Province, Ontario, Canada: 1. Sequence of Igneous activity determined by zircon U-Pb geochronology. *Chemical Geology*, vol. 79, pp. 183-200.

Davis, D.W., and Lin, S. 2003. Unraveling the geologic history of the Hemlo Archean gold deposit, Superior Province, Canada; a U-Pb geochronological study. *Economic Geology and the Bulletin of the Society of Economic Geologists* 98, pp. 51-67.

Farrand, W.R. and Drexler, C.W. 1985. Late Wisconsinan and Holocene history of the Lake Superior basin; *In Quaternary Evolution of the Great Lakes*, Geological Association of Canada, Special Paper 30, pp.17-32.

Gartner, J.F. 1979a. Schreiber area (NTS 42D/NW), District of Thunder Bay; Ontario Geological Survey, Northern Ontario Engineering Geology Terrain Study 59, 15p.

Gartner, J.F. 1979b. Roslyn Lake area (NTS 42E/SW), District of Thunder Bay; Ontario Geological Survey, Northern Ontario Engineering Geology Terrain Study 43, 12p.

GDAL, 2012. Geospatial Data Abstraction Library, <http://www.gdal.org/>

GOCAD Mining Suite, Mira Geoscience Ltd., 2012. [http://www.mirageoscience.com/software/gocad\\_mining\\_suite.php](http://www.mirageoscience.com/software/gocad_mining_suite.php)

GOCAD, Paradigm Ltd.,  
<http://www.pdgm.com/Products/GOCAD.aspx>

Gupta, V., Paterson, N., Reford, S., Kwan, K., Hatch, D., and Macleod, I., 1989, Single master aeromagnetic grid and magnetic colour maps for the province of Ontario: in Summary of field work and other activities 1989, Ontario Geological Survey Miscellaneous Paper 146, pp.244-250.

Hamilton M.A., David, D.W., Buchan, K.L. and Halls H.C. 2002. Precise U-Pb dating of reversely magnetized Marathon diabase dykes and implications for emplacement of giant dyke swarms along the southern margin of the Superior Province, Ontario. Geological Survey of Canada, Current Research 2002-F6, 10p.

International Association of Geodesy (IAG) Sixteenth General Assembly (1975) proceedings, Grenoble, France, Bulletin Géodésique 118, pp.365.

International Atomic Energy Agency (IAEA), 2003. Guidelines for radioelement mapping using gamma ray spectrometry data, IAEA-TECDOC-1363.

Jackson, S.L. 1998. Stratigraphy, structure and metamorphism; Part 1, p.1--58, in S.L. Jackson, G.P. Beakhouse and D.W. Davis, Geological Setting of the Hemlo Gold Deposit; an Interim Progress Report, Ontario Geological Survey, Open File Report 5977, 121p.

Johns, G.W., McIlraith, S., and Stott, G.M. 2003. Precambrian geology compilation map–Longlac sheet; Ontario Geological Survey, Map 2667, scale 1:250 000.

Lin, S. 2001. Stratigraphic and Structural Setting of the Hemlo Gold Deposit, Ontario, Canada. Economic Geology, v. 96, pp. 477–507.

Marmont, S. 1984. The Terrace Bay Batholith and Associated Mineralization. Ontario Geological Survey Open File Report 5514, 95p.

Miller, H.G., and Singh, V., 1994. Potential field tilt - a new concept for location of potential field sources. Journal of applied Geophysics, Vol. 32, Issues 2-3, August 1994, pp. 213-217.

Ministry of Natural Resources (MNR), 2012. Licence and permit list. [http://www.mnr.gov.on.ca/en/Business/Aggregates/2ColumnSubPage/STDPROD\\_091593.html](http://www.mnr.gov.on.ca/en/Business/Aggregates/2ColumnSubPage/STDPROD_091593.html)

Ministry of Northern Development and Mines (MNDM). 2012. Geo-Claims Internet Application. [http://www.mndm.gov.on.ca/mines/claimaps\\_e.asp](http://www.mndm.gov.on.ca/mines/claimaps_e.asp).

Morris, T.F. 2000. Quaternary geology mapping and overburden sampling, Schreiber area, northwestern Ontario; *In* Summary of Field Work and Other Activities 2000, Ontario Geological Survey, Open File Report 6032, pp.33-1 to 33-7.

Morris, T.F. 2001. Geochemical and till pebble lithology data related to the Schreiber-Killala Lake overburden mapping and sampling program, Northwestern Ontario; Ontario Geological Survey, Miscellaneous Release – Data 74.

Muir, T.L. 2003. Structural evolution of the Hemlo greenstone belt in the vicinity of the world-class Hemlo gold deposit. Can. J. Earth Sci. v40, pp. 395-430.

Nabighian, M.N. 1972. The analytic signal of two-dimensional magnetic bodies with

polygonal cross-section: Its properties and use for automated anomaly interpretation. *Geophysics*, vol. 37, pp. 507-517.

Natural Resources of Canada (NRCan), 2005. Geoscience Data Repository, Gravity point data description, [http://gdrdap.agg.nrcan.gc.ca/geodap/docs/GDR-DAP\\_gravity\\_19may2005.pdf](http://gdrdap.agg.nrcan.gc.ca/geodap/docs/GDR-DAP_gravity_19may2005.pdf)

Natural Resources of Canada (NRCan), 2012a. Aeromagnetic and Electromagnetic data, Canadian Aeromagnetic Data Base, [http://gdr.nrcan.gc.ca/aeromag/about\\_e.php](http://gdr.nrcan.gc.ca/aeromag/about_e.php)

Natural Resources of Canada (NRCan), Gravity data, 2012b. Canadian Gravity Anomaly Data Base, [http://gdr.nrcan.gc.ca/gravity/about\\_e.php](http://gdr.nrcan.gc.ca/gravity/about_e.php)

Natural Resources of Canada (NRCan), 2012c. Radioactivity data, Airborne gamma-ray spectrometry, [http://gdr.nrcan.gc.ca/gamma/about\\_e.php](http://gdr.nrcan.gc.ca/gamma/about_e.php)

Nuclear Waste Management Organization (NWMO), 2010. Moving forward together: Process for selecting a site for Canada's deep geological repository for used nuclear fuel, May 2010.

NWMO, 2013. Preliminary Assessment for Siting a Deep Geological Repository for Canada's Used Nuclear Fuel - Township of Schreiber, Ontario - Findings from Phase One Studies. NWMO Report Number APM-REP-06144-0033.

Osmani, I.A. 1991. Proterozoic mafic dike swarms in the Superior Province of Ontario. *In* *Geology of Ontario*, Ontario Geological Survey, Special Volume 4, Part 1, pp.661-681.

Ontario Geological Survey (OGS). 2003. Schreiber Area, Ontario Airborne Geophysical Surveys, Magnetic and Electromagnetic Data, Geophysical Data Set 1104 – Revised, 2003.

Ontario Geological Survey (OGS).. 2011. 1:250 000 Scale Bedrock Geology of Ontario; Ontario Geological Survey, Miscellaneous Release-Data 126-revised.

Ontario Geological Survey (OGS), Geophysical Atlas of Ontario, 2012. [http://www.mndm.gov.on.ca/mines/ogs/gpxatlas/default\\_e.asp](http://www.mndm.gov.on.ca/mines/ogs/gpxatlas/default_e.asp)

Pesonen, L.J. and Halls, H.C. 1983. Geomagnetic field intensity and reversal asymmetry in late Precambrian Keweenawan rocks. *Geophys. J. R. Astr. Soc.* Vol. 73, pp. 241-270.

Peterman, Z.E. and Day, W. 1989. Early Proterozoic activity on Archean faults in the Western Superior Province – evidence from pseudotachylite. *Geology*, vol. 17, pp. 1089-1092.

Polat, A. 1998. Geodynamics of the Late Archean Wawa Subprovince greenstone belts, Superior Province, Canada. PhD Thesis, Department of Geological Sciences, University of Saskatchewan, Saskatoon, 249p.

Polat, A., Kerrich, R. and Wyman, D.A. 1998. The late Archean Schreiber–Hemlo and White River–Dayohessarah greenstone belts, Superior Province: collages of oceanic plateaus, oceanic arcs, and subduction–accretion complexes. *Tectonophysics*, vol. 289, pp. 295–326.

Polat, A. and Kerrich, R. 1999. Formation of an Archean tectonic mélange in the Schreiber–Hemlo greenstone belt, Superior Province, Canada: Implications for Archean subduction–accretion process; *Tectonics*, v. 18, pp.733–755.

Reford, S.W., Gupta, V.K., Paterson, N.R., Kwan, K.C.H., and Macleod, I.N., 1990, Ontario master aeromagnetic grid: A blueprint for detailed compilation of magnetic data on a regional scale: in *Expanded Abstracts, Society of Exploration Geophysicists, 60th Annual International Meeting, San Francisco, v.1.*, pp.617-619.

Sado, E.V. and Carswell, B.F. 1987. Surficial geology of northern Ontario; Ontario Geological Survey, Map 2518, scale 1:1,200,000.

Santaguida, F. 2002. Precambrian geology compilation series–Schreiber sheet; Ontario Geological Survey, Map 2665, scale 1:250 000.

Smyk, M.C. and Schnieders, B.R. 1995. Geology of the Schreiber Greenstone Assemblage and its Gold and Base Metal Mineralization. Institute on Lake Superior Geology 41st Annual Meeting, Proceedings Volume 41, Field Trip Guidebook, 86p.

SRK Consulting Inc., 2013. Phase 1 Geoscientific Desktop Preliminary Assessment, Lineament Interpretation, Township of Schreiber, Ontario. Prepared for Nuclear Waste Management Organization (NWMO). NWMO Report Number: APM-REP-06144-0038.

Szewczyk, Z., J. and G.F. West, 1976. Gravity study of an Archean granitic area northwest of Ignace, Ontario *Canadian Journal of Earth Sciences* 13, pp. 1119-1130

Telford, W. M., Geldart, L. P., Sheriff, R. E., 1990. *Applied Geophysics* Second Edition. Cambridge University Press, 1990-10-26, 792 p.

Thurston, P.C. 1991. Geology of Ontario: Introduction. in *Geology of Ontario*, Ontario Geological Survey, Special Volume 4, Part 1, pp. 3-25.

Williams, H. R., G.M. Stott, K.B. Heather, T.L. Muir and R.P. Sage. 1991. Wawa Subprovince. in *Geology of Ontario*, Ontario Geological Survey, Special Volume 4, Part 1, pp. 485-525.

WinDisp, 2012. Scientific Computing and Applications, J. Paine, <http://www.scicomap.com/prod01.htm>

Zoltai, S. C. 1965. Surficial geology of the Thunder Bay map area; Ontario Department of Lands and Forests. Map S265.



## Figures

Figure 1: Township of Schreiber and Surrounding Area

Figure 2: Regional Tectonic Setting of Schreiber and Surrounding Area

Figure 3: Local Bedrock Geology of the Schreiber Area

Figure 4: Terrain Features of the Schreiber Area

Figure 5: Magnetic and Electromagnetic Survey Flight lines in the Schreiber Area

Figure 6: Very Low Frequency Electromagnetic and Radiometric Flight Lines in the Schreiber Area

Figure 7: Reduced to Pole Residual Magnetic Field in the Schreiber Area

Figure 8: First Vertical Derivative of Reduced to Pole Residual Magnetic Field in the Schreiber Area

Figure 9: Second Vertical Derivative of Reduced to Pole Residual Magnetic Field in the Schreiber Area

Figure 10: Tilt Angle of Reduced to Pole Magnetic Field in the Schreiber Area

Figure 11: Analytical Signal of Residual Magnetic Field in the Schreiber Area

Figure 12: Bouguer Gravity Field with Station Locations in the Schreiber Area

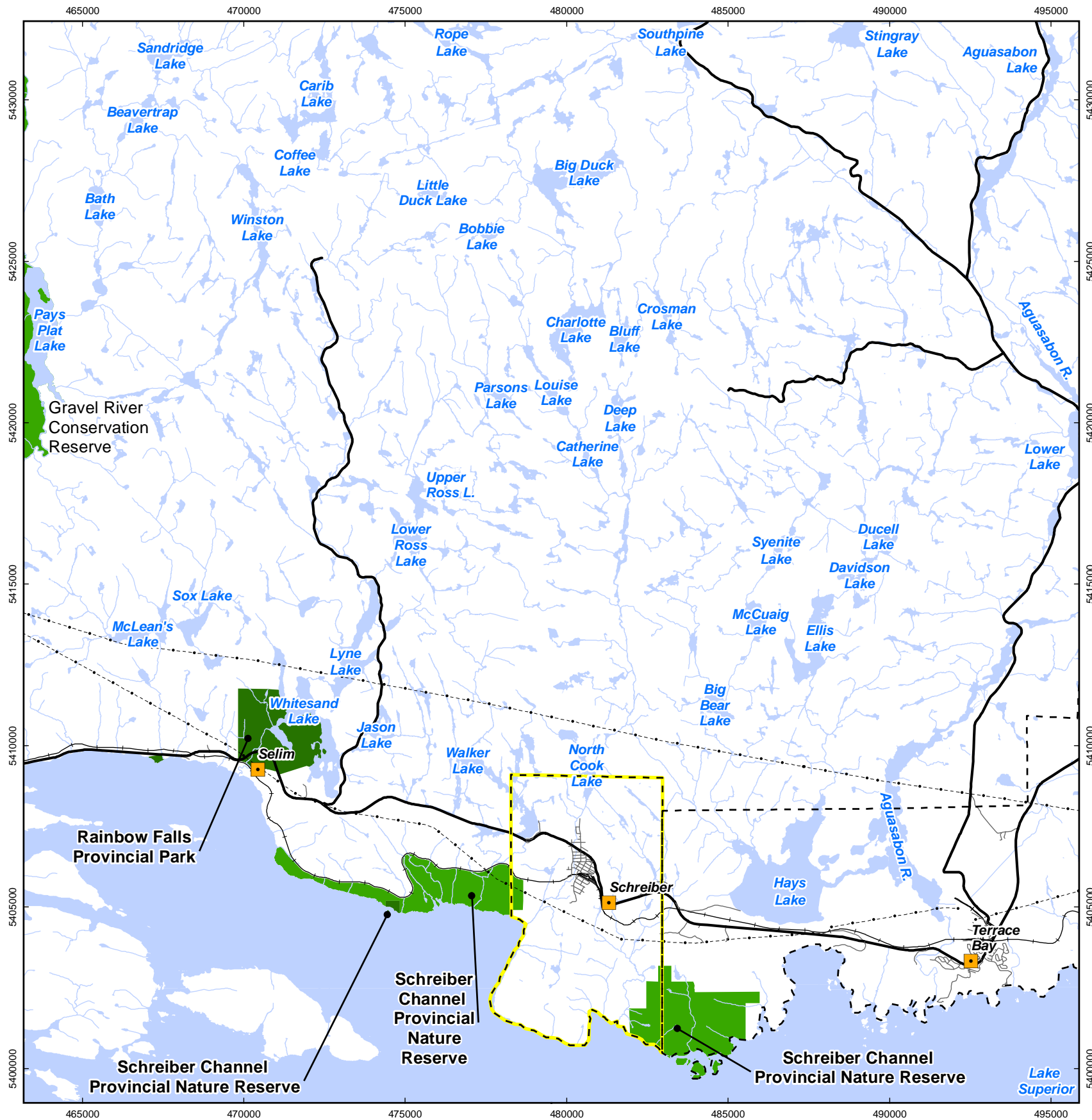
Figure 13: Radiometric Ternary Image in the Schreiber Area

Figure 14: Very Low Frequency Electromagnetic (VLF-EM) Data in the Schreiber Area

Figure 15: Apparent Resistivity from Low Frequency (877 Hz) Electromagnetic Data in the Schreiber Area

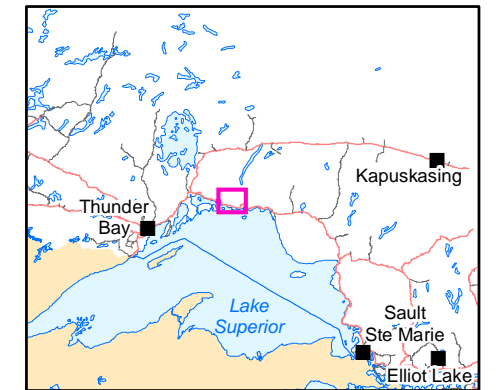
Figure 16: Geophysical Interpretation Showing Distribution of Bedrock Units for the Schreiber area





**Legend**

- City / Towns
- ▭ Township of Schreiber
- ▭ Township of Terrace Bay
- Main Road
- Local Road
- Railway
- Transmission Line
- Watercourse
- Waterbody
- Protected Areas
- Provincial Park
- Conservation Reserve



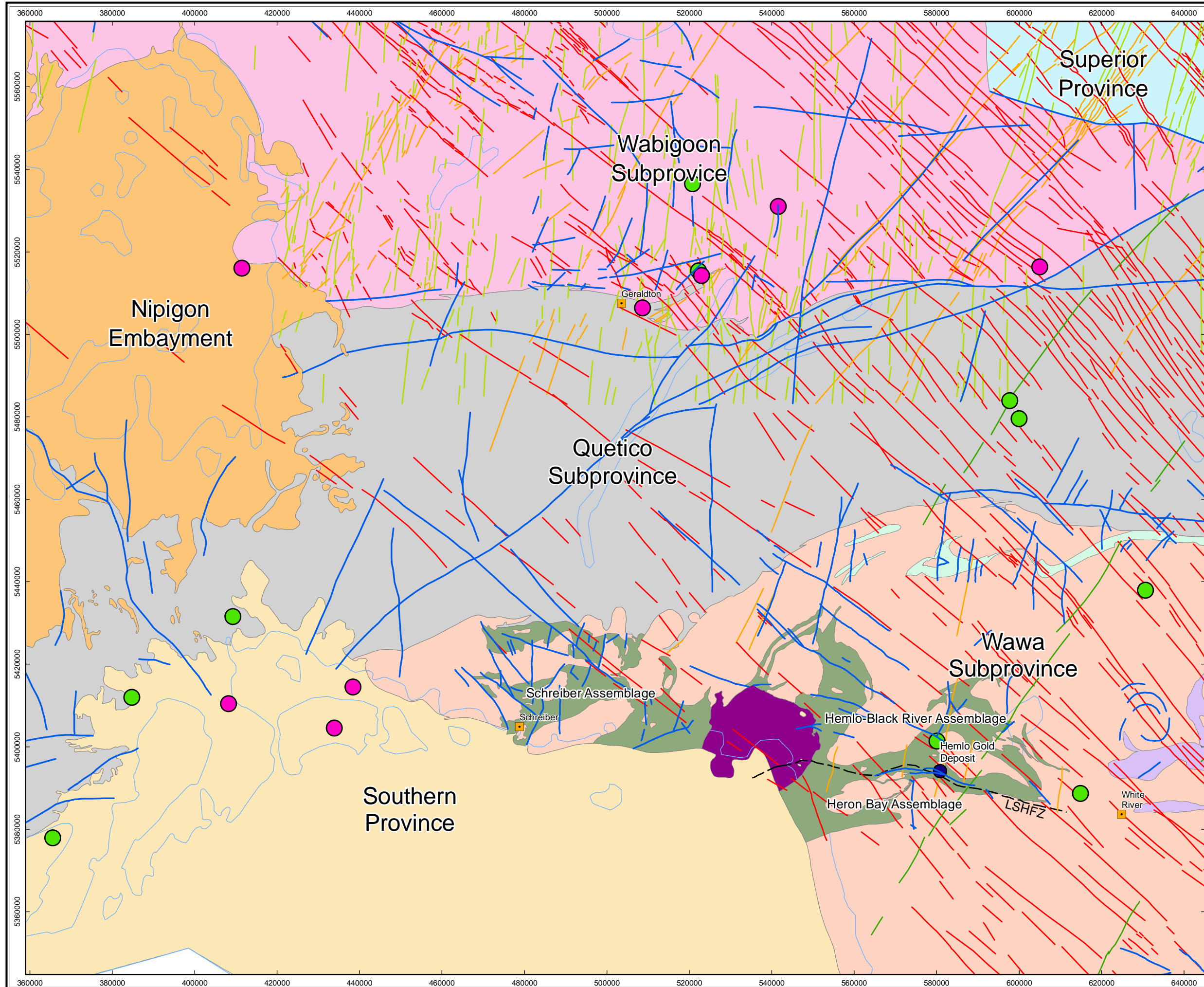
Data Sources:  
 Parks: LIO CLUPA designation  
 Rail: LIO Railway  
 Road: LIO Road Segment  
 Township: LIO Township  
 Utility: LIO Utility Line  
 Waterbody: LIO Waterbody  
 Watercourse: LIO Watercourse  
 Figure reproduced from AECOM (2013)



PROJECT  
 Phase 1 Geoscientific Desktop Preliminary Assessment,  
 Geophysics Study, Schreiber Area, Ontario

TITLE  
**Township of Schreiber and Surrounding Area**

DESIGN	GHF	14 Aug 2012	<b>Figure 1</b>	REVISION 7
GIS	JA	07 Aug 2013		UTM ZONE 16
CHECK	IV	07 Aug 2013		NAD 1983
REVIEW	IV	07 Aug 2013		1:150,000



**Legend**

- Community
- Waterbody
- Hemlo Gold Deposit
- Lake Superior-Hemlo Fault Zone (LSHFZ)
- Geological Subprovince Boundary
- Fault

**Seismic Events (Magnitude)**

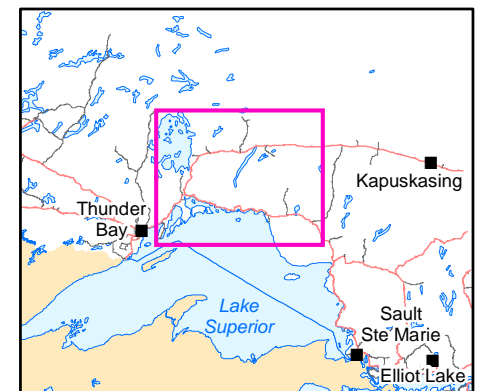
- 1.0 - 2.0
- 2.1 - 3.0

**Dykes**

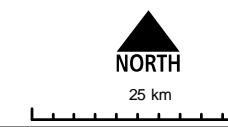
- Biscotasing mafic dyke
- Marathon mafic dyke
- Marathon, Kapuskasing or Biscotasing mafic dyke
- Matachewan mafic dyke

**Regional Tectonic Geology**

- Nipigon Embayment
- Quetico Subprovince
- Southern Province
- Superior Province
- Wabigoon Subprovince
- Wawa Subprovince
- Schreiber-Hemlo Greenstone Belt
- Coldwell Alkalic Complex
- Manitouwadge-Hornepayne Greenstone Belt
- White River-Dayohessarah Greenstone Belt



Data Sources:  
 Bedrock: OGS MRD 126-REV-1 (1:250,000)  
 Earthquake: NRCAN Earthquake Database  
 Figure reproduced from AECOM (2013)

  
 NORTH  
 25 km

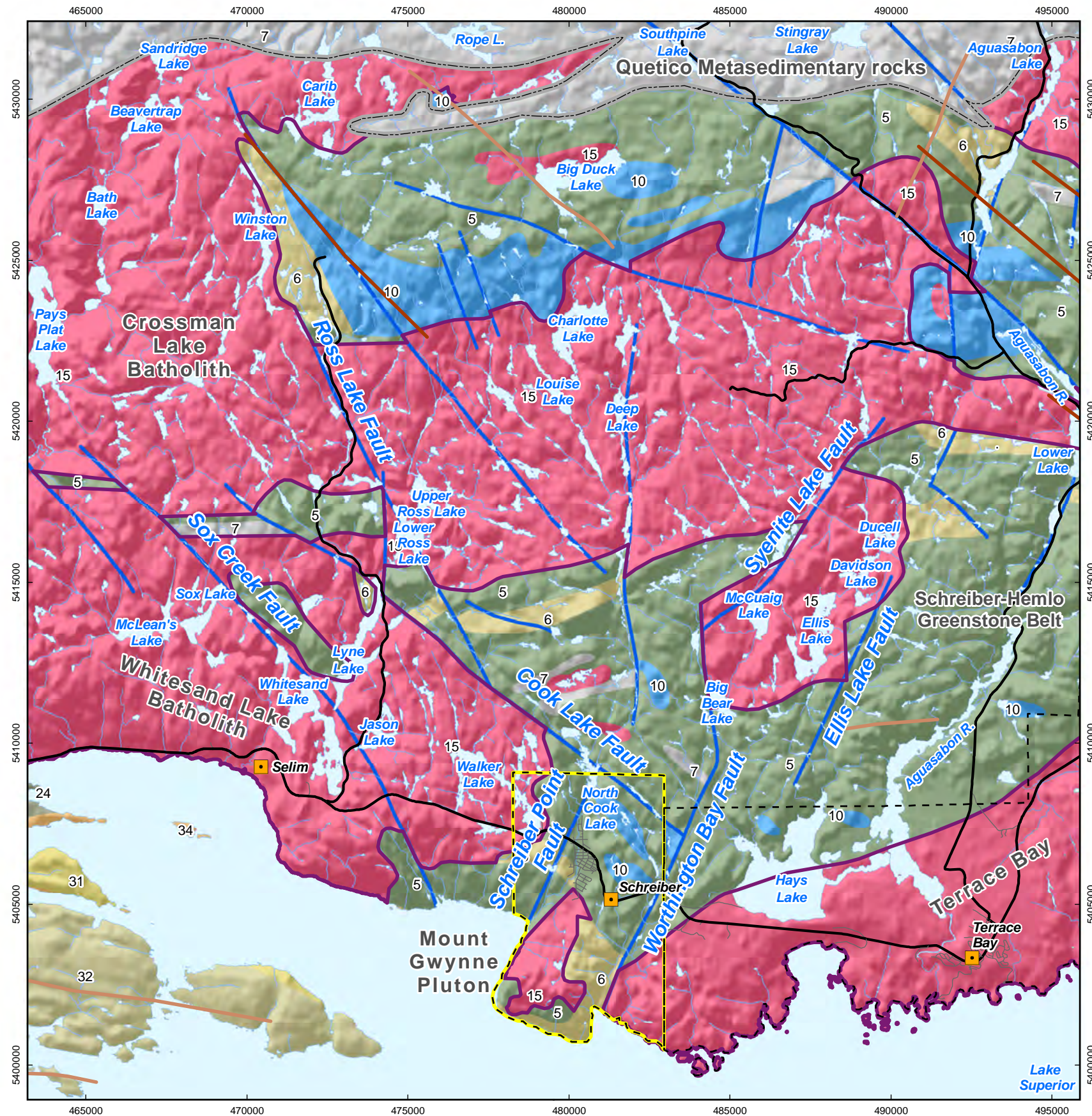
**AECOM**

PROJECT  
 Phase 1 Geoscientific Desktop Preliminary Assessment,  
 Geophysics Study, Schreiber Area, Ontario

TITLE  
**Regional Tectonic Setting of  
 Schreiber and Surrounding Area**

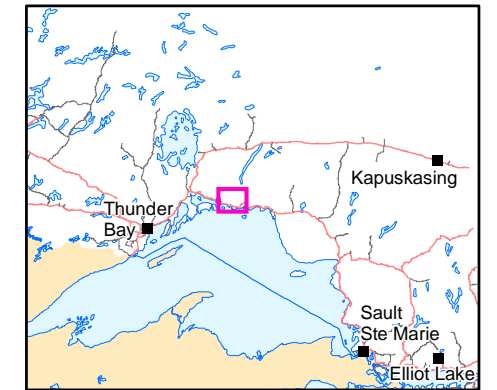
DESIGN	GHF	14 Aug 2012	<b>Figure 2</b>	REVISION 3
GIS	GHF	30 Nov 2012		UTM ZONE 16
CHECK	IV	08 Aug 2013		NAD 1983
REVIEW	IV	08 Aug 2013		1:892,000





**LEGEND**

- City / Towns
  - Township of Schreiber
  - Township of Terrace Bay
  - Main Road
  - Local Road
  - Watercourse
  - Waterbody
- Dykes**
- Marathon, Kapuskasing or Biscotasing Mafic Dyke
  - Matachewan Mafic Dyke
  - Dyke (other)
  - Fault
  - Quetico/Wawa Subprovince boundary
- Bedrock Geology (Youngest to Oldest)**
- 34. Mafic dykes and related intrusive rocks (Keweenawan age) (circa 1.1 to 1.2 Ga)
  - 32. Osler Gp., Maminse Point Fm., Michipicoten Island Fm.
  - 31. Sibley Gp.
  - 24. Sedimentary rocks
  - 15. Massive granodiorite to granite
  - 11. Gneissic tonalite suite
  - 10. Mafic and ultramafic rocks
  - 7. Metasedimentary rocks
  - 6. Felsic to intermediate metavolcanic rocks
  - 5. Mafic to intermediate metavolcanic rocks
  - 2. Felsic to intermediate metavolcanic rock
  - Batholith / Pluton



Data Sources:  
 Bedrock: OGS MRD 126-REV1 (1:250,000)  
 Faults: OGS MRD 126-REV1 (1:250,000)  
 Dike: OGS MRD 126-REV1 (1:250,000)  
 Batholith: Generalized from OGS 2006  
 Cities/Towns: LIO Cities and Towns  
 Road: LIO Road Segment  
 Township: LIO Township  
 Waterbody: LIO Waterbody  
 Watercourse: LIO Watercourse  
 Figure reproduced from AECOM (2013)



4.5 km

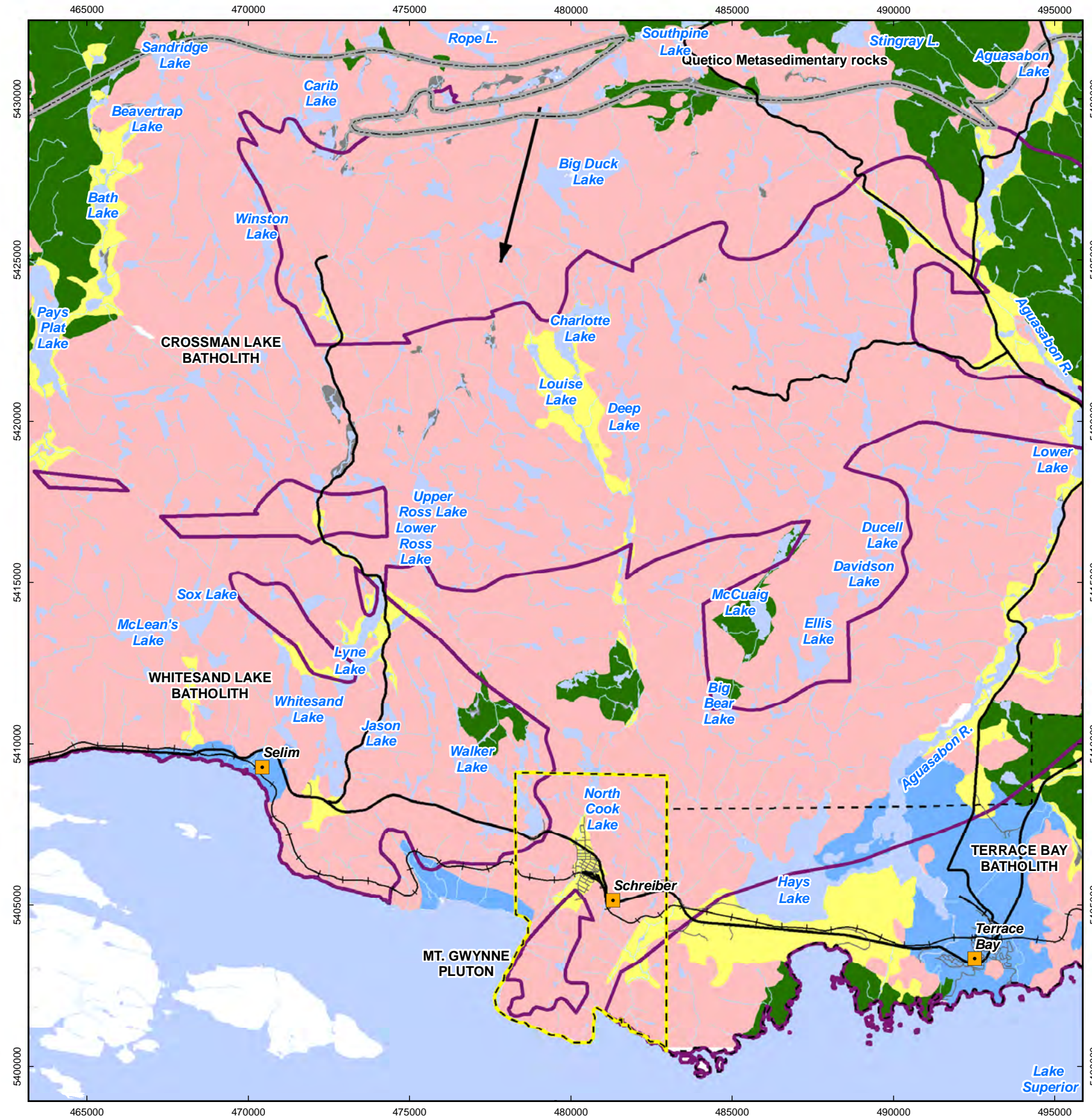


PROJECT  
 Phase 1 Geoscientific Desktop Preliminary Assessment,  
 Geophysics Study, Schreiber Area, Ontario

TITLE  
**Local Bedrock Geology of the Schreiber Area**

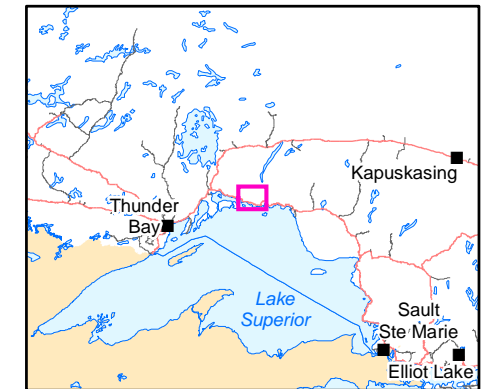
DESIGN	GHF	14 Aug 2012	<b>Figure 3</b>	REVISION 7
GIS	GHF/JA	02 Aug 2013		UTM ZONE 16
CHECK	IV	02 Aug 2013		NAD 1983
REVIEW	IV	02 Aug 2013		1:150,000





**LEGEND**

- Cities/Towns
  - Township of Schreiber
  - Township of Terrace Bay
  - Main Road
  - Local Road
  - Railways
  - Watercourse
  - Waterbody
  - Quetico/Wawa Subprovince boundary
  - Outline of Batholith / Pluton
- Surficial Geology**
- Morainal Terrain
  - Glaciofluvial Terrain
  - Glaciolacustrine Terrain
  - Organic Terrain
  - Bedrock Terrain
- Average Ice-Flow Direction for Area



Data Sources:  
 Overburden: OGS MRD-160 (1:100,000)  
 Batholith: Generalized from OGS 2006  
 Cities/Towns: LIO Cities and Towns  
 Road: LIO Road Segment  
 Township: LIO Township  
 Waterbody: LIO Waterbody  
 Watercourse: LIO Watercourse  
 Figure reproduced from AECOM (2013)

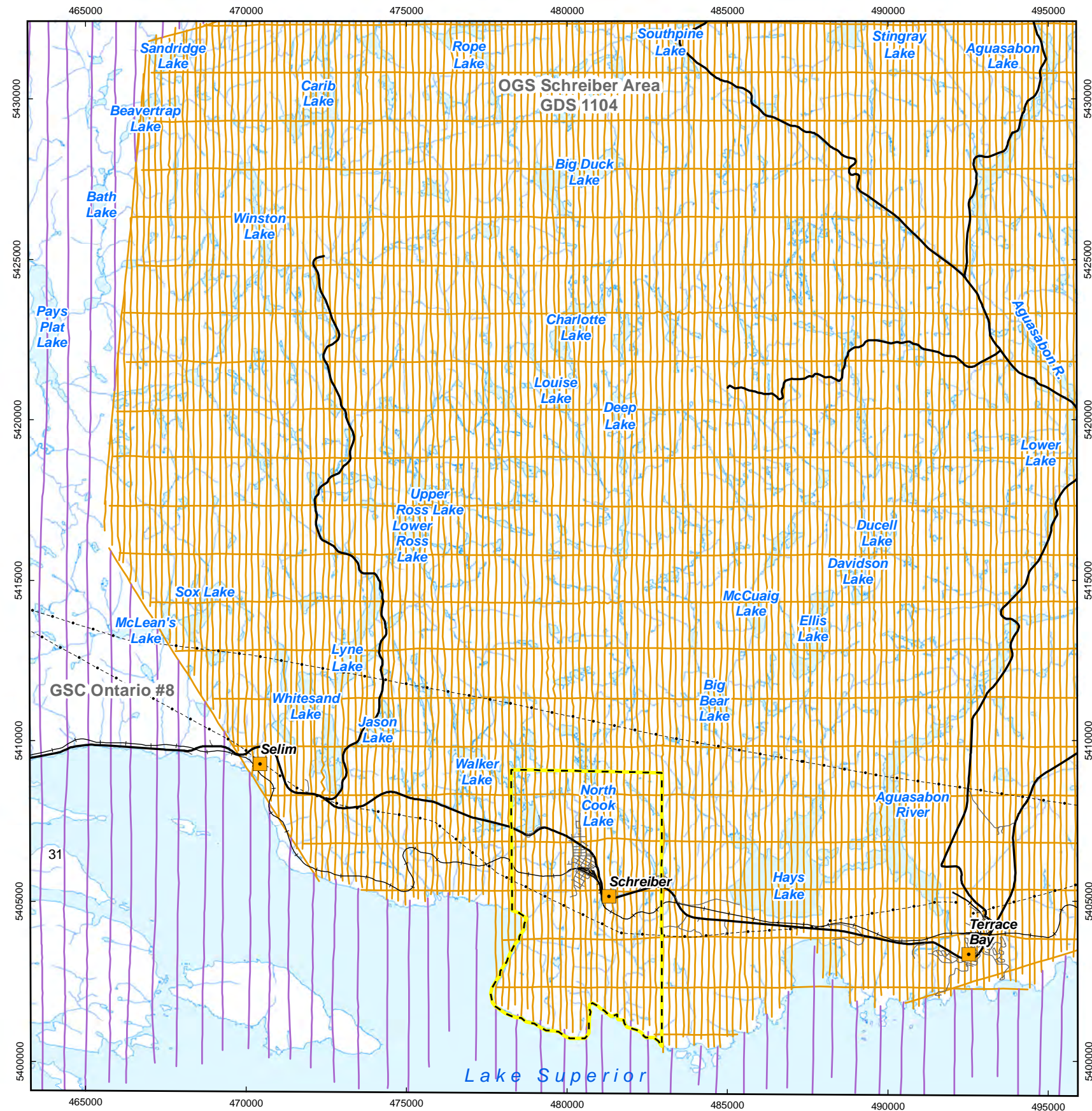


PROJECT  
 Phase 1 Geoscientific Desktop Preliminary Assessment,  
 Geophysics Study, Schreiber Area, Ontario

TITLE  
**Terrain Features of the Schreiber Area**

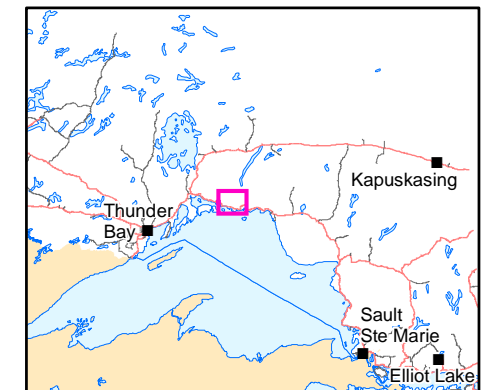
DESIGN	GHF	14 Aug 2012	<b>Figure 4</b>	REVISION 7
GIS	GHF/JA	02 Aug 2013		UTM ZONE 16
CHECK	IV	02 Aug 2013		NAD 1983
REVIEW	IV	02 Aug 2013		1:150,000





**LEGEND**

- City / Towns
- ▭ Township of Schreiber
- Main Road
- Local Road
- Railway
- Transmission Line
- Watercourse
- Waterbody
- OGS Schreiber Area survey GDS1104
- GSC Ontario #8



Data Sources:  
 Road: LIO Road Segment  
 Township: LIO Township  
 Waterbody: LIO Waterbody  
 Geophysical Data:  
 OGS Schreiber Area survey GDS1104  
 GSC Ontario #8

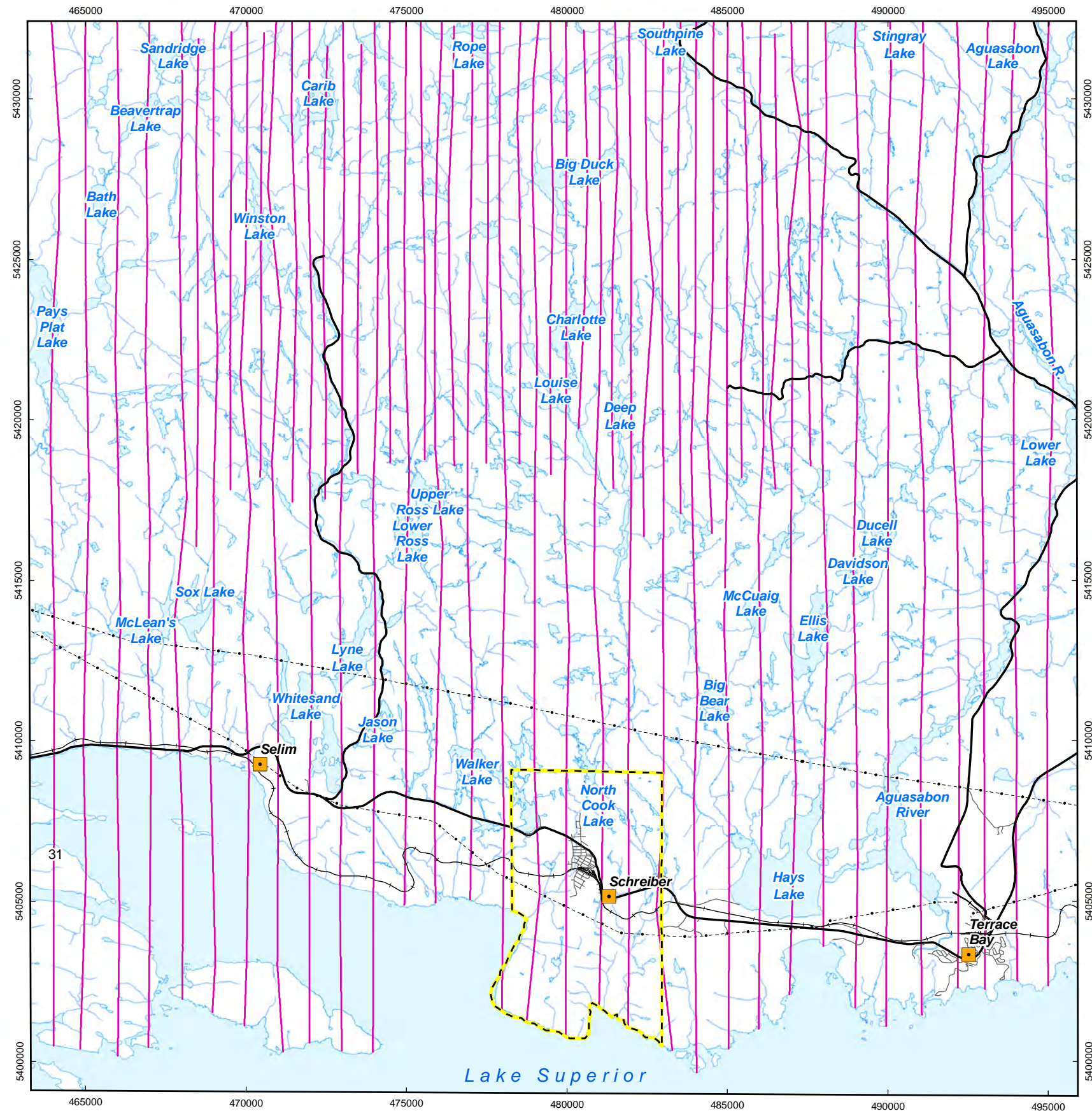


PROJECT  
 Phase 1 Geoscientific Desktop Preliminary Assessment,  
 Geophysics Study, Schreiber Area, Ontario

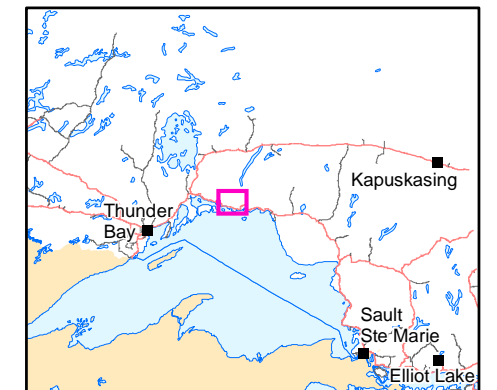
TITLE  
**Magnetic and Electromagnetic Survey Flight Lines  
 in the Schreiber Area**

DESIGN	GHF	14 Aug 2012	<b>Figure 5</b>	REVISION 7
GIS	JA	07 Aug 2013		UTM ZONE 16
CHECK	IV	07 Aug 2013		NAD 1983
REVIEW	IV	07 Aug 2013		1:150,000





- LEGEND**
- City / Towns
  - ▭ Township of Schreiber
  - Main Road
  - Local Road
  - Railway
  - Transmission Line
  - Watercourse
  - Waterbody
  - VLF Profile, Schreiber (GSC2514)



Data Sources:  
 Road: LIO Road Segment  
 Township: LIO Township  
 Waterbody: LIO Waterbody  
 Geophysical Data:  
 GSC Schreiber survey GSC2514



PROJECT  
 Phase 1 Geoscientific Desktop Preliminary Assessment,  
 Geophysics Study, Schreiber Area, Ontario

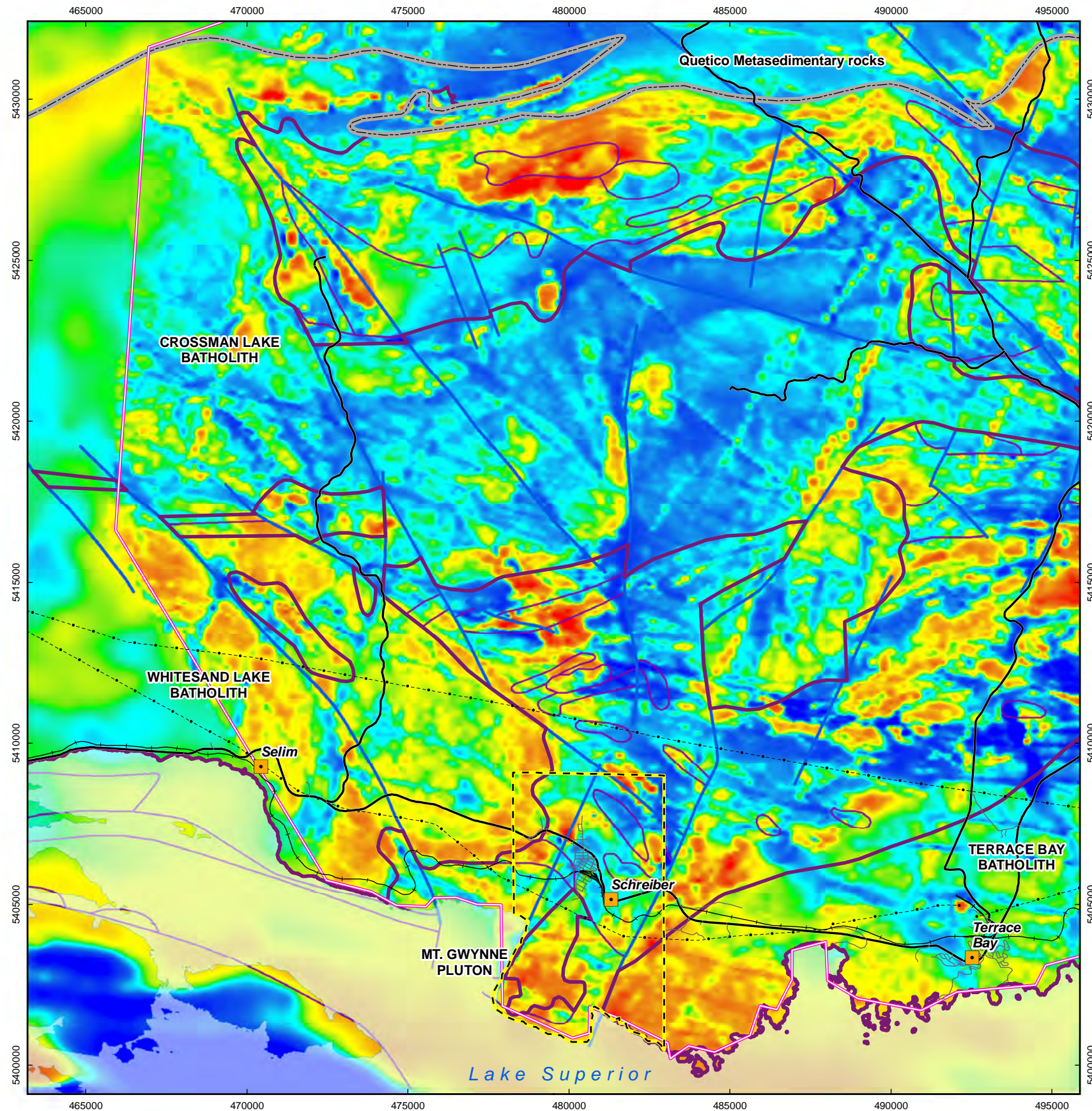
TITLE  
**Very Low Frequency Electromagnetic and  
 Radiometric Flight Lines in the Schreiber Area**

DESIGN	GHF	14 Aug 2012
GIS	JA	07 Aug 2013
CHECK	IV	07 Aug 2013
REVIEW	IV	07 Aug 2013

**Figure 6**

REVISION 7
UTM ZONE 16
NAD 1983
1:150,000

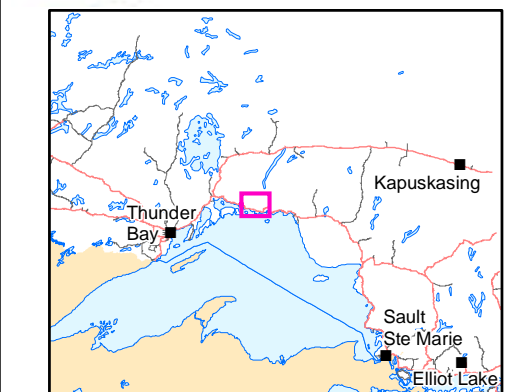
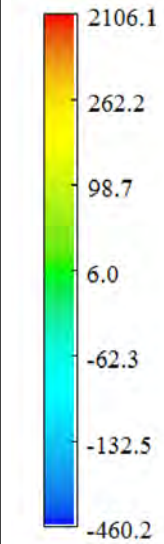




**LEGEND**

- City / Towns
- Township of Schreiber
- Main Road
- Local Road
- Railway
- Transmission Line
- Lake Superior
- Mapped Fault
- Geological Contact
- Quetico-Wawa Subprovince boundary
- Batholith / Pluton
- OGS Schreiber Area (GDS1104)

*Residual Magnetic Field (nT)*



Data Sources:  
 Road: LIO Road Segment  
 Township: LIO Township  
 Waterbody: LIO Waterbody  
 Geology: Bedrock Geology of Ontario MRD126, Rev1  
 Geophysical Data:  
 OGS Schreiber Area survey GDS1104  
 GSC Magnetic 200m Compilation



4.5 km

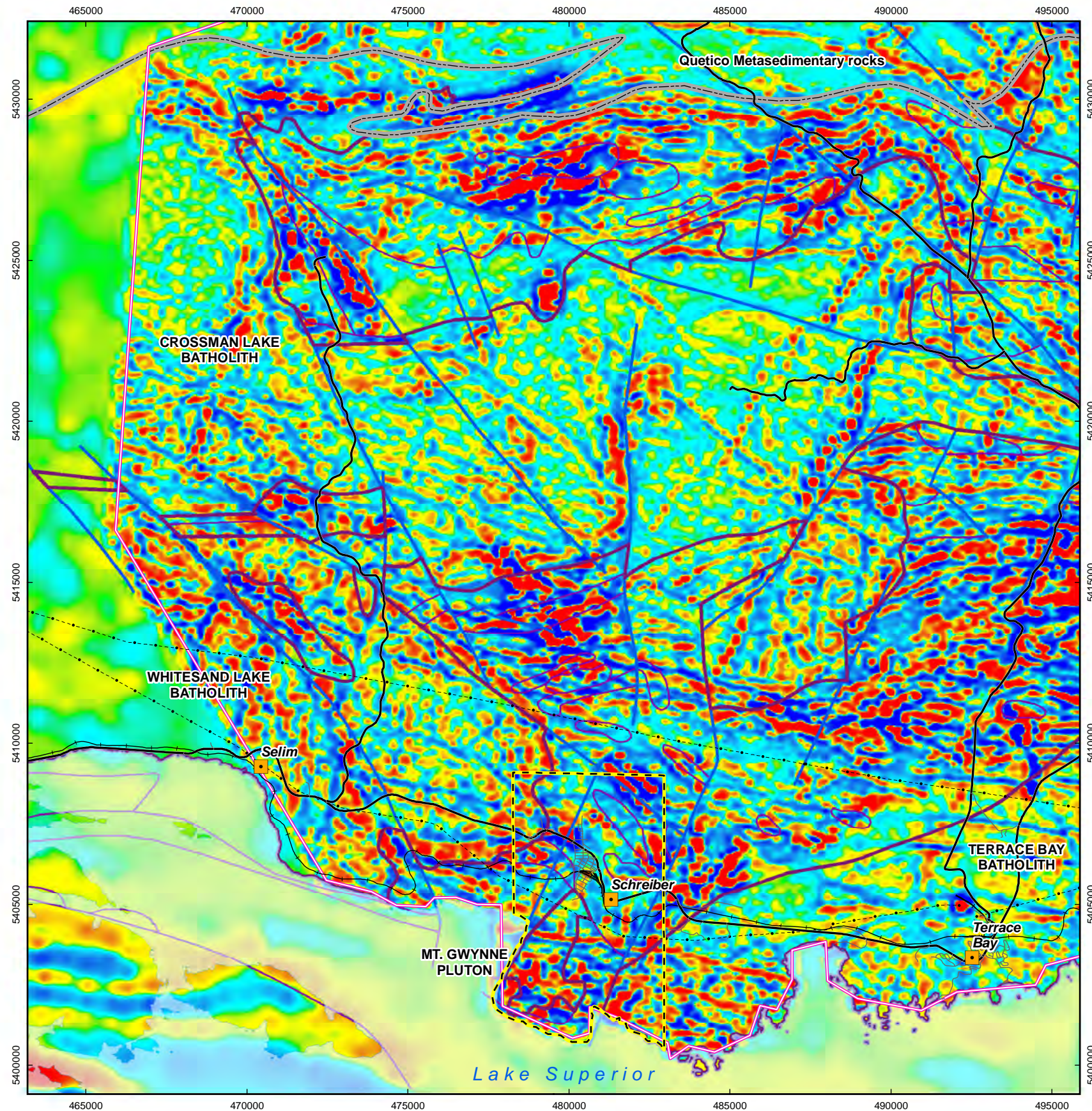


PROJECT  
 Phase 1 Geoscientific Desktop Preliminary Assessment,  
 Geophysics Study, Schreiber Area, Ontario

TITLE  
**Reduced to Pole Residual Magnetic Field  
 in the Schreiber Area**

DESIGN	GHF	14 Aug 2012	<b>Figure 7</b>	REVISION 7
GIS	JA	07 Aug 2013		UTM ZONE 16
CHECK	IV	07 Aug 2013		NAD 1983
REVIEW	IV	07 Aug 2013		1:150,000

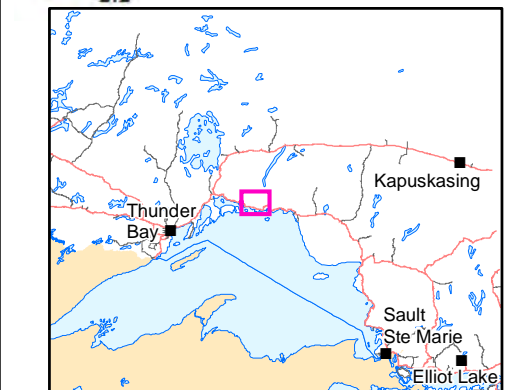
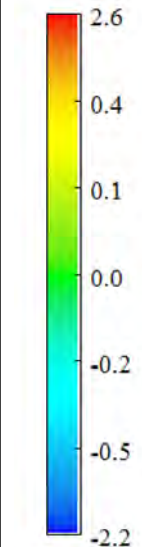




**LEGEND**

- City / Towns
- Township of Schreiber
- Main Road
- Local Road
- Railway
- Transmission Line
- Lake Superior
- Mapped Fault
- Geological Contact
- Quetico-Wawa Subprovince boundary
- Batholith / Pluton
- OGS Schreiber Area (GDS1104)

*First Vertical Derivative (nT/m)*



Data Sources:

- Road: LIO Road Segment
- Township: LIO Township
- Waterbody: LIO Waterbody
- Geology: Bedrock Geology of Ontario MRD126, Rev1
- Geophysical Data: OGS Schreiber Area survey GDS1104
- GSC Magnetic 200m Compilation



NORTH

4.5 km



PROJECT  
Phase 1 Geoscientific Desktop Preliminary Assessment,  
Geophysics Study, Schreiber Area, Ontario

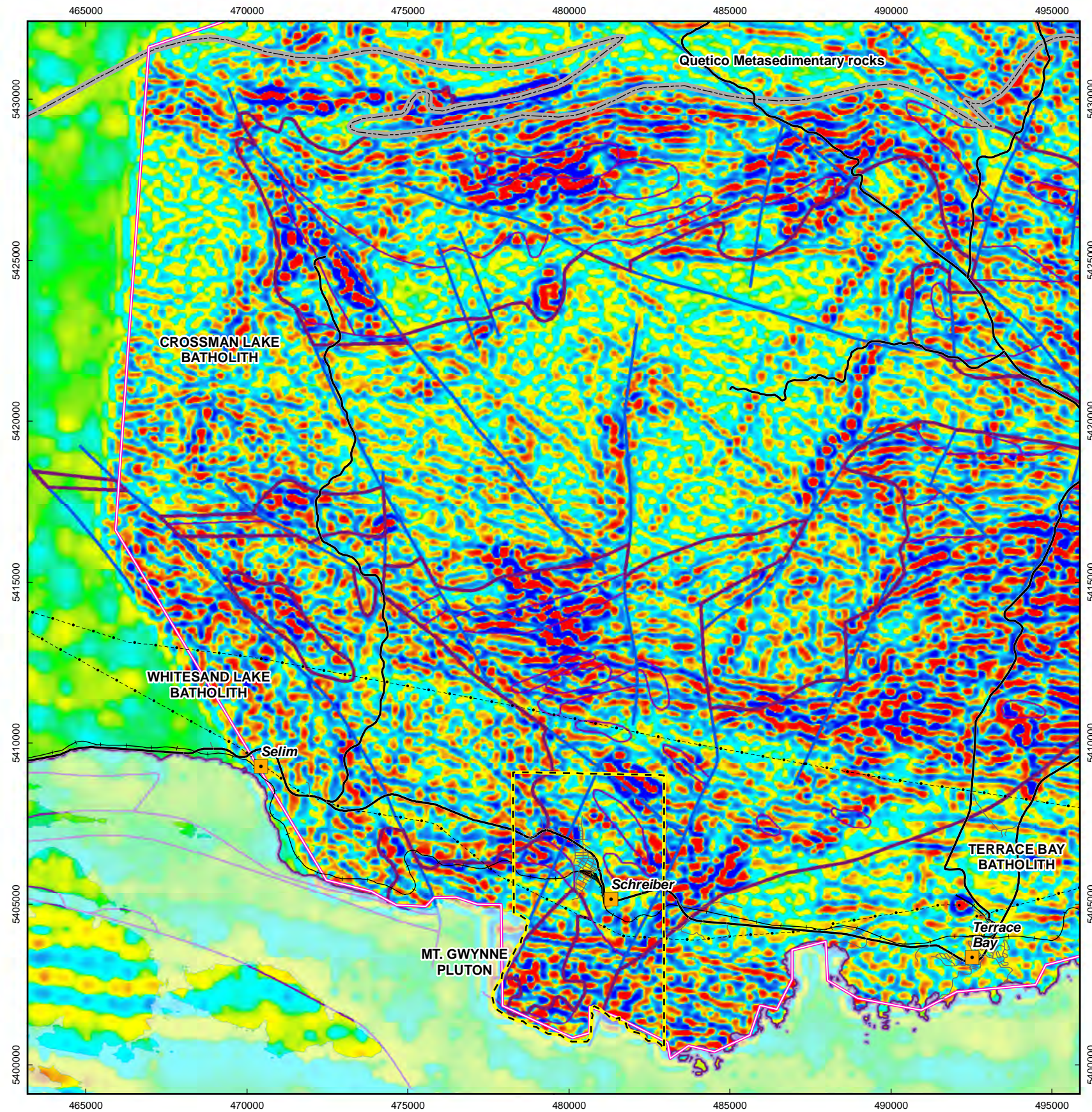
TITLE  
**First Vertical Derivative of Reduced to Pole  
Residual Magnetic Field in the Schreiber Area**

DESIGN	GHF	14 Aug 2012
GIS	JA	07 Aug 2013
CHECK	IV	07 Aug 2013
REVIEW	IV	07 Aug 2013

**Figure 8**

REVISION 7
UTM ZONE 16
NAD 1983
1:150,000

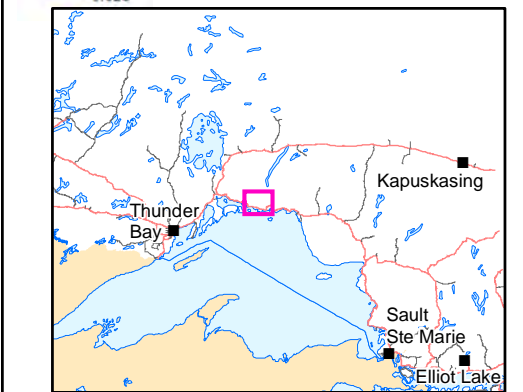
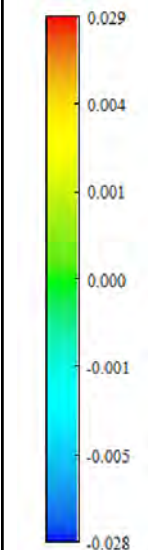




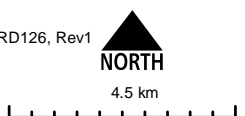
**LEGEND**

- City / Towns
- Township of Schreiber
- Main Road
- Local Road
- Railway
- Transmission Line
- Lake Superior
- Mapped Fault
- Geological Contact
- Quetico-Wawa Subprovince boundary
- Batholith / Pluton
- OGS Schreiber Area (GDS1104)

*Second Vertical Derivative (nT/m<sup>2</sup>)*



Data Sources:  
 Road: LIO Road Segment  
 Township: LIO Township  
 Waterbody: LIO Waterbody  
 Geology: Bedrock Geology of Ontario MRD126, Rev1  
 Geophysical Data:  
 OGS Schreiber Area survey GDS1104  
 GSC Magnetic 200m Compilation



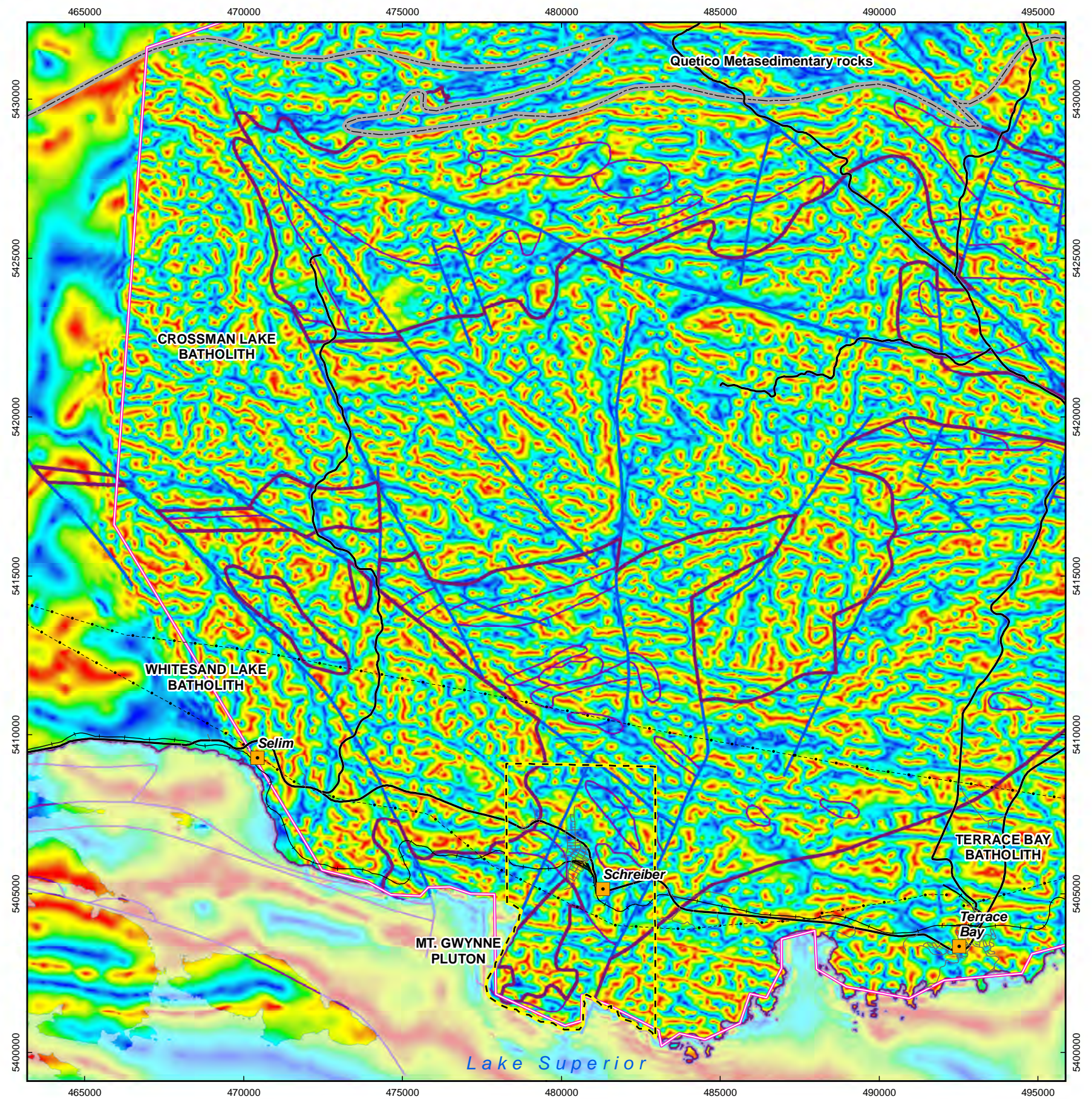
PROJECT  
 Phase 1 Geoscientific Desktop Preliminary Assessment,  
 Geophysics Study, Schreiber Area, Ontario

TITLE  
**Second Vertical Derivative of Reduced to Pole  
 Residual Magnetic Field in the Schreiber Area**

DESIGN	GHF	14 Aug 2012	<b>Figure 9</b>	REVISION 7
GIS	JA	07 Aug 2013		UTM ZONE 16
CHECK	IV	07 Aug 2013		NAD 1983
REVIEW	IV	07 Aug 2013		1:150,000

Lake Superior





**LEGEND**

- City / Towns
- Township of Schreiber
- Main Road
- Local Road
- Railway
- Transmission Line
- Lake Superior
- Mapped Fault
- Geological Contact
- Quetico-Wawa Subprovince boundary
- Batholith / Pluton
- OGS Schreiber Area (GDS1104)

*Tilt Angle (° degrees)*

90.0  
49.5  
19.5  
-11.4  
-38.9  
-61.4  
-90.0

Data Sources:  
 Road: LIO Road Segment  
 Township: LIO Township  
 Waterbody: LIO Waterbody  
 Geology: Bedrock Geology of Ontario MRD126, Rev1  
 Geophysical Data:  
 OGS Schreiber Area survey GDS1104  
 GSC Magnetic 200m Compilation

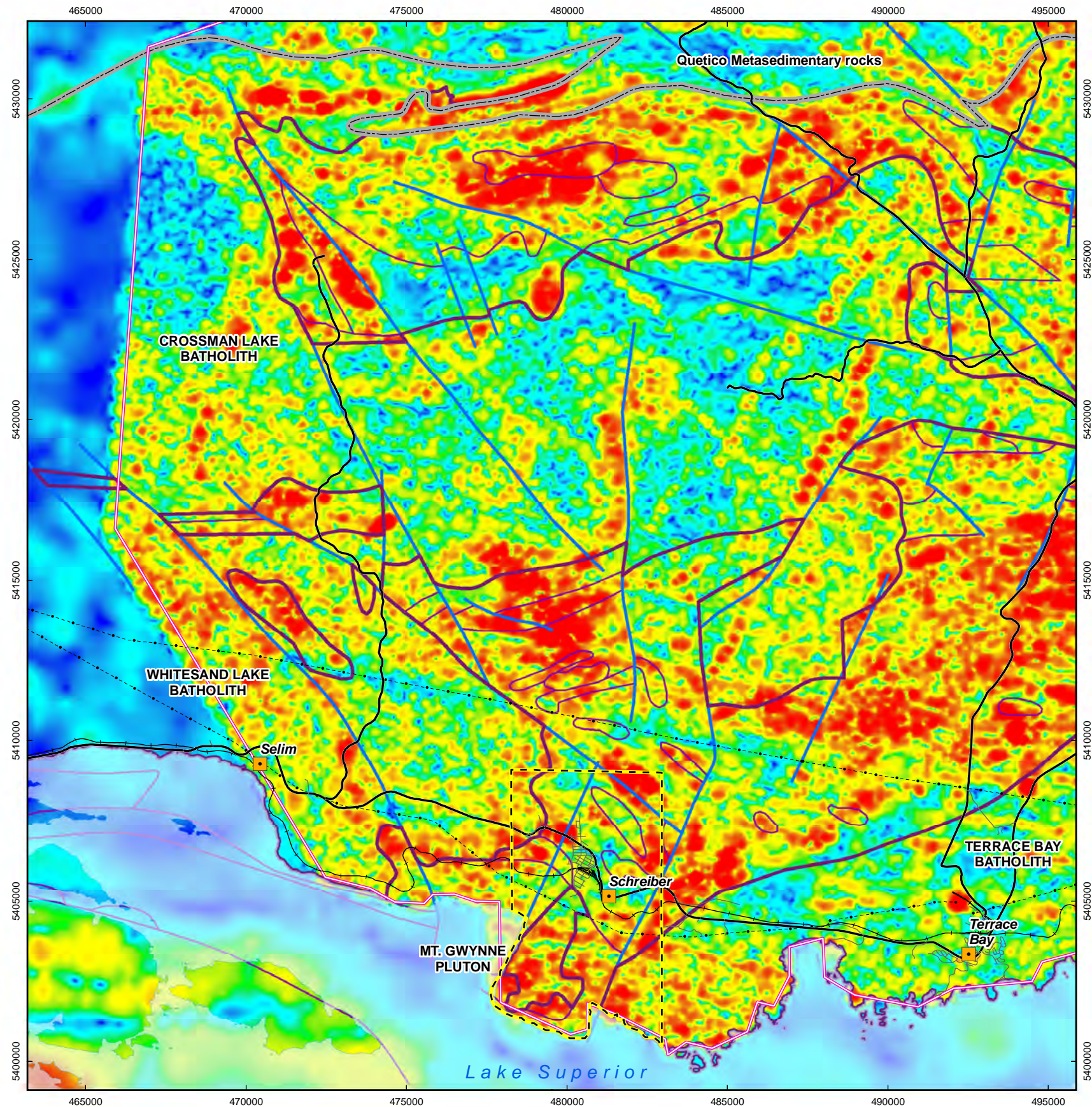
NORTH  
4.5 km

PROJECT  
Phase 1 Geoscientific Desktop Preliminary Assessment,  
Geophysics Study, Schreiber Area, Ontario

TITLE  
**Tilt Angle of Reduced to Pole Magnetic Field  
in the Schreiber Area**

DESIGN	GHF	14 Aug 2012	<b>Figure 10</b>	REVISION 7
GIS	JA	07 Aug 2013		UTM ZONE 16
CHECK	IV	07 Aug 2013		NAD 1983
REVIEW	IV	07 Aug 2013		1:150,000

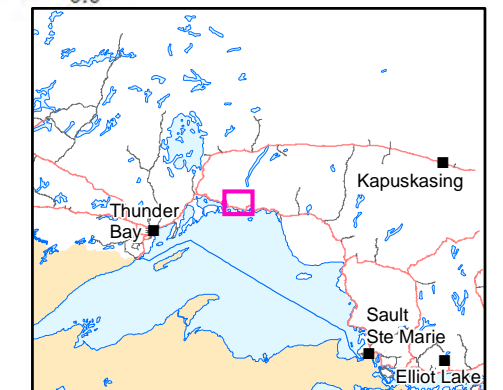
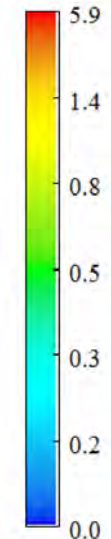




**LEGEND**

- City / Towns
- Township of Schreiber
- Main Road
- Local Road
- Railway
- Transmission Line
- Lake Superior
- Mapped Fault
- Geological Contact
- Quetico/Wawa Subprovince boundary
- Batholith / Pluton
- OGS Schreiber Area (GDS1104)

Analytic signal amplitude (nT/m)



Data Sources:  
 Road: LIO Road Segment  
 Township: LIO Township  
 Waterbody: LIO Waterbody  
 Geology: Bedrock Geology of Ontario MRD126, Rev1  
 Geophysical Data:  
 OGS Schreiber Area survey GDS1104  
 GSC Magnetic 200m Compilation



4.5 km



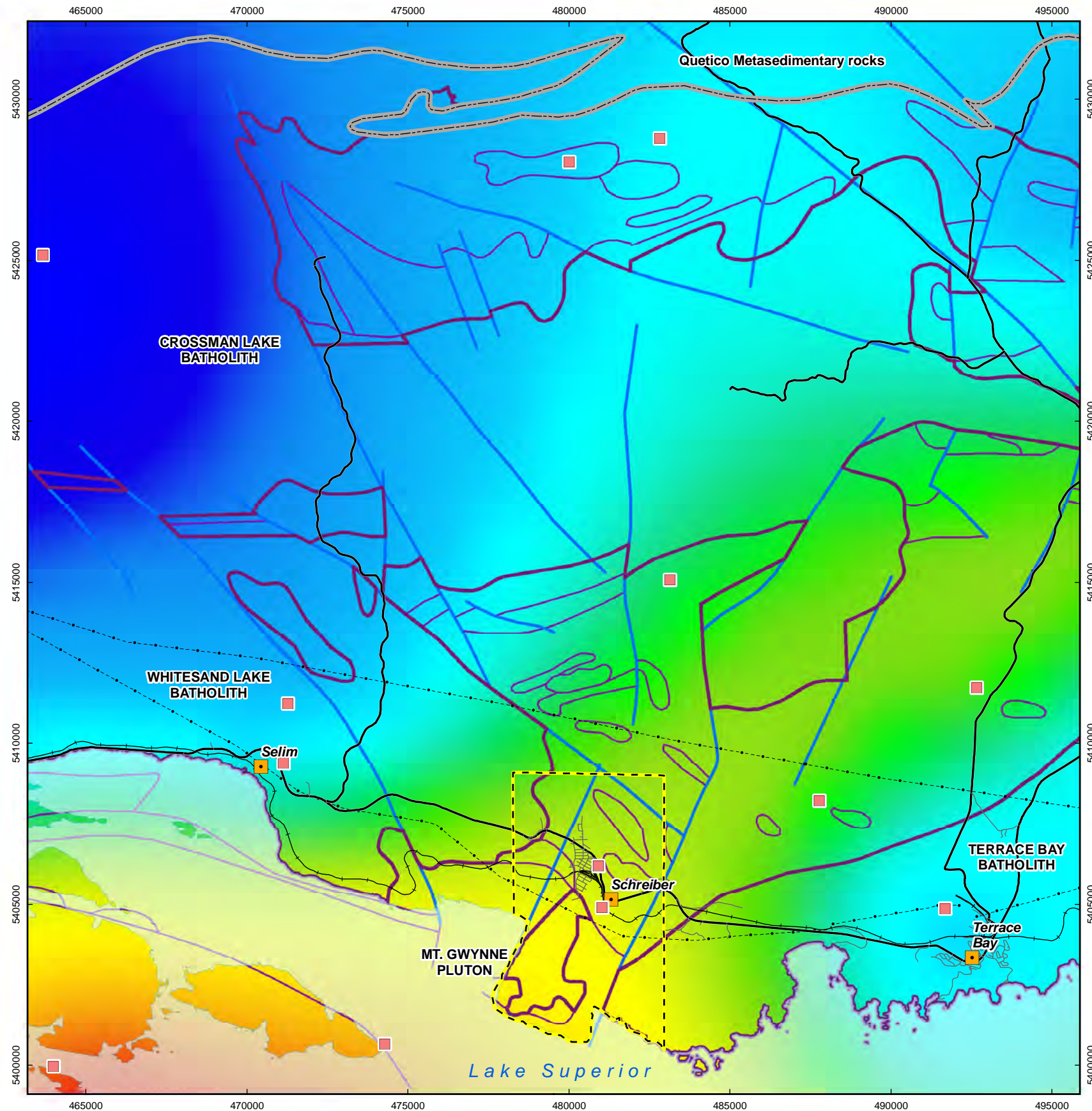
PROJECT  
 Phase 1 Geoscientific Desktop Preliminary Assessment,  
 Geophysics Study, Schreiber Area, Ontario

TITLE  
**Analytical Signal of Residual Magnetic Field  
 in the Schreiber Area**

DESIGN	GHF	14 Aug 2012	<b>Figure 11</b>	REVISION 7
GIS	GHF	07 Aug 2013		UTM ZONE 16
CHECK	IV	07 Aug 2013		NAD 1983
REVIEW	IV	07 Aug 2013		1:150,000



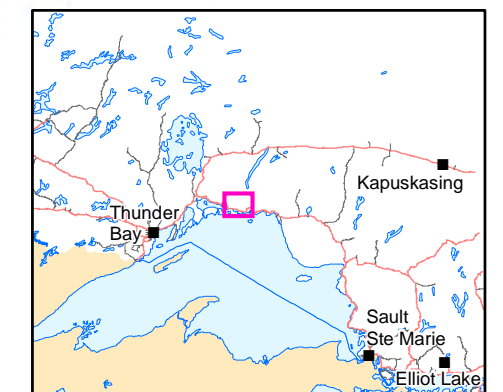
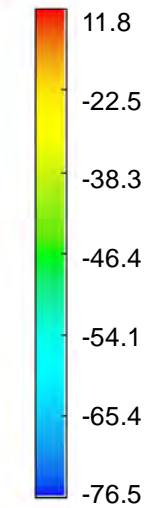
Name: Mira\_NWMO\_Schreiber\_Fig12\_GRAV\_rev07



**LEGEND**

- City / Towns
- Township of Schreiber
- Main Road
- Local Road
- Railway
- Transmission Line
- Lake Superior
- Mapped Fault
- Geological Contact
- Quetico/Wawa Subprovince boundary
- Batholith / Pluton
- Station - Canadian Gravity Database

*Bouguer Gravity Anomaly (mGal)*



Data Sources:  
 Road: LIO Road Segment  
 Township: LIO Township  
 Waterbody: LIO Waterbody  
 Geology: Bedrock Geology of Ontario MRD126, Rev1  
 Geophysical Data:  
 GSC Canadian Gravity Database (CGDB)



4.5 km

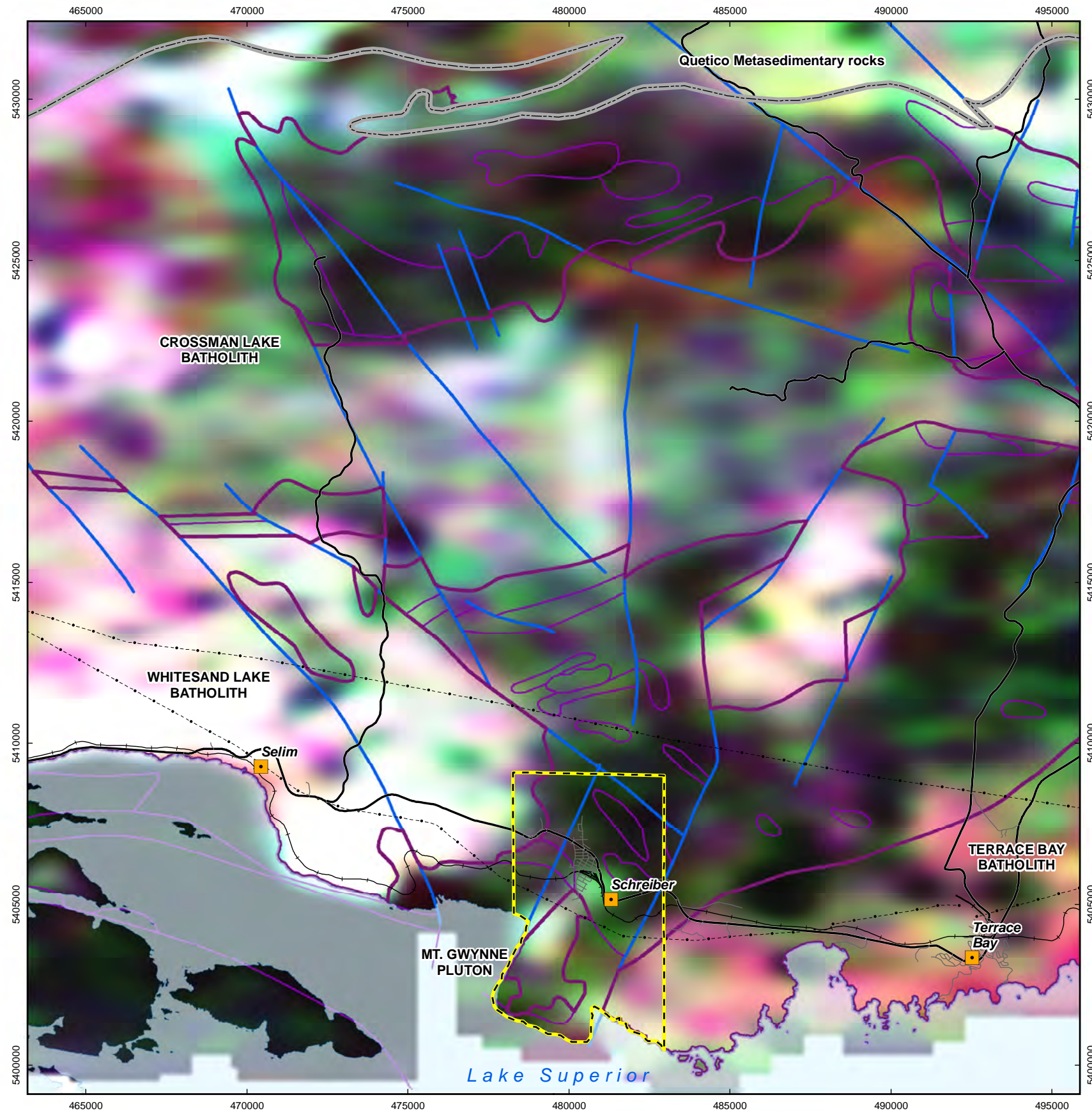


PROJECT  
 Phase 1 Geoscientific Desktop Preliminary Assessment,  
 Geophysics Study, Schreiber Area, Ontario

TITLE  
**Bouguer Gravity Field with Station Locations  
 in the Schreiber Area**

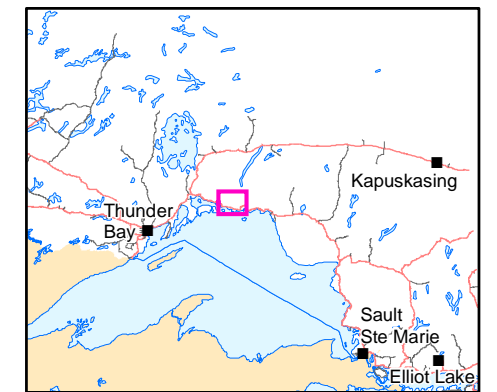
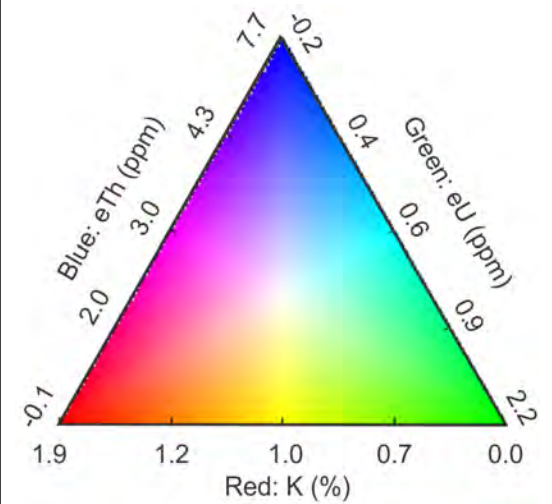
DESIGN	GHF	14 Aug 2012	<b>Figure 12</b>	REVISION 7
GIS	JA	07 Aug 2013		UTM ZONE 16
CHECK	IV	07 Aug 2013		NAD 1983
REVIEW	IV	07 Aug 2013		1:150,000





**LEGEND**

- City / Towns
- Township of Schreiber
- Main Road
- Local Road
- Railway
- Transmission Line
- Lake Superior
- Mapped Fault
- Geological Contact
- Quetico/Wawa Subprovince boundary
- Batholith / Pluton



Data Sources:

- Road: LIO Road Segment
- Township: LIO Township
- Waterbody: LIO Waterbody
- Geology: Bedrock Geology of Ontario MRD126, Rev1
- Geophysical Data: GSC Schreiber survey GSC2514



4.5 km

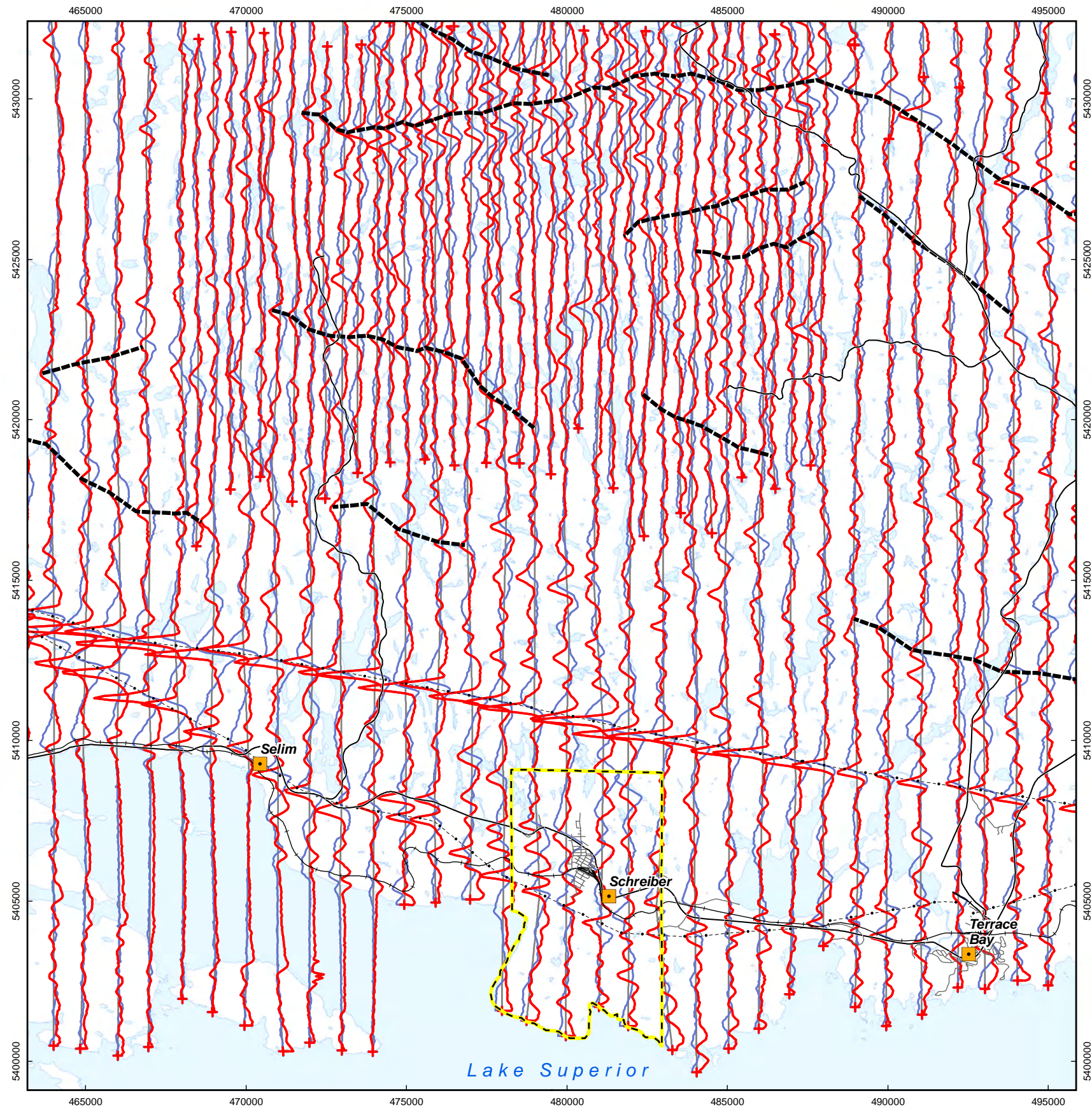


PROJECT  
Phase 1 Geoscientific Desktop Preliminary Assessment,  
Geophysics Study, Schreiber Area, Ontario

TITLE  
**Radiometric Ternary Image (RGB = K-eU-eTh)  
in the Schreiber Area**

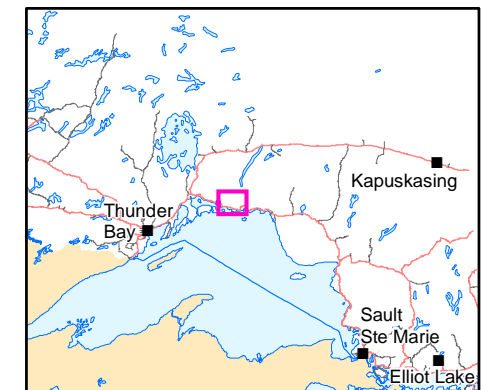
DESIGN	GHF	14 Aug 2012	<b>Figure 13</b>	REVISION 7
GIS	JA	07 Aug 2013		UTM ZONE 16
CHECK	IV	07 Aug 2013		NAD 1983
REVIEW	IV	07 Aug 2013		1:150,000



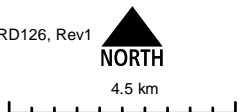


**LEGEND**

- City / Towns
- Township of Schreiber
- Main Road
- Local Road
- Railway
- Transmission Line
- Waterbody
- VLF Interpreted Contact
- Schreiber VLF Total Field
- Schreiber VLF Quadrature
- Schreiber VLF Flightline



Data Sources:  
 Road: LIO Road Segment  
 Township: LIO Township  
 Waterbody: LIO Waterbody  
 Geology: Bedrock Geology of Ontario MRD126, Rev1  
 Geophysical Data:  
 GSC Schreiber survey GSC2514

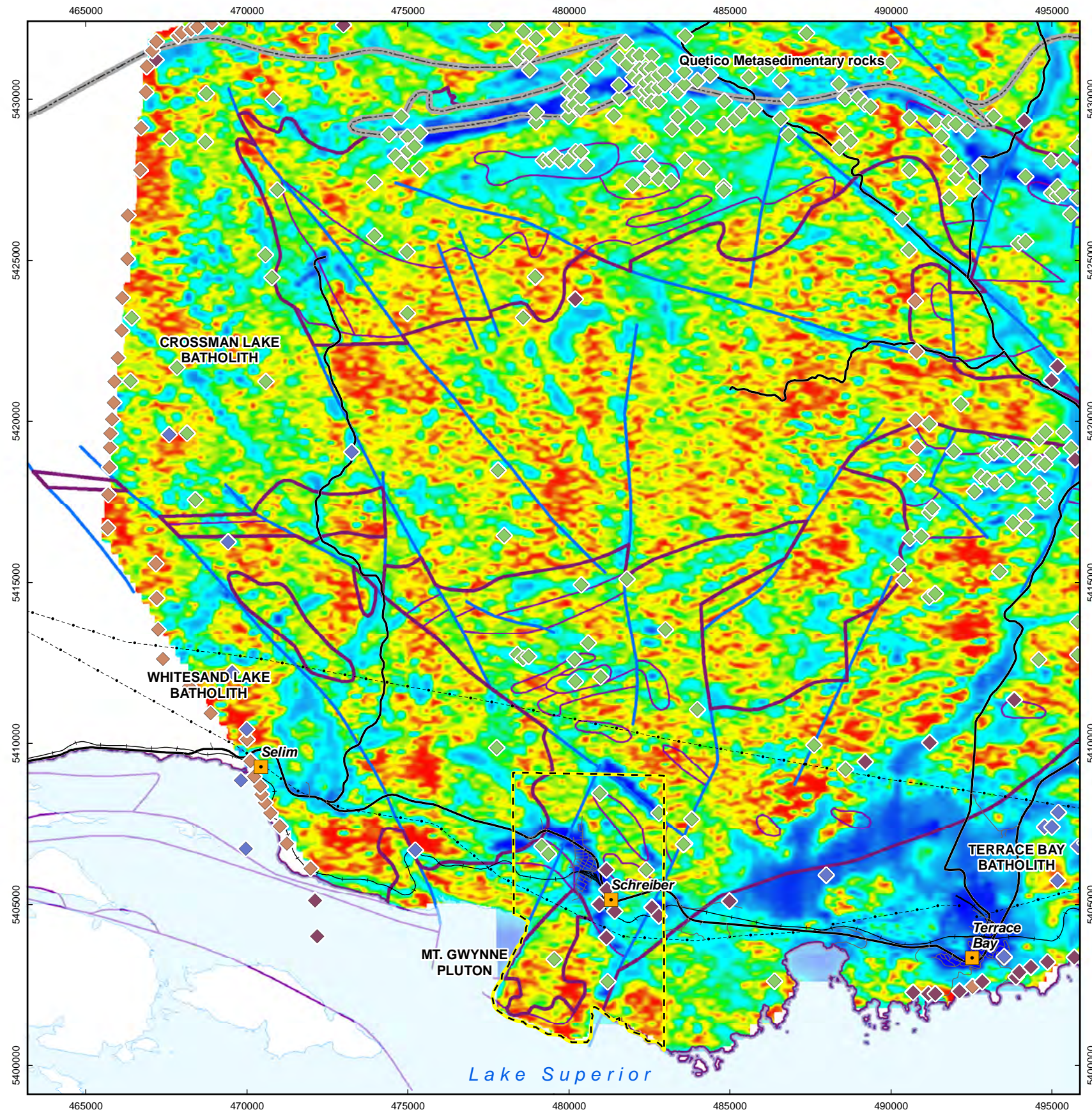


PROJECT  
 Phase 1 Geoscientific Desktop Preliminary Assessment,  
 Geophysics Study, Schreiber Area, Ontario

TITLE  
**Very Low Frequency Electromagnetic (VLF EM) Data  
 in the Schreiber Area**

DESIGN	GHF	14 Aug 2012	<b>Figure 14</b>	REVISION 7
GIS	JA	07 Aug 2013		UTM ZONE 16
CHECK	IV	07 Aug 2013		NAD 1983
REVIEW	IV	07 Aug 2013		1:150,000





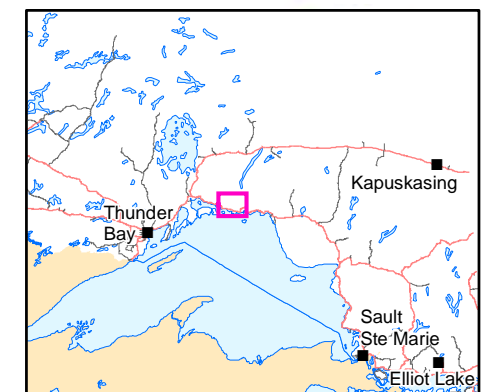
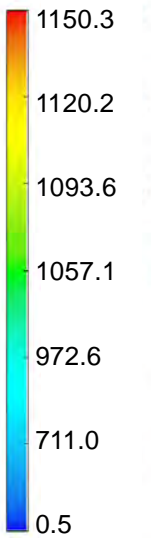
**LEGEND**

- City / Towns
- Township of Schreiber
- Main Road
- Local Road
- Railway
- Transmission Line
- Lake Superior
- Mapped Fault
- Geological Contact
- Quetico-Wawa Subprovince boundary
- Batholith / Pluton

**EM anomalies**

- Bedrock conductor
- Cultural conductor
- Dyke-like conductor
- Flat lying conductor

Apparent resistivity (Ohm.m)



Data Sources:  
 Road: LIO Road Segment  
 Township: LIO Township  
 Waterbody: LIO Waterbody  
 Geology: Bedrock Geology of Ontario MRD126, Rev1  
 Geophysical Data:  
 OGS Schreiber Area survey GDS1104



4.5 km

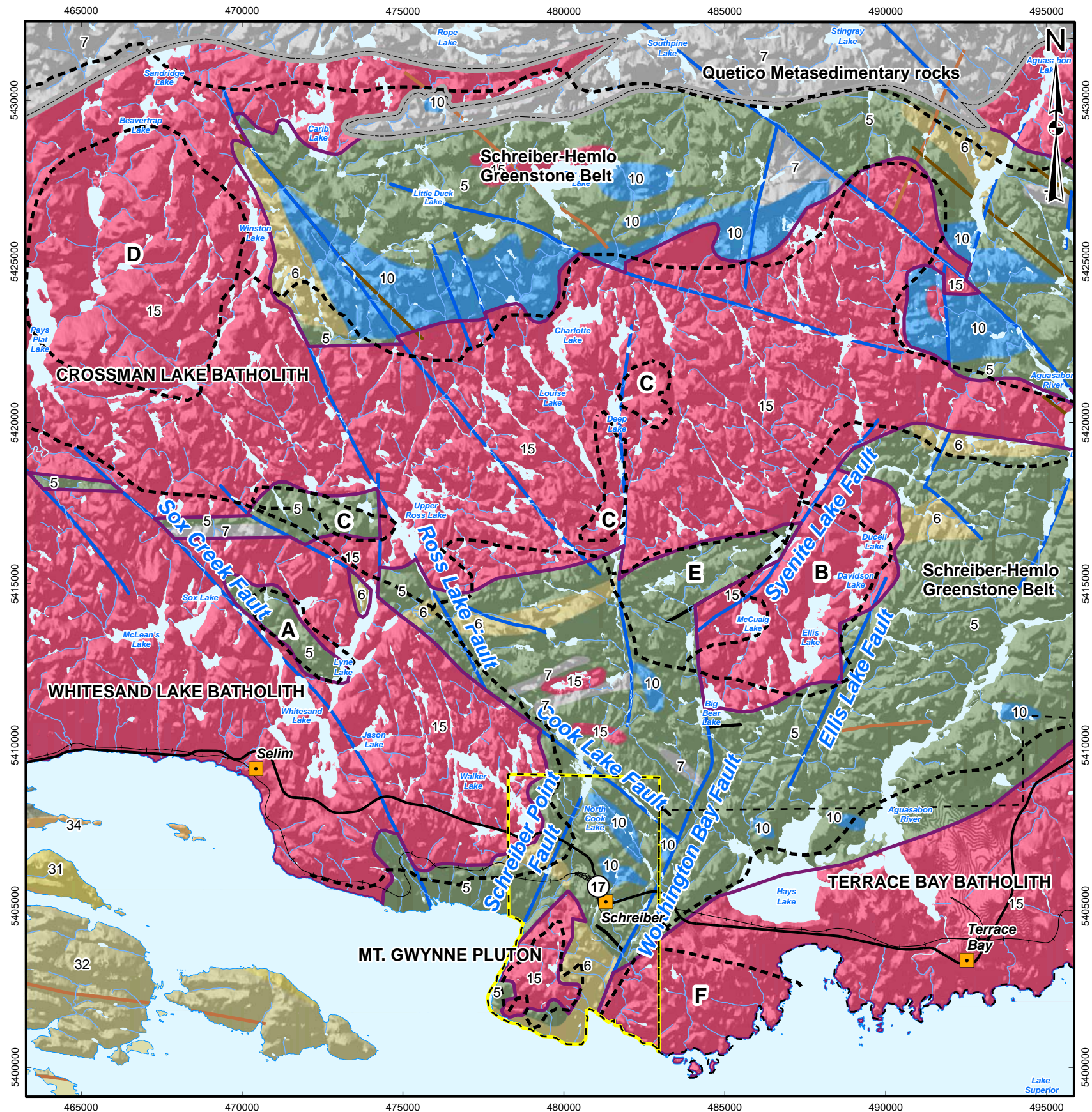


PROJECT  
 Phase 1 Geoscientific Desktop Preliminary Assessment,  
 Geophysics Study, Schreiber Area, Ontario

TITLE  
**Apparent Resistivity from Low Frequency (877 Hz)  
 Electromagnetic Data in the Schreiber Area**

DESIGN	GHF	14 Aug 2012	<b>Figure 15</b>	REVISION 7
GIS	JA	07 Aug 2013		UTM ZONE 16
CHECK	IV	07 Aug 2013		NAD 1983
REVIEW	IV	07 Aug 2013		1:150,000





**LEGEND**

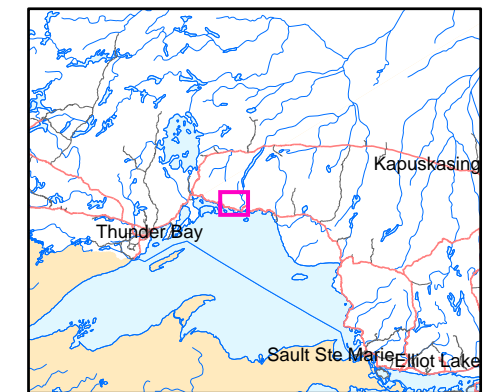
- City / Towns
- Schreiber Area
- Township of Schreiber
- Township of Terrace Bay
- Main Road
- Railway
- Watercourse, Permanent
- Watercourse, Intermittent
- Waterbody, Permanent
- Mapped Fault
- Iron Formation
- Quetico-Wawa Subprovince Boundary
- Geologic Unit Interpreted from Geophysics
- Outline of batholith/pluton

**Mapped Dyke**

- Marathon, Kapuskasing or Biscotasing Mafic Dyke
- Matachewan Mafic Dyke
- Dyke (Other)

**Bedrock Geology (Youngest to Oldest)**

- 34. Mafic intrusive rocks (Keweenawan age)
- 32. Osler Gp., Mamainse Point Fm., Michipicoten Island Fm.
- 31. Sibley Gp.
- 24. Animikie Gp.
- 15. Massive granodiorite to granite
- 11. Gneissic tonalite suite
- 10. Mafic and ultramafic rocks
- 7. Metasedimentary rocks
- 6. Felsic to intermediate metavolcanic rocks
- 5. Mafic to intermediate metavolcanic rocks
- 2. Felsic to intermediate metavolcanic rocks



Data Sources:  
 Bedrock: OGS MRD 126-REV1 (1:250,000)  
 Faults: OGS MRD 126-REV1 (1:250,000)  
 Dykes: OGS MRD 126-REV1 (1:250,000)  
 Batholith: Generalized from OGS 2006  
 Base Data: MNR LIO, obtained 2009-2013

5 km



PROJECT  
 PHASE 1 GEOSCIENTIFIC DESKTOP PRELIMINARY ASSESSMENT  
 GEOPHYSICS STUDY, SCHREIBER AREA, ONTARIO

TITLE  
**Geophysical Interpretation showing distribution of  
 bedrock units for the Schreiber Area**

DESIGN	GHF	14 Aug 2012	<b>FIGURE 16</b>	REVISION 4
GIS	GHF	26 Feb 2013		UTM ZONE 16
CHECK	CB	26 Feb 2013		NAD 1983
REVIEW	CB	26 Feb 2013		1:150,000